ANL/PHY-94/1

ANL/PHY-94/1

Proceedings

of

The Argonne Physics Division Workshop

on

DOUBLE PHOTOIONIZATION OF HELIUM WITH SYNCHROTRON X-RAYS

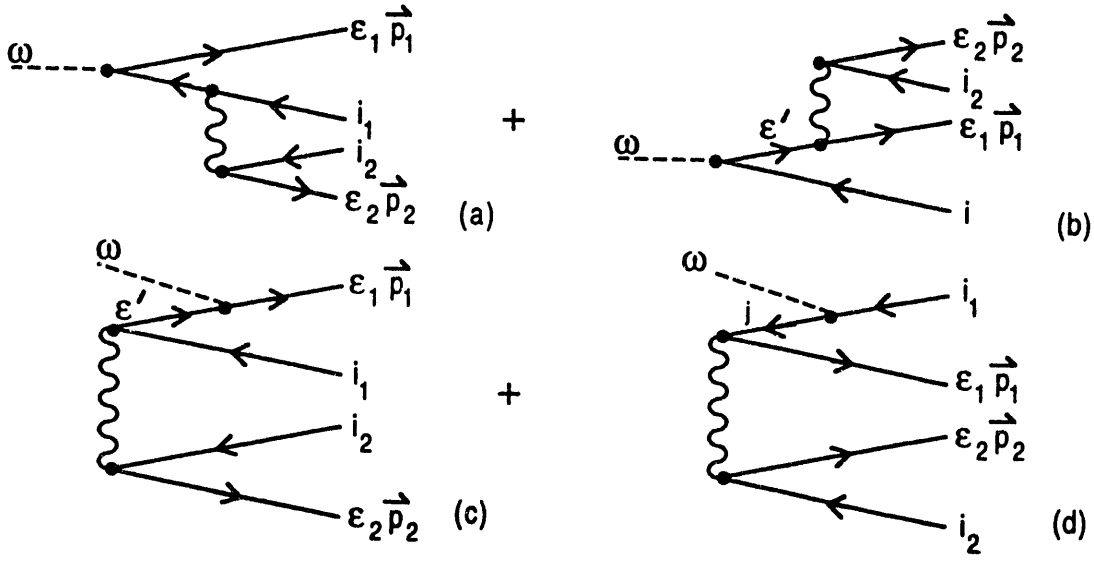

held at Argonne National Laboratory on Monday and Tuesday, October 4 and 5, 1993

Reproduced from the best available copy.

Available to DOE and DOE contractors from the
Office of Scientific and Technical Information
P.O. Box 62
Oak Ridge, TN 37831
Prices available from (615) 576-8401

Available to the public from the
National Technical Information Service
U.S. Department of Commerce
5285 Port Royal Road
Springfield, VA 22161

ANL/PHY-94/1

ARGONNE NATIONAL LABORATORY
9700 South Cass Avenue
Argonne, IL 60439

Proceedings

of
The Workshop on

DOUBLE PHOTOIONIZATION OF HELIUM WITH SYNCHROTRON X-RAYS

Held at Argonne
on Monday and Tuesday,
October 4 and 5, 1993.

Organizing Committee

Yoshiro Azuma, ANL-Physics Division
Gordon Berry, ANL-Physics Division

January 1994

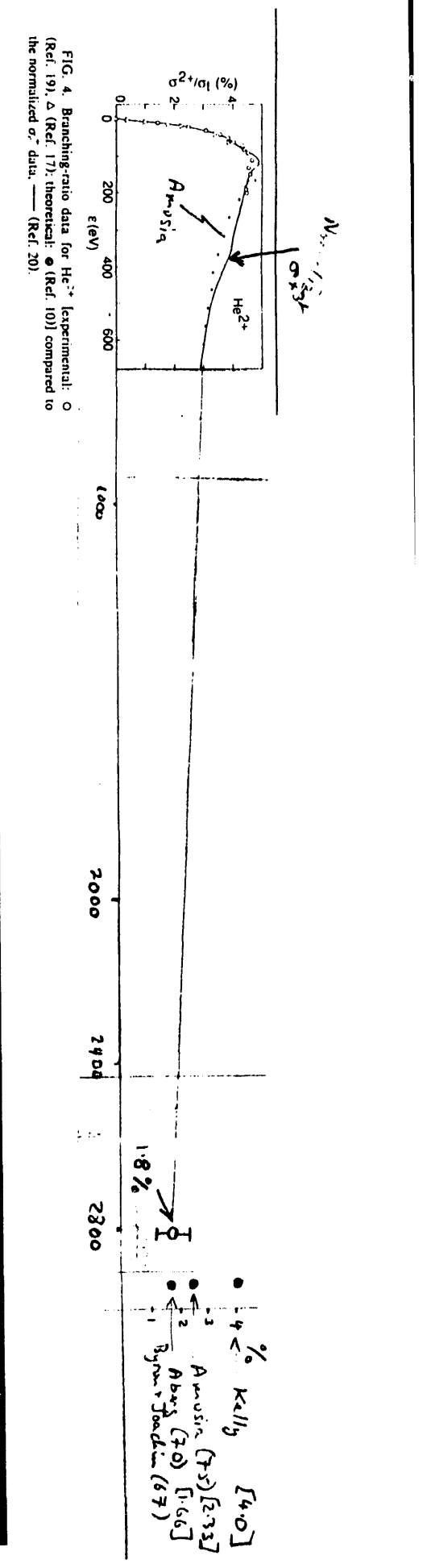

FIG. 4. Branching-ratio data for He^{2+} [experimental: o (Ref. 19), Δ (Ref. 17); theoretical: • (Ref. 10)] compared to the normalized σ_t^+ data. —— (Ref. 20).

:=

Preface

This book contains the Proceedings of the workshop on "**Double Photoionization of Helium with Synchrotron X-rays**", held at Argonne on October 4 and 5, 1993. The workshop was held to bring together the different groups working on this problem of intense current interest. The past two years have witnessed an enormous experimental and theoretical effort to help understand this basic problem of atomic physics. The contributions included here give witness to this explosive growth of the past one to two years, and we hope that the workshop has provided a forum for a collective view of the next steps in the study of photoionization of the simplest atomic systems.

In order to keep to a rapid time line for publishing, these Proceedings have been put together in a very informal manner, and thus, some of the contributions have been arranged just from copies of the overhead figures presented at the workshop. We thank those speakers who prepared manuscripts after the conference at very short notice. We believe that on balance the Proceedings provide an excellent snapshot of where progress now is in the field and an excellent resource for work completed in the past.

The success of such a rapidly organized workshop owes much to the hard work of many people: Firstly, we thank Rose Lorenz on whose back fell many of the organizing headaches, deadlines, and minor/major irritations. We thank her for her smiling efficiency. We thank many of the speakers for organizing their schedules at such short notice, and agreeing to talk. Our colleagues in the atomic physics synchrotron radiation group, Don Gemmell and Tom LeBrun helped to make sure nothing had been forgotten. The support of Mitio Inokuti was helpful in initial discussions to have a workshop. It was extremely unfortunate that the illness of our colleague Paul Cowan prevented his taking part in the conference or its organization. His expertise in this field was very much missed during the workshop. We wish him every success on his road to recovery, and to his contributions in the future.

We thank Walter Henning, Director of the Physics Division, for his continuing support and for his opening remarks at the workshop. We thank David Moncton, Associate Laboratory Director of the Advance Photon Source, for guiding us on a tour of that facility; many of the workshop participants look forward to utilizing the Advanced Photon Source. We also acknowledge financial support from the University of Chicago Board of Governors, from Frank Fradin, Associate Laboratory Director for Physical Research at Argonne, and from the Department of Energy, Division of Chemical Sciences: this help was essential in enabling us to provide support for the workshop participants. We appreciate the support of the last in our continuing research into the photoionization of helium.

Yoshiro Azuma
Gordon Berry
The Organizing Committee

December 17, 1993

WORKSHOP ON

DOUBLE-PHOTOIONIZATION OF HELIUM WITH SYNCHROTRON X-RAYS

Table of Contents

17.

WORKSHOP ON
DOUBLE PHOTOIONIZATION OF HELIUM WITH SYNCHROTRON X-RAYS

Argonne National Laboratory
October 4-5, 1993
Bldg. 203, Room R-150

MONDAY, OCTOBER 4

9:00 AM - 11:30 AM	Registration
11:30 AM - 1:00 PM	Lunch, Argonne Cafeteria, Bldg. 213
1:00 PM **Welcome**	**Walter Henning**
Session 1	Chair, **Magnus Westerlind**
1:05 PM - 1:35 PM	**Yoshiro Azuma** "Introduction and Recent Absorption Measurements"
1:45 PM - 2:30 PM	**Jim McGuire and Steve Manson** "Overview and Comparison of Photoionization with Charged Particle Impact"
2:45 PM - 3:15 PM	**Jon Levin** "He^{++}/He^{+} Measurements, 2 to 12 keV"
3:30 PM- 4:00 PM	Coffee Break
Session 2	Chair, **Teijo Åberg**
4:00 PM - 4:30 PM	**Paul Bergstrom** "Compton Scattering of Photons from Electrons Bound in Light Elements"
4:45 PM - 5:15 PM	**James Samson** "Electron Ionization and the Compton Effect in He^{+}"
5:30 PM - 6:00 PM	**Miron Amusia** "Elimination of Two Atomic Electrons by a Single High Energy Photon"
7:00 PM - 7:30 PM	Cocktails & Dinner

Sponsored by Argonne National Laboratory with additional support from The University of Chicago Board of Governors for Argonne National Laboratory

TUESDAY, OCTOBER 5

Session 3 — Chair, **Dennis Lindle**

8:30 AM - 9:00 AM	**Nora Berrah** "Double Photoionization of Helium at Intermediate Energies"
9:15 AM - 9:45 AM	**Hossein Sadeghpour** "Double Photoionization: Coulomb Explosion, Dipole Gauge Dependence, and ..."
10:00 AM - 10:15 AM	Coffee Break

Session 4 — Chair, **Richard Pratt**

10:15 AM - 10:45 AM	**Joachim Burgdörfer** "Photoionization and Compton Scattering by High Energy Photon Impact on Helium"
11:00 AM - 11:30 AM	**Roger Bartlett** "The effect of Compton Scattering on the Double to Single Ionization Ratio in Helium"
11:45 AM - 12:15 PM	**Ken-Ichi Hino** "Double Photoionization of He by using MBPT and the BBK Wave Function"
12:30 PM - 1:30 PM	Lunch

Session 5

1:30 PM - 3:00 PM	Chair, **John Cooper** Panel Discussion **Ivan Sellin, Teijo Åberg, Steve Manson, Mitio Inokuti**
3:00 PM - 3:15 PM	Summary: **Gordon Berry**
3:30 PM - 4:30 PM	Tour of the Advanced Photon Source

Sponsored by Argonne National Laboratory with additional support from The University of Chicago Board of Governors for Argonne National Laboratory

List of Attendees to the workshop

Name	Affiliation
Åberg, Maire	self
Åberg, Teijo	Department of Physics, University of Helinski
Ali, Rami	Physics Division, Argonne National Laboratory
Amusia, Agneta	self
Amusia, Miron	Physics Division, Argonne National Laboratory
Azuma, Yoichiro	Physics Division, Argonne National Laboratory
Bartlett, Roger	Los Alamos National Laboratory
Bergstrom, Paul	Department of Physics, University of Tennessee
Berkowitz, Joseph	Chemistry Division, Argonne National Laboratory
Berrah, Nora	Department of Physics, University of Western Michigan
Berry, Gordon	Physics Division, Argonne National Laboratory
Bohn, John	Department of Physics, University of Chicago
Branko, Ruscic	Chemistry Division, Argonne National Laboratory
Bruch, Reinhard	Department of Physics, University of Nevada
Burgdörfer, Joachim	Department of Physics, University of Tennessee
Childs, William	Physics Division, Argonne National Laboratory
Cooper, John	Department of Physics, University of Maryland
Cowan, Paul	Physics Division, Argonne National Laboratory
Dunford, Robert	Physics Division, Argonne National Laboratory
Fano, Ugo	Department of Physics, University of Chicago
Gemmell, Donald	Physics Division, Argonne National Laboratory
Gerdes, Stina	self
Henning, Walter	Physics Division, Argonne National Laboratory
Hino, Ken-ichi	Department of Physics, University of Tennessee
Inokuti, Mitio	Environmental Research Division, Argonne National Laboratory
Kanter, Elliot	Physics Division, Argonne National Laboratory
Kimura, Mineo	Environmental Research Division, Argonne National Laboratory
Kurtz, Charles	Physics Division, Argonne National Laboratory
LeBrun, Thomas	Physics Division, Argonne National Laboratory
Levin, Jon	Department of Physics, University of Tennessee
Lindle, Dennis	Department of Physics, University of Nevada
Manson, Steven	Department of Physics, Georgia State University
McGuire, James	Department of Physics, Jim Tulane University
Montano, Pedro	Material Sciences Division, Argonne National Laboratory
Pratt, Richard	Department of Physics, University of Pittsburgh
Sadeghpour, Hossein	Department of Physics, Harvard University
Samson, James	Department of Physics, University of Nebraska
Sellin, Ivan	Oak Ridge National Laboratory
Stehman, Robert	Department of Chemistry, Northeastern Illiinois University

Suleiman, Jamal	Physics Division, Argonne National Laboratory
Tani, Smio	Department of Physics, Marquette University, Milwaukee
Westerlind, Magnus	Department of Physics, University of Tennessee
Young, Linda	Physics Division, Argonne National Laboratory
Zabransky, Bruce	Physics Division, Argonne National Laboratory

Introduction and recent absorption measurements

Yoshiro Azuma

Physics Division, Argonne National Laboratory, Argonne, IL 60439

1. Introduction

Helium is the simplest, neutral atom that exhibits electron-electron correlation effects and photons provide the cleanest probes of atomic structure. In fact the first atomic physics experiment with synchrotron radiation was the measurement of doubly excited nsnp autoionizing resonances of helium (Madden & Codling 1963). This and subsequent experiments on double photo excitation/ionization in the uv region near threshold stimulated major developments in the theory of electron correlation effects (Cooper et al. 1963, Fano 1983) and led to the formulation of new correlational quantum numbers (Herrick and Sinanoglu 1975, Lin 1984). Active interplay between theory and experiments in the uv region near threshold still continues. Recent developments include the pursuit of hyperspherical close coupling (HSCC) calculations (Tang, Watanabe, et al. 1992, 1993) and high resolution absorption measurements (Domke et al. 1991, 1992).

Theoretical studies on helium double photoionization were extended to the high photon energy region, which is the subject of this workshop, through the 1970s. A number of authors pursued the many body perturbation (MBPT) approach (Byron & Joachain 1967, Brown 1970, Amusia et al 1974, Carter & Kelly 1981) and Åberg (1970) evaluated the high energy limit by sudden approximation. However, further developments in the 1980's was slower, except for the comparison of the high energy limits of σ^{++}/σ^{+} for charged particle impact and photoionization by McGuire (1984). Perhaps the lapse was mainly due to the complete lack of experimental data beyond a single data point of the double-to-single photoionization ratio s++/s+ at 600 eV measured with an x-ray tube source (Carlson 1967).

The situation took a drastic turn in the 90's with the new time-of-flight measurement utilizing synchrotron x-rays by a collaboration including ORNL, the University of Tennessee, ANL, and NIST, of the double-to-single photoionization ratio σ^{++}/σ^{+} at 2.8 keV photon energy (Levin et al. 1991). Also, a new attempt to predict the ratio with a semiempirical calculation was made by Samson (1990). His suggestion was to derive the double photoionization cross-section as the product of single photoionization cross section and the electron impact ionization cross section of a singly charged ion. This paper addressed photon energies of up to approximately 600 eV with remarkable success, but extension of this approach to higher energies would yield an exceedingly small ratio and no asymptotic value. Nevertheless, the intuitive clarity and simplicity of this idea was appealing, and became instrumental in stimulating further experimental work in the high photon energy region. Since then, a number of experimental works have appeared in rapid succession (Bartlett et al. 1992, Samson et al. 1992, Levin et al. 1993, Berrah et al. 1993).

Interactive theoretical efforts have been equally high. Further MBPT calculations have been pursued (Ishihara et al. 1992, Sadeghpour & Dalgarno 1993, Teng & Shakeshaft 1993, Hino et al. 1993a, 1993b). Efforts were made to extend the calculations to the iso-electronic sequence and to analyze the importance of the respective MBPT amplitudes on the choice of the gauge (length, velocity, acceleration) of the electric dipole operator (Sadeghpour & Dalgarno 1993). A most recent development has been the incorporation of single and double ionization by Compton scattering (Samson et al. 1993, Andersson & Burgdörfer 1993) which was neglected in many of the previous works.

The recent rapid growth of the number of papers published on this subject can be seen on Table I, which lists titles of papers in major refereed journals. This year's entry on the table includes only up to September, and we hear about a number of further papers that are just about to come out. It is perhaps fair to call this an "explosive development" and it will be very interesting to see how far this will take us.

Table I. *Titles of recent papers on double photoionization of helium with synchrotron x-rays in major refereed journals.*

1990 1. Proportionality of Electron-Impact Ionization to Double Photoionization, Samson PRL.

1991 1. Measurement of the Ratio of Double-to-single Photoionization of Helium at 2.8 keV using Synchrotron Radiation. Levin et al. PRL
2. Photoionization of two electrons in helium Ishihara et al. PRA RC.

1992 1. Double photoionization of atomic helium and its isoelectronic partners at x-ray energies. Dalgarno and Sadeghpour. PRA RC.
2. Single-photon double ionization of He and Ne Bartlett et al. PRA.
3. Probability for double photoionization of He and Ne Samson et al. PRA
4. High Energy Behavior of the Double Photoionization of Helium from 2 to 12 keV. Levin et al. PRA RC.

1993 (up to September)
1. Double ionization of helium by a single high-energy photon. Teng and Shakeshaft PRA RC.
2. Excitation-ionization and double ionization of Helium by high-energy photon impact. Andersson and Burgdorfer PRL
3. Comment on Measurement of the Ratio of Double-to Single Photoionization of Helium at 2.8 keV Using Synchrotron Radiation Samson et al. PRL.
4. Probing Electron Correlations in Double Photoionization of He at Intermediate Energies. Berrah et al. PRA RC.
5. Double ionization of He by high-energy photon impact Hino 1993a PRA.
6 Double photoionization of helium using many-body perturbation theory Hino et al. 1993b PRA.
7. Double photoionization of helium: Use of correlated two-electron continuum wave function. Kornberg and Miraglia. PRA

2. Absolute cross-section measurements at NSLS

(Y. Azuma, H.G. Berry, D.S. Gemmell, J. Suleiman, M. Westerlind, I.A.Sellin and J.P.Kirkland)

The following is a brief progress report of our series of measurements of the total attenuation cross-section of helium for photons in the energy range of 2 to 15 keV. It is over this region that the transition should take place from photoionization dominance with lower photon energies to Compton scattering dominance with higher photon energies.

The measurements took place at the National Synchrotron Light Source (NSLS) x-ray ring at Brookhaven National Laboratory, utilizing beam-lines X-24A, X-23B, and X-23A2. Instead of employing the "Double Ion-chamber Method" and scanning the photon energy as usually done for gas phase absorption spectroscopy, we fixed the photon energy at each data point and measured the photon beam transmission as a function of target thickness. This was necessary for absolute measurements of the very low cross-sections, down to less than two barns. A schematic of the experimental setup is shown on figure 1. The 1 meter long, 3.5 cm diameter cell, fitted with 3/8" diameter 3-mil kapton windows on both ends was filled with helium up to as high as 10 atmospheres. For measurements in the lower photon energy end, 1-mil mylar windows were used to allow better photon beam transmission and pressures were kept to below 2 atmospheres. Another difficulty due to the low cross section, which limited previous works (Bearden 1966, McCray et al. 1970) is that the measurement becomes very sensitive to even small amounts of impurities that have much higher cross sections. We used 99.9999% pure, neon-free helium, and the remaining 1 ppm gases were expected to affect the cross-section measured cross sections by less than 1%. A neon filled ionization chamber recorded the incident photon flux up-beam of the He cell, and a PIN diode monitored the transmission down-beam. The ratios of these two signals provide the raw absorption data. Slits in front of the ionization chamber defined the photon-beam size, typically 1 mm square, within the chamber.

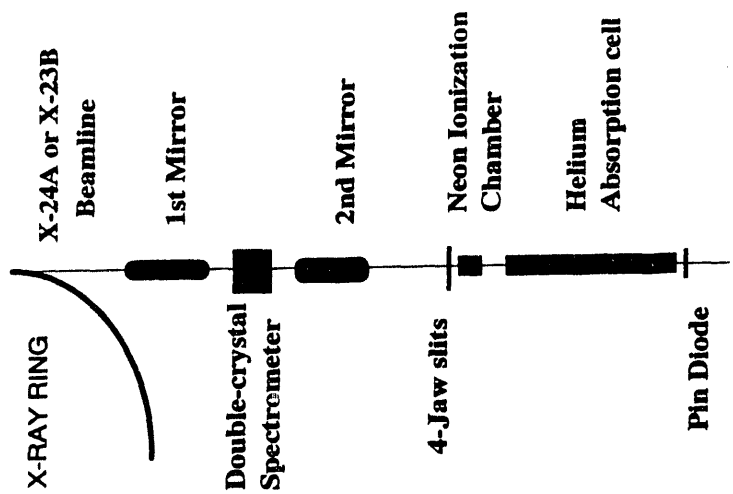

Figure 1. *Schematic of the helium absorption experimental arrangement.*

At each photon energy, we measured the absorption ratio for 12 to 15 helium pressures typically between 100 and 6000 torr. Figure 2 shows two semi-logarithmic absorption curves, each slope being proportional to the attenuation coefficient at the given photon energy. Figure 3 summarizes the current status of the measurements of absolute cross-sections and makes comparison with theory as well as previous measurements.

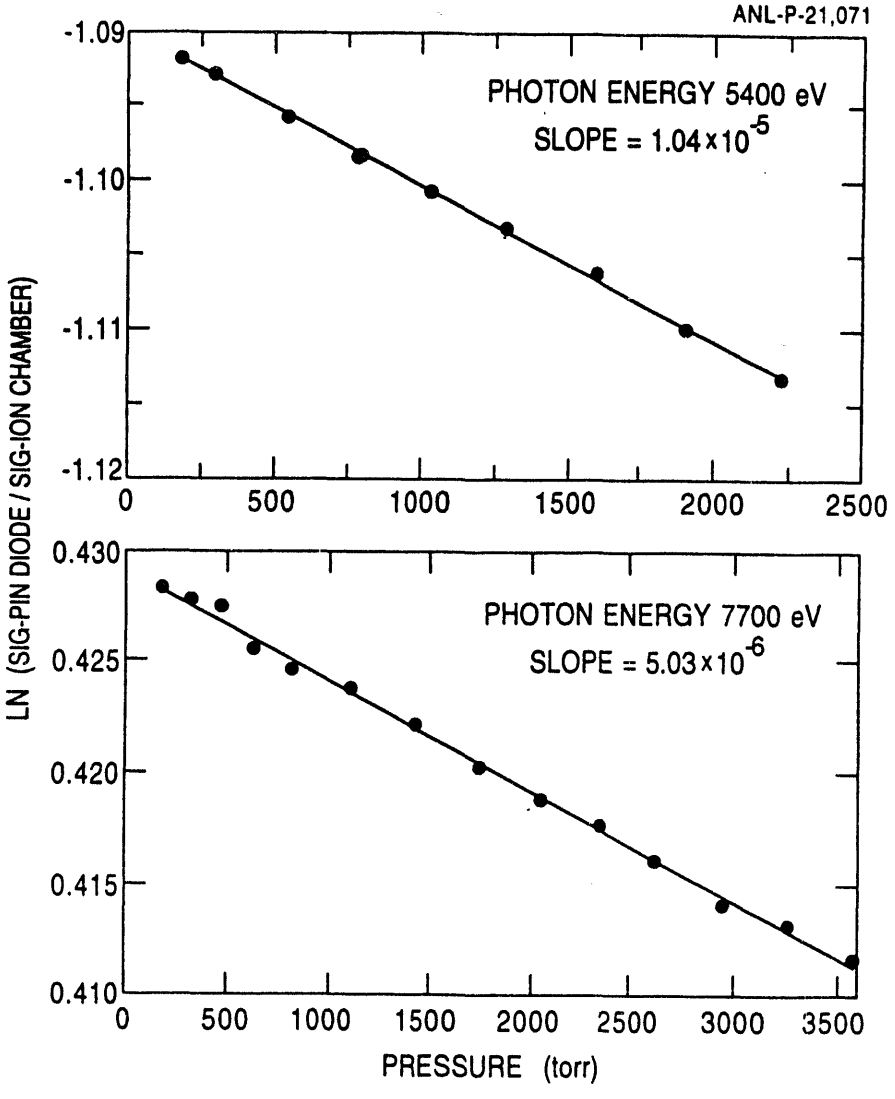

Figure 2. *Pressure dependence of the absorption in helium at two different photon energies.*

The experimental data show an energy dependence close to E-3.5 at lower energy, and tends to level off asymptotically at higher energies. The higher energy value is close to 1.33 barns which is twice the non-relativistic limit of the Klein-Nishina formula for a single free electron (helium has two electrons). Thus the change over from photoionization dominance to Compton scattering dominance is very clearly observed and verifies that the experimental data of the ionization ratio σ^{++}/σ^{+} was due to Compton scattering above 6 keV.

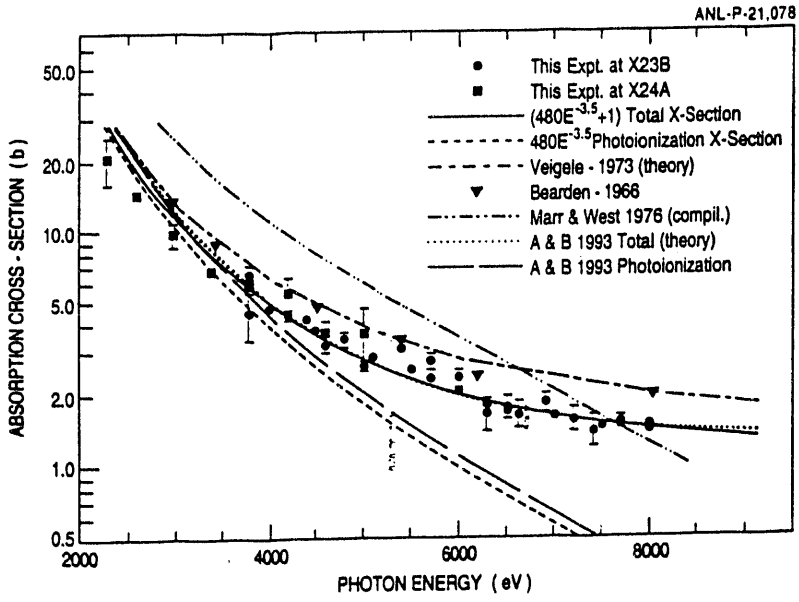

Figure 3. *Comparisons of our measured absorption cross sections with theories (for details, see text of other proceedings papers).*

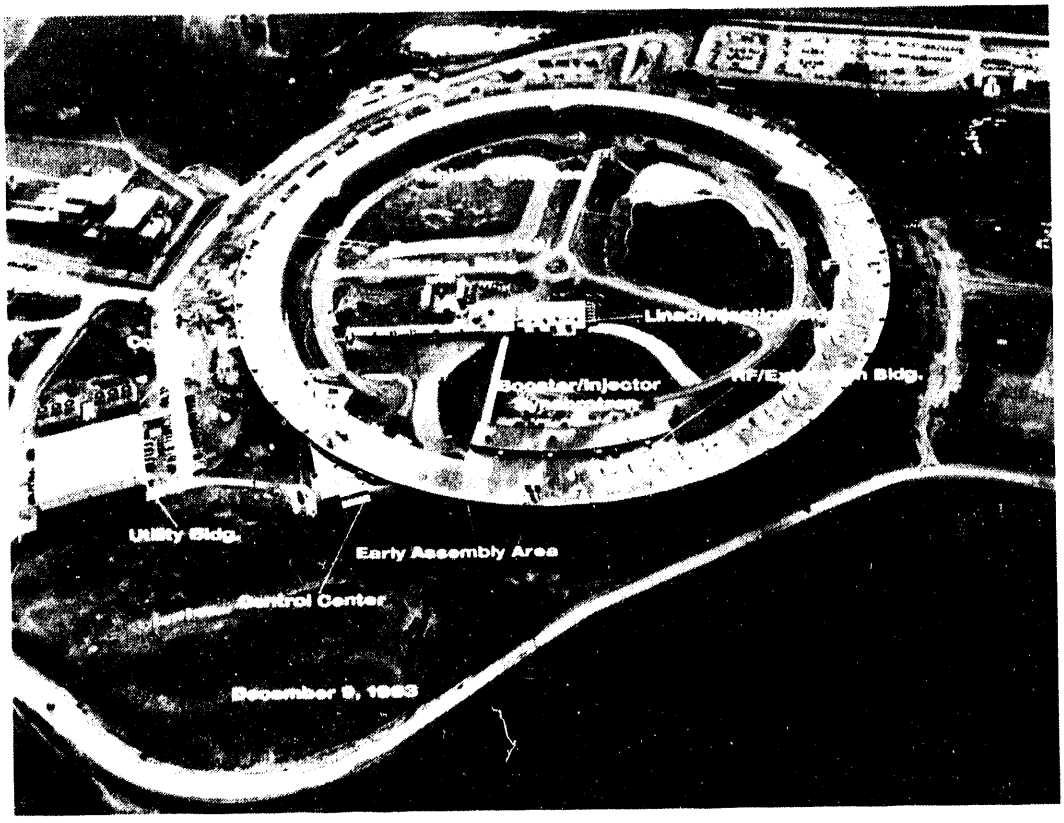

Figure 4. *View of the Advanced Photon Source (APS) at Argonne - 1993.*

3. Future opportunities at the Advanced Photon Source and other third generation synchrotron light sources.

It should be noted that following the on-going experimental efforts on the σ^{++}/σ^{+} as well as absolute cross section measurements, the next phase experimental developments should include increasingly differential detections of electrons, ions and Compton photons involving coincidence as well as angular distributions. Electron-electron angular correlation measurements may shed light to the respective roles of various interaction diagrams in the MBPT approach. The list of possibilities include measurements of, electron kinetic energy distribution, electron angular distribution, electron-electron coincidence (angular correlations), electron-ion coincidence, photon-electron coincidence, photon-ion coincidence.

Clearly not all of them are currently feasible, especially in the x-ray region. In the uv region, measurements of energy and angle-resolved double photoionization in helium was achieved recently (Schwartzkopf et al. 1993). At the ANL/NIST X-24a beam line of NSLS, x-ray ring, some highly differential measurements on Ar K-edge region with its much greater cross section have been made on Auger electron photoion coincidence (Levin et al. 1989) and electron photon coincidence (LeBrun et al.1993). Very roughly speaking, the 5 orders of magnitude decrease in cross section for He in the x-ray region can be at least partially compensated by the 4 or 5 order of magnitude increase in photon beam intensity compared to X-24A, by utilizing the undulator sources of the Advanced Photon Source (APS) currently under construction at Argonne shown on figure 4. It is our hope to see such experimental research flourish at the new light source.

Also important would be the extension to similar measurements of the isoelectronic sequence H-, Li^{+}, Be^{++}, etc. to follow the nuclear charge dependence. Since these ionic targets will be even more tenuous than the neutral He target, many of the interesting measurements will depend on the availability of the very high photon flux from the insertion devices of the new third generation synchrotron light sources.

REFERENCES

*Work supported by the U.S. Department of Energy, Office of Basic Energy Sciences under contract No. W-31-109-ENG-38.

Åberg T., 1970 Phys. Rev. **A2** 1726.
Amusia M.Ya., Drukarev E.G., Gorshkov V.G., and Kazachkov M.P., 1975 J. Phys. **B 8** 1248
Andersson L.R., and Burgdörfer J., 1993 Phys. Rev. Lett. **71** (1) 50.
Bartlett R.J., Walsh P.J., He Z.X., Chung Y., Lee E.-M, and Samson J.A.R., 1992 Phys. Rev. **A46** (9) 5594
Bearden A.J., 1966, J. Appl. Phys. **37**, 1681.
Berrah N., Heiser F., Wehlitz R., Levin J.C., Whitfield S.B., Viefhaus J., Sellin I.A., Becker U.,

1993, Phys. Rev. **A 48** (2) R1292.
Brown R.L. 1970, Phys. Rev. **A 1** 586.
Byron F.W. and Joachain C.J., 1967, Phys. Rev. **164** 1
Carlson T.A. 1967 Phys. Rev. **156**, 142.
Carter S.L. and Kelly H.P., 1981, Phys. Rev. **A 24** 170
Cooper J.W., Fano U. and Prats F. 1963, Phys. Rev. Lett. **10** 518
Dalgarno A. and Sadeghpour H.R. 1992, Phys. Rev. **A 46**, (7) R3591
Domke M., Xue C., Puschmann A., Mandel T., Hudson E., Shirley D.A., Kaindl G., Greene C.H., Sadeghpour H.R., and Peterson H. 1991, Phys. Rev. Lett. **66** 1306.
Domke M., Remmers G., and Kaindl G. 1992 Phys. Rev. Lett. **69** 1171.
Fano U. 1983 Rep. Prog. Phys. **49** 97.
Herrick D.R. and Sinanoglu O., 1975, Phys. Rev. **A 11** 97.
Hino K., Phys. Rev. 1993a, **A 47** (6) 4845.
Hino K., Ishihara T., Shimizu F., Toshima N, and McGuire J.H., 1993b, Phys. Rev. **A 48** 1271.
Ishihara T., Hino K., and McGuire J.H., 1991 Phys. Rev. **A 44**, R6980
Kornberg M.A. and Miraglia J.E., 1993, Phys. Rev. **A 48** (5), 3714.
LeBrun T., 1993, private communications.
Levin J.C., Biedermann C., Keller N., Liljeby L., O C.-S., Short R.T., Sellin I.A., 1990, Phys. Rev. Lett. **65** (8), 988.
Levin J.C., Lindle D.W., Keller N., Miller R.D., Azuma Y., Berrah Mansour N., Berry H.G., Sellin I.A., 1991, Phys. Rev. Lett. **67** (8), 968.
Levin J.C., Sellin I.A., Johnson B.M., Lindle D.W., Miller R.D., Berrah N., Azuma Y., Berry H.G., and Lee D.-H. 1993, Phys. Rev. **A 47** (1) R16.
Lin C.D., 1984, Phys. Rev. **A 29** 1019.
Madden R.P. and Codling K. 1963, Phys. Rev. Lett. **10** 516
Marr G.V. and West J.B., 1976, Atomic and Nuclear Data Tables **18**, 497.
McCrary J.H., Looney L.D., Atwater H.F., 1970, J. Appl. Phys. **41**, 3570.
McGuire J.H. 1984, J. Phys. **B 17** L779.
Samson J.A.R., 1990, Phys. Rev. Lett. **65**, 2861.
Samson J.A.R., R.J. Bartlett, and He Z.X., 1992, Phys. Rev. **A 46** (11) 7277.
Samson J.A.R., Greene C.H., Bartlett R.J. 1993, Phys. Rev. Lett. **71** (1) 201.
Schwarzkopf O., Krassig B., Elmiger J., Schmidt V., 1993, Phys. Rev. Lett. **70** (20) 3008.
Teng Z. and Shakeshaft R., 1993, Phys. Rev. **A 47** (5) R3487.
Veigele W.J., 1973, Atomic Data Tables **5**, 51.

Overview and comparison of photoionization with charged particle impact

James McGuire

Department of Physics, Tulane University, New Orleans LA

Neither birth nor death nor most of the processes in between can best be described in terms of the transition of a single electron.

The interesting puzzles of the human universe have not all yet been solved.

Abstract

What are the mechanisms for the two electron transitions in fast collisions of atoms with wavepackets of electromagnetic fields (charged particles and photons)?

Charge particles <==> Photons

- Charged particles and photons both carry $\boldsymbol{E}$ fields.
- $\boldsymbol{E}$ fields act via virtual photons.
- A charged particle is surrounded (or "dressed") by virtual photons.
- Virtual photons are not observable, and energy is not conserved within $\Delta\epsilon \geq \hbar/\Delta t$.

σ^{++} at high incident energies

Three bodies are required: hence it is a direct probe of few body physics.
High incident energy means that the collision time is very small, and hence not enough time to be very complicated.
This is one of the simplest dynamic few body problems.

Table I. $R=\sigma^{++}/\sigma^{+}$ in helium

Process	Ratio
Photoionization (total σ)	1.7×10^{-2} (±20%)
Ionization by $\gamma^{\pm}$, $e^{\pm}$ (total σ)	3×10^{-3} (±20%)
Ionization by N^{+7} (total σ)	1×10^{-2} (?)
Ionization by e^{-} (differential σ, small Q)	same as photons
Ionization by p^{+} (differential σ, binary encounter large Q)	2×10^{-2} (± 30%)
Ionization by neutral atoms (total σ)	?
Photoexcitation to n=2 (total σ)	5%
Excitation by $p^{\pm}$, $e^{\pm}$ (n=2)	?
Capture	?
Transfer Ionization/Transfer	$2\text{-}4 \times 10^{-2}$ (?)

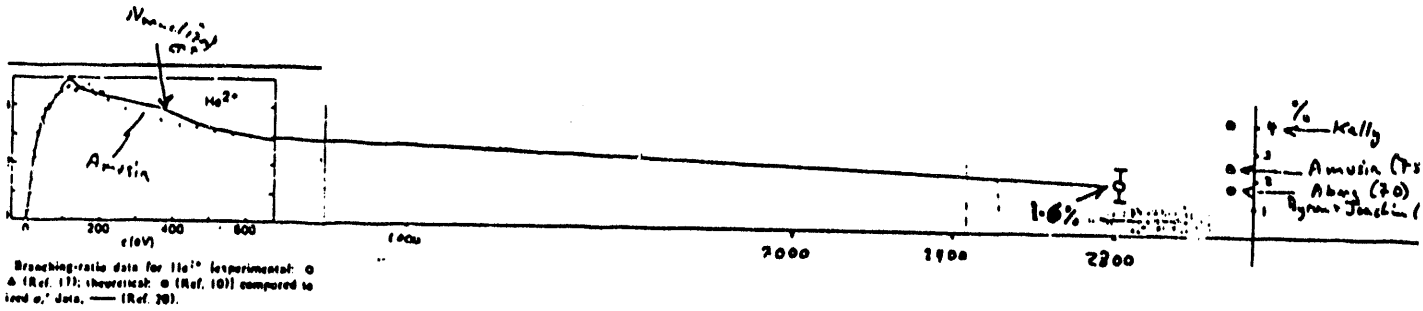

Figure 1. *The first high energy measurement (at 2.8 keV, by Levin et al, 1991).*

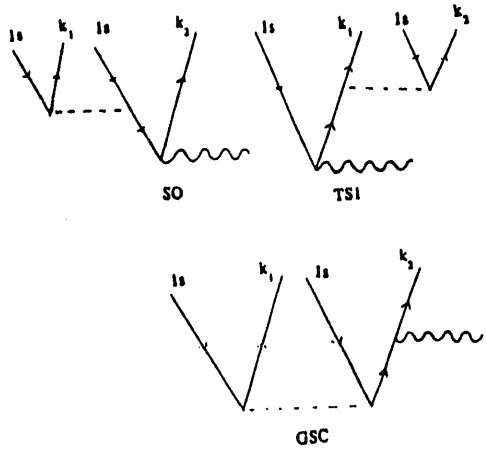

Figure 2. *Many body perturbation theory diagrams*

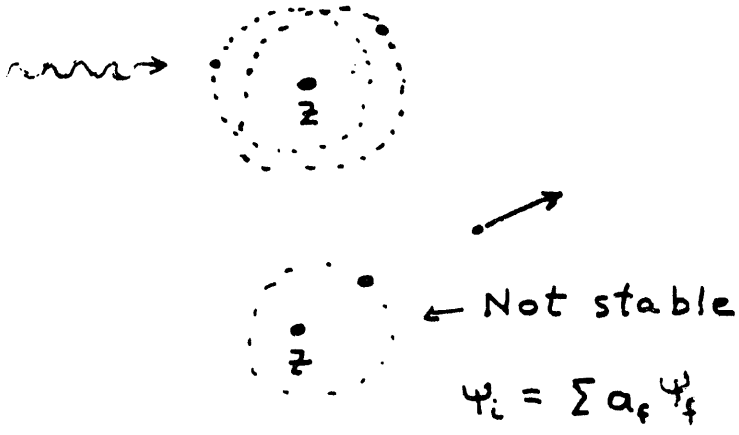

Figure 3. *Shakeoff.*

$$P_{shake} = |a_f|^2 = |\langle \psi_f | \psi_i \rangle|^2$$

$$\sigma^{++} = P_{shake} \cdot \tfrac{1}{2}\sigma^{+}$$

So that $$R_\gamma = \sigma^{++}/\sigma^{+} = \tfrac{1}{2}P_{shake}$$

But $\tfrac{1}{2}P_{shake}$ is too small.

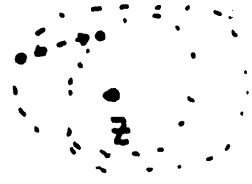

Figure 4. *Ground state correlation. Calculated by Byron and Joachain, and by Åberg => limit for* R = 1.7%; *and by Dalgarno => limit of 3.4%, late corrected to 1.7%.*

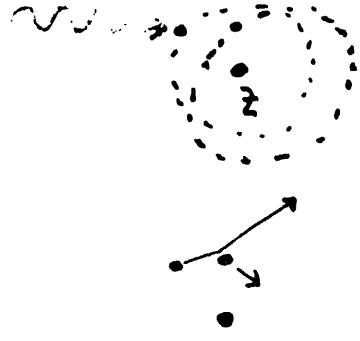

Figure 5. *Final state correlation. This two-step 1 (TS1) is not negligible (Amusia, Drukarev, Gorshkov, Kazachkov, lowest order Feynman diagrams) give limit* R = *2.3%. Also calculated by Carter and Kelly.*

Mechanisms for σ^{++}

Shakeoff and Ground state correlation are needed.
As regards TS1, Byron and Joachain, Åberg, Dalgarno, and Amusia et al claim it is unnecessary; while Carter and Kelly, and Ishihara et al claim it is essential. Both groups now agree that the asymptotic limit for the charge state ratio is close to 1.6%.

It seems unlikely that TS1 is both unnecessary and essential.

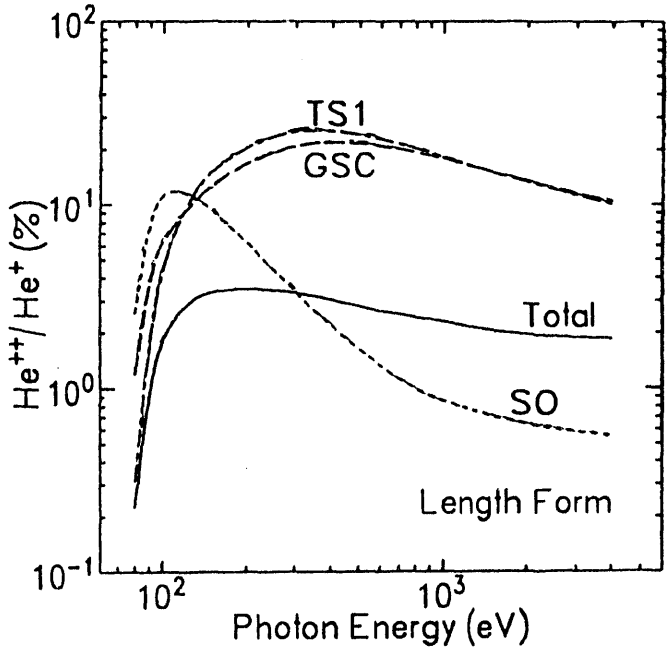

Figure 6. *Individual contributions to the charge state ratio, from the calculations of Hino, Ishihara and McGuire; using the length form of the operators.*

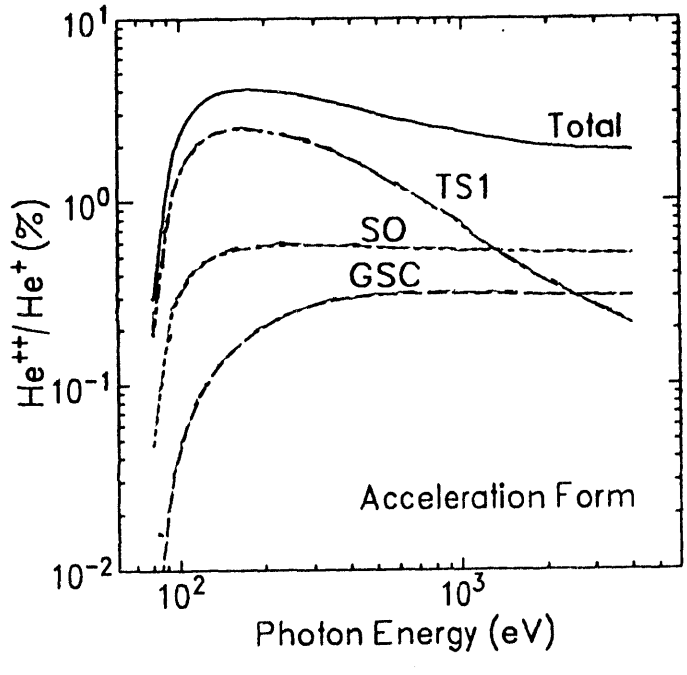

Figure 7. *Individual contributions to the charge state ratio, from the calculations of Hino, Ishihara and McGuire; using the acceleration form of the operators.*

Notes from figures 6 and 7: ==>

- The MBPT amplitudes vary with L, V and A forms (or gauges).
- The sum of all first order MBPT terms is form *independent* (Thank goodness!).
- The MBPT terms have no consistent meaning as mechanisms of double ionization unless one defines the form of the dipole interaction.
- All potentials vary with gauge. (This question arises in any approximate scattering calculation.)
- In the Coulomb gauge (dipole form) the interaction between two charged particles is given by Z_1Z_2/R.

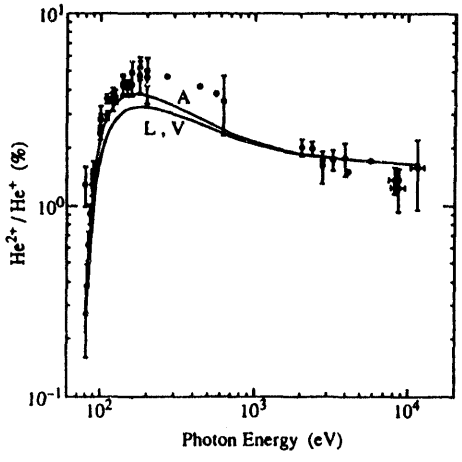

Figure 8. *Comparison of theory with experiment for the charge ratio.*

As pointed out in the papers of Samson, Bartlett and Greene, and Andersson and Burgdörfer, the photoionization cross-section at high energy should be proportional to the (-7/2) power of the photon energy. However, this decrease turns into a constant at high energy as the influence of Compton scattering comes into play, as observed in the data of Azuma et al.(shown schematically in Figure 9.

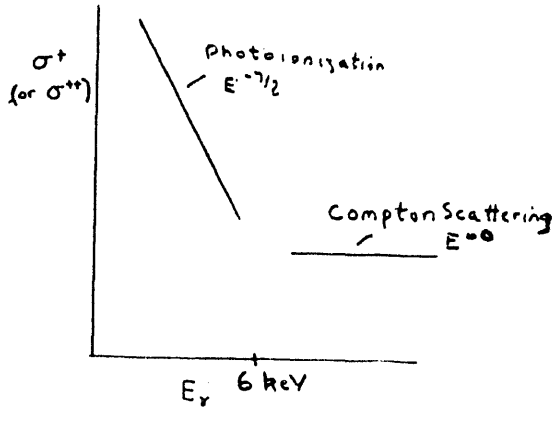

Figure 9. *Schematic variation of helium photoionization cross sections.*

The differences between photoionization and Compton scattering

- $p \cdot A \neq A^2$.
- no final $\gamma \neq \int d\Omega_\gamma$.
- dipole terms ≠ non-dipole terms.

First order scattering amplitudes

Compton: $f_C \sim < f|e^{i(\vec{k}_i - \vec{k}_f)\cdot\vec{r}}|i >$

Charged particles: $f_Z \sim < f|e^{i(\vec{k}_i - \vec{k}_f)\cdot\vec{r}}|i >$

Cross sections for both Compton scattering and scattering by fast charged particles are expressed in terms of the Generalized Oscillator Strength (GOS).

Relation of Compton to charge particle scattering

$$\frac{d\sigma_C}{dQ} = \frac{r_{cl}^2}{a_0^2}\frac{v^2}{8k_i^2 Z^2}\left(1 + \left(\frac{k_i^2 + k_f^2 - Q^2}{2k_i k_f}\right)^2\right) Q^4 \frac{d\sigma_Z}{dQ}$$

- This is valid for arbitrary final states, |f>, including both single and double ionization.
- This could be tested experimentally by observing differential cross sections for Compton scattering and comparing them to existing data for differential cross sections by charged particle impact weighted by the factors in the above relation.
- This may also be used to evaluate cross sections for Compton scattering by modifying existing computer codes for single and double ionization by charged particle impact.

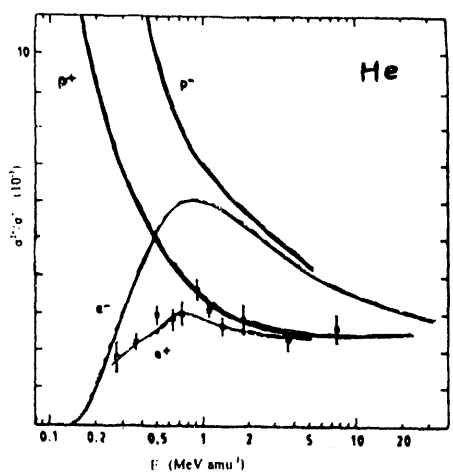

Figure 10. *Charge ratio from charged particle impact.*

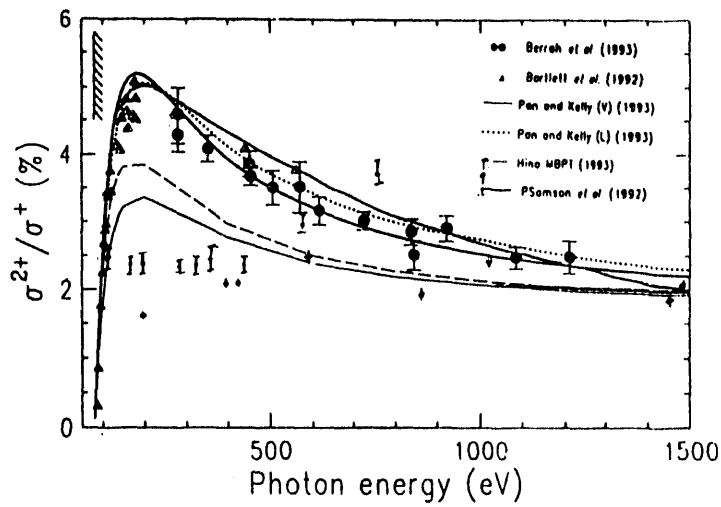

Figure 11. *Charge ratio from photon impact.*

Relationship between Z and γ in first order

Photons annihilate and give their energy to the ejected electron. Charged particles do not annihilate and give a distribution ρ of ejected electron energies ϵ.

At a fixed electron energy ϵ:

$$\frac{d\sigma_Z}{d\epsilon} = \frac{Z^2}{2\pi\alpha}\frac{\ln v^2}{v^2}\frac{\sigma_\gamma(\epsilon)}{\epsilon}$$

After integration over the density of final states $\rho(\epsilon)$,

$$R_Z = \int_{I++}^{\infty} R_\gamma(\epsilon)\ \rho^+(\epsilon)\ d\epsilon$$

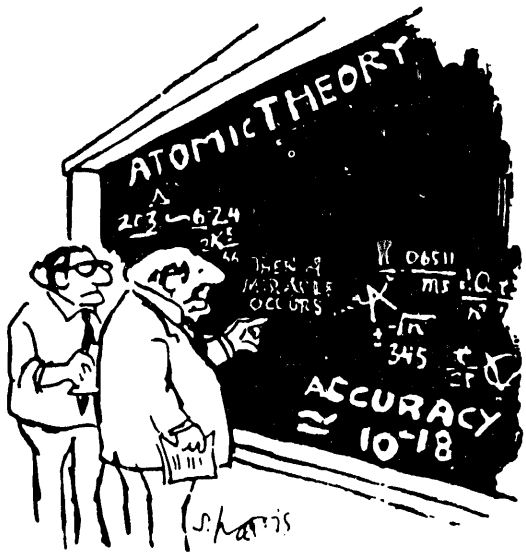

Figure 11. *"I think you should be more explicit here in step two."*

Second order processes

- Direct double excitation, excitation-ionization, ... by a charged particle
- Direct double ionization, et al.... by one photon.
- Auger transitions
- Autoionization
- Raman scattering
- Compton scattering
- Thomas processes for mass (and charge) transfer.

Interpretation of second order scattering

$$P(\mathbf{B}) = |a(\mathbf{B})|^2$$

$$a(\mathbf{B}) = lim_{t\to\infty} < \psi_f|\psi_i(t) >$$

$$= < f|\ U(+\infty,-\infty)\ |i >$$

$$= < f|T \exp\left(-i\int_{-\infty}^{+\infty} V(t)dt\right)|i >$$

$$= -i\int_{-\infty}^{+\infty} e^{i(\epsilon_f-\epsilon_i)t_1} < \bar{f}|\ V(t_1)|\bar{i} > dt_1$$

$$+\frac{(-i)^2}{2!}\int_{-\infty}^{+\infty} dt_2 \int_{-\infty}^{+\infty} dt_1 e^{-i\epsilon_f t_2} \sum_{\bar{I}}$$

$$[< \bar{f}|V(t_2)|\bar{I} > e^{-i\epsilon_I(t_2-t_1)} < \bar{I}|V(t_1)|\bar{i} >$$

$e^{-i\epsilon_i t_1}$ + higher order terms.

$$\frac{T}{2}e^{-i\epsilon(t_2-t_1)}$$

$$= \Theta(t_2-t_1)e^{-i\epsilon(t_2-t_1)}$$

$$= \frac{i}{2\pi}\int_{-\infty}^{+\infty} e^{-i\omega(t_2-t_1)}\frac{1}{\omega-\epsilon+i\eta}d\omega$$

$$= \frac{i}{2\pi}\int_{-\infty}^{+\infty} e^{-i\omega(t_2-t_1)}\left\{-i\pi\delta(\omega-\epsilon) + \mathcal{P}\frac{1}{\omega-\epsilon}\right\}d\omega$$

$$= \frac{1}{2}[\ 1 + (T-\bar{1})\ ]e^{-i\epsilon(t_2-t_1)}$$

no time ordering — time ordering

- Determines the shape of resonance profiles.
- Interferes with the space correlation first order term in double electron transitions (Z^3 term).
- Can be large - half of total counting rates.

Meaning of T-1

- Energy **non**-conserving - from $\omega \neq \epsilon$.
- Reduces to zero when $\hbar \to 0$ or $\Delta\epsilon \to \infty$.
- Has no classical analogue.
- Measures correlation in time: *Prop - < Prop >*
- Obeys a dispersion relation - is equal to an integral over the classical, energy-conserving, non-time ordered term.
- Is 90 degrees out of phase with the classical, energy-conserving, non-time ordered term.

SUMMARY

- Z and γ carry EM fields.
- (T-1) → energy non-conservation, purely quantum, time correlation Z^3 effects.
- The MBPT terms have no consistent meaning as mechanisms of double ionization unless one defines the form of the dipole interaction.
- Compton scattering differs from photoannihilation, but may give a similar charge ratio ***R***. Why is not clear.

The ratio of double to single ionization of helium: the relationship of photon and bare charged particle impact ionization

Steven T. Manson

Dept. of Physics and Astronomy, Georgia State University, Atlanta, Georgia 30303, USA

Consider the photoionization of the He atom in its ground, $1s^2\,{}^1S$, state. The cross section for each ionization channel shall be termed $\sigma^j_{\gamma,i}(h\nu)$, where i=1 or 2, the charge state of the final ion, j designates the rest of the quantum numbers defining the ionization channel, and $h\nu$ is the photon energy. The ratio of double to single ionization of He by photons is thus given by

$$R_\gamma(h\nu) = \frac{\sum_j \sigma^j_{\gamma,2}(h\nu)}{\sum_j \sigma^j_{\gamma,1}(h\nu)} \,. \qquad (1)$$

The channels in the sum for single ionization are all of the $n\ell\epsilon\ell'\,{}^1P$ final states, i.e., the He^+ ion left in its ground state or any discrete excited state. For double ionization the possible final channels are the $\epsilon\ell\epsilon'\ell'\,{}^1P$ states subject to the conservation of energy, $h\nu = \epsilon+\epsilon'+I_2$, where I_2 is the double ionization potential; actually then, the sum over channels in the denominator of Eq.(1) is really an integral over the possible energy sharings of the two ejected electrons plus a sum over the possible angular momenta of the individual electrons. It must be realized, however, that the designations of various states referred to signify only the configuration with the largest coefficient in a CI expansion. In fact, without CI, neither the double ionization process, nor the ionization plus excitation, would be possible since the transition operator for photoionization (in any of its forms) is a sum of single-particle operators; under the action of such an operator, two electrons changing state are not possible. The major contributions to the double ionization cross section arise from $1s\epsilon s\,{}^1S$ and $(n,\epsilon)s\epsilon's\,{}^1S$ mixing with the dominant $1s^2\,{}^1S$ configuration of the initial state, and $1s\epsilon p\,{}^1P$ mixing with the dominant $\epsilon s\epsilon'p\,{}^1P$ configuration of the final state.

For later use, it is of interest to cast the ratio in terms of differential oscillator strength, i.e.,

$$\sigma^j_{\gamma,i} \equiv 4\pi^2\alpha a_0^2 \frac{df^j_i(\Delta E)}{d(\Delta E)} \qquad (2)$$

where α is the fine structure constant, a_0 is the Bohr radius, and ΔE (=$h\nu$) is the energy transferred to the atom. In terms of the oscillator strength, then, the double to single

photoionization ratio [Eq. (1)] can be written as

$$R_\gamma(h\nu) = \frac{\sum_j df_2^j(\Delta E=h\nu)/d(\Delta E)}{\sum_j df_1^j(\Delta E=h\nu)/d(\Delta E)} \quad . \tag{3}$$

Now consider the single and double ionization of He by fast bare charged particles of charge z, mass M and velocity v. Define the reduced incident energy $T = \frac{1}{2}mv^2$, where m is the electron mass. The cross section for each ionization channel, differential in the energy transfer ΔE, will be written as $d\sigma^{j,T}_{i,z,M}(\Delta E)/d(\Delta E)$, where i and j are as in the photoionization case. The ratio of double to single ionization by charged particles, as a function of energy transfer ΔE is, thus given by

$$R^T_{z,M}(\Delta E) = \frac{\sum_j d\sigma^{j,T}_{2,z,M}(\Delta E)/d(\Delta E)}{\sum_j d\sigma^{j,T}_{1,z,m}(\Delta E)/d(\Delta E)} \quad . \tag{4}$$

The sums in Eq.(4) are over all channels, just as in Eq.(1). It is important to note that for charged particle impact, charge transfer processes can also produce singly and doubly charged target ions. The cross sections dealt with here are only for the ionization process, however.

For reasonably high incident energy of the charged particle, the first Born approximation is applicable [1]. Furthermore, for small energy transfer, the Born cross section can be expanded in T, the reduced incident energy, as [1]

$$\frac{d\sigma^{j,T}_{i,z,M}(\Delta E)}{d(\Delta E)} = \frac{4\pi a_0^2 z^2}{T/R}\left[\left(\frac{R}{\Delta E}\right)\frac{df_i^j(\Delta E)}{d(\Delta E)}\ln\left(\frac{4T}{R}\right)+B_i^j(\Delta E)\right]+O\left(\frac{R^2}{T^2}\right) \tag{5}$$

where R = 13.6 eV and $B_i^j(\Delta E)$ is a function of target properties only. When $\Delta E/T \ll 1$, retaining only the first two terms of Eq.(5) is an excellent approximation. In such a case, the ratio of Eq.(4) is independent of z and M, the charge and mass of the incident projectile, and can be written as

$$R^T(\Delta E) = \frac{\sum_j \left[(R/\Delta E)df_2^j(\Delta E)/d(\Delta E)\ln(4T/R)+B_2^j(\Delta E)\right]}{\sum_j \left[(R/\Delta E)df_1^j(\Delta E)/d(\Delta E)\ln(4T/R)+B_1^j(\Delta E)\right]} \tag{6a}$$

$$= R_\gamma(\Delta E)\frac{1+\sum_j B_2^j(\Delta E)/\sum_j [(R/\Delta E)df_2^j(\Delta E)/d(\Delta E)\ln(4T/R)]}{1+\sum_j B_1^j(\Delta E)/\sum_j [(R/\Delta E)df_1^j(\Delta E)/d(\Delta E)\ln(4T/R)]} \qquad (6b)$$

$$= R_\gamma(\Delta E)F(\Delta E,T) \ . \qquad (6c)$$

Now the function $F(\Delta E,T)$ is of order unity, but the details are target-dependent. In the limit of such high T that ln(4T/R) becomes large enough to allow the second term in the numerator and the denominator of Eq.(6b) to be neglected, i.e., $F(\Delta E,T)\rightarrow 1$, one obtains the simple relation

$$R^T(\Delta E) = R_\gamma(\Delta E) \qquad (7)$$

independent of T. In this limit then, the ratio of double ionization to single charged particle impact ionization at a particular energy loss, ΔE, is independent of the incident particle velocity (energy), mass or charge and equal to the ratio for photon impact at photon energy $h\nu = \Delta E$. It is important to emphasize that the charged particle ratio that is related to the photoionization is for a **fixed** energy transfer, ΔE, for both the single and double ionization process. This is **not** the same thing as a ratio of electrons of a given energy resulting from the single and double ionization by charged particle impact.

Up to this point, we have considered only non-relativistic kinematics. It is of interest, however, to inquire as to what modifications are introduced if the incident charged particle is relativistic. In the relativistic range, with T replaced by its definition ($\frac{1}{2}mv^2$) and introducing $\beta=v/c$, Eq.(5) becomes [1]

$$\frac{d\sigma_{i,z,M}^{j,T}(\Delta E)}{d(\Delta E)} = \frac{8\pi a_0^2 z^2}{mv^2/R}\left[\left(\frac{R}{\Delta E}\right)\frac{df_i^j(\Delta E)}{d(\Delta E)}\left\{\ln\left(\frac{2mv^2}{R}\right)-\ln(1-\beta^2)-\beta^2\right\}+B_i^j(\Delta E)\right]+O\left(\frac{1}{(8V)^4}\right)$$

where the essential difference from Eq.(5) is the addition of the two β-dependent terms; thus, the ratio of Eq.(6b) is modified to

$$R_T(\Delta E) = R_\gamma(\Delta E)\frac{1+\sum_j B_2^j(\Delta E)/\sum_j [(R/\Delta E)df_2^j(\Delta E)/d(\Delta E)\{\ln(2mv^2/R)-\ln(1-\beta^2)-\beta^2\}]}{1+\sum_j B_1^j(\Delta E)/\sum_j [(R/\Delta E)df_1^j(\Delta E)/d(\Delta E)\{\ln(2mv^2/R)-\ln(1-\beta^2)-\beta^2\}]} \qquad (9)$$

where the only change is seen to be the replacement of $\ln(4T/R)$ by $\ln(2mv^2/R)-\ln(1-\beta^2)-\beta^2$.

Thus, relativistic incident charged particles do not alter the non-relativistic results is any significant way; at high enough incident energy, Eq.(7) still holds.

For large energy transfer, where $\Delta E/T$ is no longer small compared to unity, the Bethe-Born expansion no longer valid, but the Born approximation is still applicable. In such a case, the dipole part of the interaction no longer dominates; in fact it contributes only a relatively small amount to the cross section. Thus many final states other than the optically allowed states discussed above are allowed and important correlations, configurations which mix with the main configuration, differ in detail from the photon case. Thus, while one would expect effects of the same order of magnitude, there is no direct relationship between the photon case and the charged particle case when $\Delta E/T$ is not small. However, recent experimental data [2], shown in Fig. 1, seems to suggest that even in the large energy transfer range, the ratio of double to single ionization of He is substantially the same as the photon case.

The ratio of total single and double ionization cross sections of He, integrated over energy transfer, ΔE, for incident bare charged particles can, however, be related to the photon ratio. This is because these total cross sections are dominated by the small energy transfer region where there is a relationship to the photon case, as has been shown above. The ratio can be written as

$$R^T_{z,M} = \frac{\sigma^T_{2,z,M}}{\sigma^T_{1,z,M}} = \frac{\sum_j \int [d\sigma^{j,T}_{2,z,M}(\Delta E)/d(\Delta E)]d(\Delta E)}{\sum_j \int [d\sigma^{j,T}_{1,z,m}(\Delta E)/d(\Delta E)]d(\Delta E)} \quad . \qquad (10)$$

Using Eq.(4) then, this can be rewritten as

$$R^T_{z,M} = \frac{\sum_j \int [R^T_{z,M}(\Delta E) d\sigma^{j,T}_{1,z,M}(\Delta E)/d(\Delta E)]d(\Delta E)}{\sum_j \int [d\sigma^{j,T}_{1,z,m}(\Delta E)/d(\Delta E)]d(\Delta E)} \quad . \qquad (11)$$

Thus, the total cross section ratio is a weighted average of the differential cross section ratio, the weighting factor being the differential cross section for single ionization over the total cross section for single ionization. Of crucial importance in Eq.(11) is the fact that although the lower limit of integration is ΔE = 24.58 eV, the ionization potential of He, the ratio $R^T_{z,M}(\Delta E)$ in the integral in the numerator of Eq.(11) is **zero** below the double ionization potential of He, ΔE = 79.98 eV. Then, since most of the total single ionization cross section comes from the small ΔE region, it is evident that the ratio of Eq.(11), the weighted average, will be much smaller than $R_{z,M}(\Delta E)$ of Eq.(4) because of the heavy weighting of the ΔE region where $R^T_{z,M}(\Delta E)$ vanishes.

If the incident energy is great enough so that Eqs.(6) apply, Eq.(11) becomes

$$R^{T}_{z,M} = \frac{\sum_{j} \int_{\cdot} [R_{\gamma}(\Delta E) F(\Delta E, T) d\sigma^{j,T}_{1,z,M}(\Delta E)/d(\Delta E)] d(\Delta E)}{\sum_{j} \int_{\cdot} [d\sigma^{j,T}_{1,z,m}(\Delta E)/d(\Delta E)] d(\Delta E)} \quad . \qquad (12)$$

Note that, strictly speaking, the integrand in the numerator of Eq.(12) is only correct for small $\Delta E/T$. However, since the contribution of small $\Delta E/T$ dominates the integral, i.e., the total single ionization cross section is dominated by low energy electrons, this is a very minor approximation. Finally, at high enough incident energies so that Eq.(7) applies, this ratio becomes

$$R^{T}_{z,M} = \frac{\sum_{j} \int_{\cdot} [R_{\gamma}(\Delta E) d\sigma^{j,T}_{1,z,M}(\Delta E)/d(\Delta E)] d(\Delta E)}{\sum_{j} \int_{\cdot} [d\sigma^{j,T}_{1,z,m}(\Delta E)/d(\Delta E)] d(\Delta E)} \qquad (13)$$

which depends only upon the photon ratio, $R_{\gamma}(\Delta E)$, and the shape of the differential single ionization cross section, i.e., the ratio of the differential single ionization cross section to the total single ionization cross section. This latter ratio approaches a limit for high enough T as can easily be demonstrated by the use of the Bethe-Born expansion. Thus, the ratio of total cross sections for double and single ionization, $R^{T}_{z,M}$ also approaches a limit for high enough T. That it approaches a limit is verified by the experimental data [3] presented in Fig. 2, which shows the ratio for a number of different charged particles over a broad range of energies. In addition, it is seen from Fig. 2 that the limit of the ratio of about 0.28 % is indeed much smaller than the asymptotic ratio for photoionization of 1.67 % [4], just as predicted above and previously [5].

References

1. M. Inokuti, Rev. Mod. Phys. **43**, 297 (1971) and references therein.
2. C. L. Cocke, R. Dorner, A.D. Gonzalez and E. Horsdal-Pedersen in XVIII ICPEAC: Abstracts of Contributed Papers, eds. T. Andersen, B. Fastrup, F. Folkmann and H. Knudsen (Aarhus, Denmark, 1993), Vol. II, p.845.
3. J. Ullrich, R. Moshammer, H. Berg, R. Mann. H. Tawara, R. Dorner, J. Euler, H. Schmidt-Bocking, S. Hagmann, C. L. Cocke, M. Unversagt, S. Lencinas and V. Mergel, Phys. Rev. Lett. **71**, 1697 (1993) and references therein.
4. K. Hino, T. Ishihara, F. Shimizu, N. Toshima and J. H. McGuire, Phys. Rev. **A 48**, 1271 (1993) and references therein.
5. J. H. McGuire, J. Phys. **B 17**, L779 (1984).

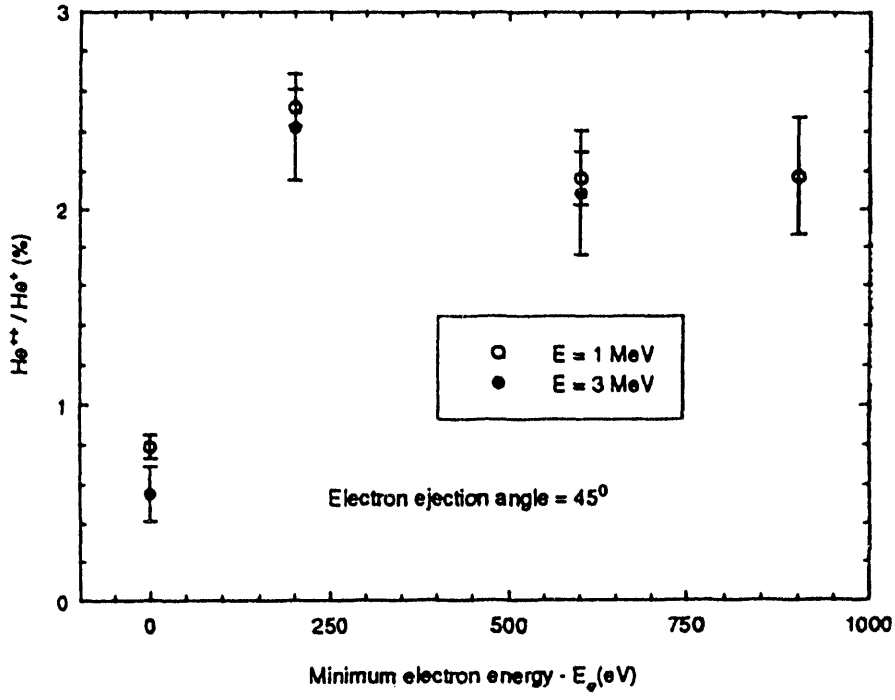

Figure 1. *Ratio of double to single ionization of He for events which generate electrons with energy exceeding a minimum value, for 1 and 3 Mev protons, from Ref. 2.*

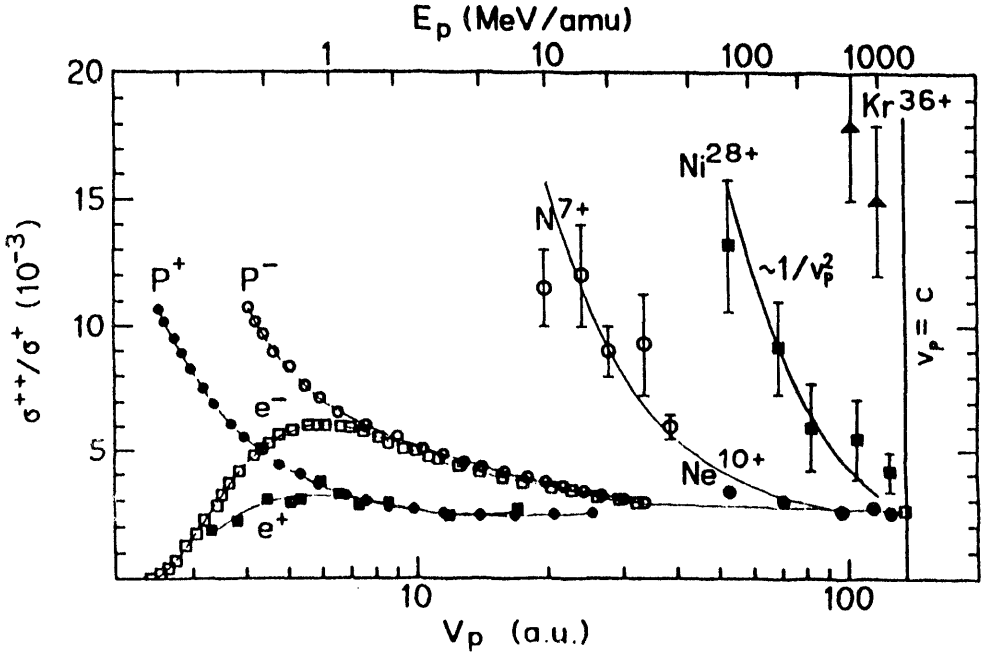

Figure 2. *Ratio of double to single ionization of He for different projectiles as a function of projectile velocity (lower scale) and energy (upper scale) from Ref. 3. The open square at the far right is for electron impact.*

Double photoionization of helium at high energies

Jon Levin

Department of Physics, University of Tennessee, Knoxville, Tennessee

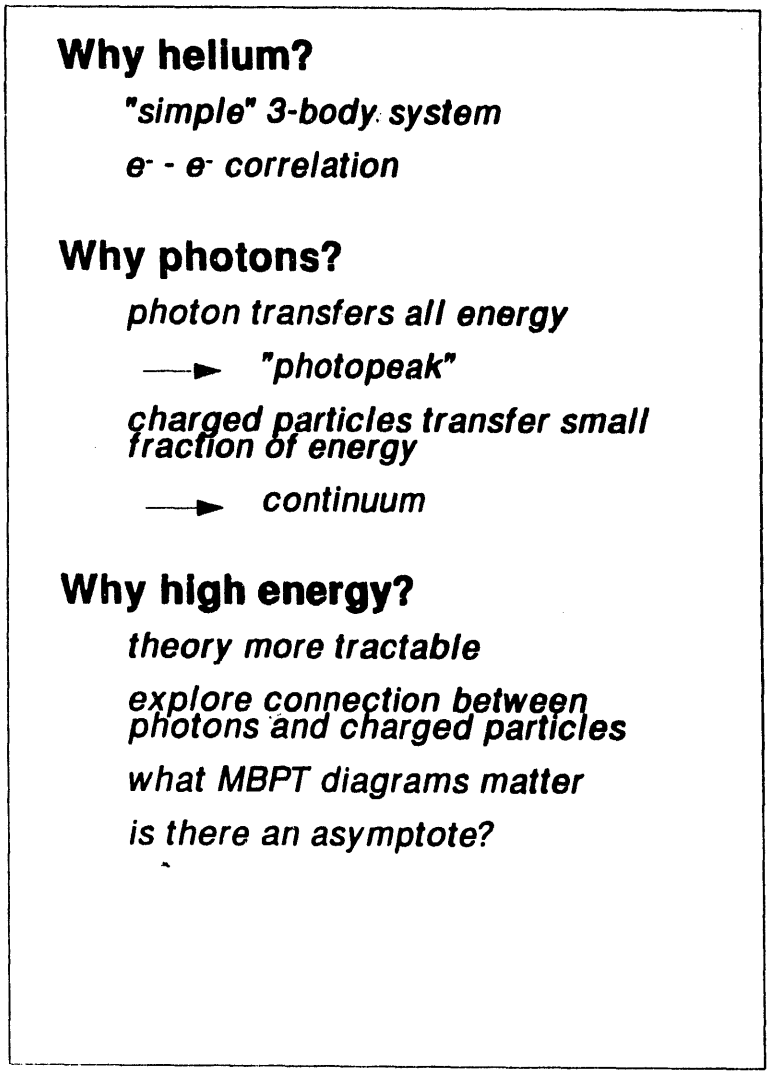

Figure 1. *The questions*

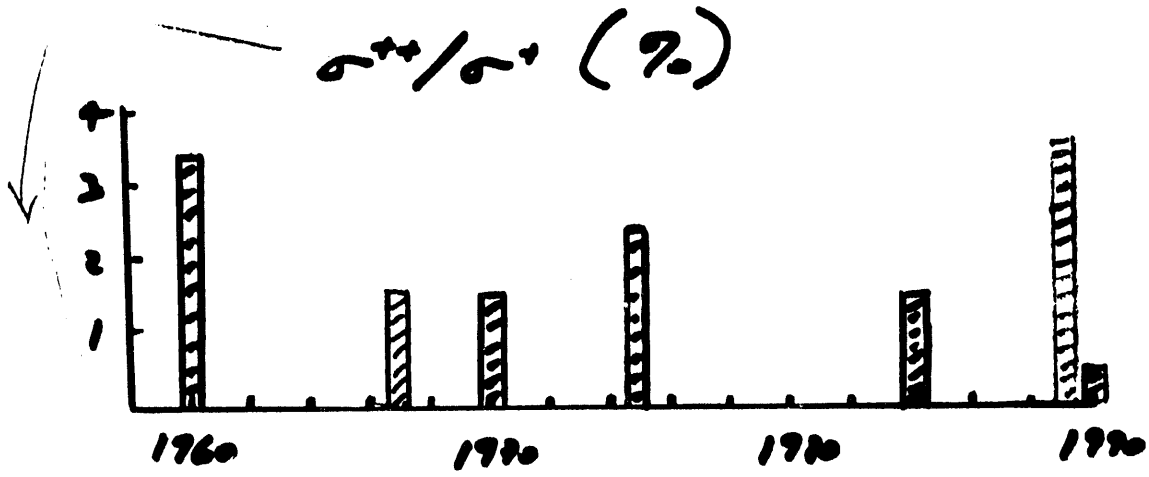

Figure 2. *Theoretical values for the asymptotic ratio: Dalgarno and Stewart (1960); Byron and Joachain (1967); Åberg (1970), Brown and Gould (1970); Amusia (1975); McGuire (1984); Hino, Ishihara and McGuire (1989); Samson (1990).*

In 1991, J.H. McGuire in Advances in Atomic, Molecular and Optical Physics, stated: "Of central importance is the value of the high energy photoionization ratio, which is not well determined".

In general. photoionization cross sections peak near threshold, while electron impact cross sections tend to peak at several times the electron binding energy. Hence photons are necessary for observations of threshold behavior.

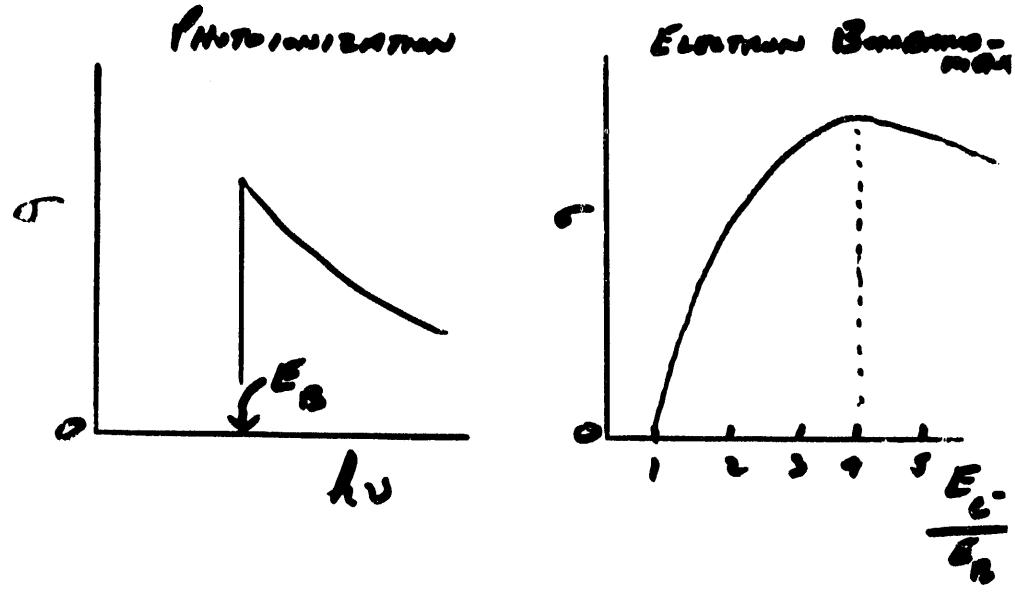

Figure 3. *Typical threshold behaviors*

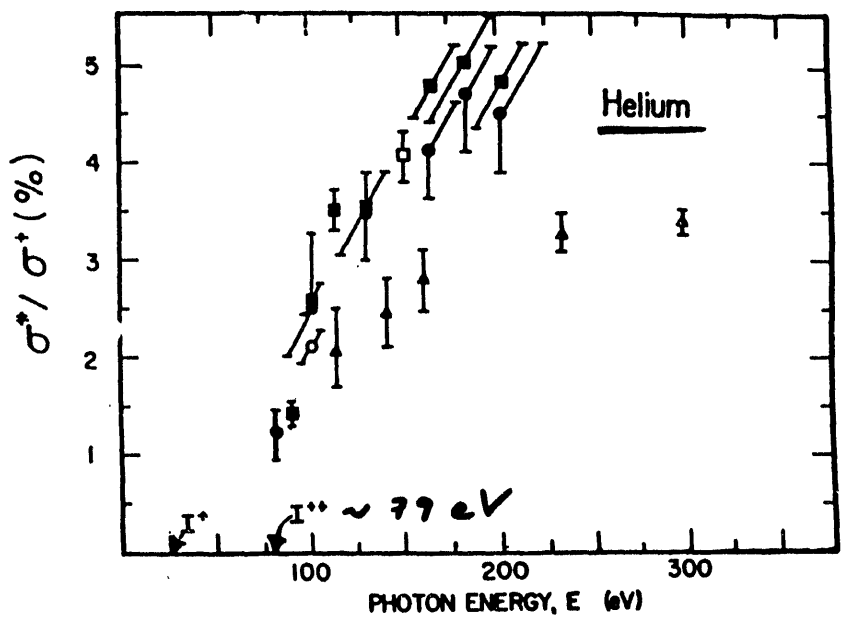

Figure 4. *Measurements of the double-to-single ionization ratio near threshold: T.A. Carlson Phys. Rev. 156, 142 (1967); Wight and Van de Wier, J. Phys. B 9, 1379 (1976); Holland, Codling, West and Mark, J. Phys. B 12, 2465 (1979),*

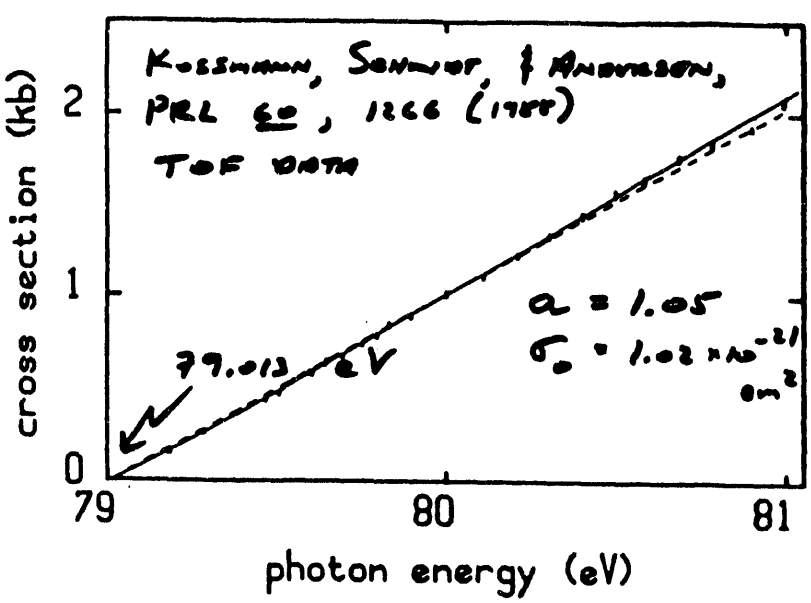

Figure 5. *Experimental confirmation of the Wannier theory near threshold:* $\sigma^{++}=\sigma_0 E^a_{Excess}$, *where* $a=1.056$ *for* $Z=2$, *and* $\sigma_0=\sigma^{++}$ *at* $E_{Excess}=1$ *eV.*

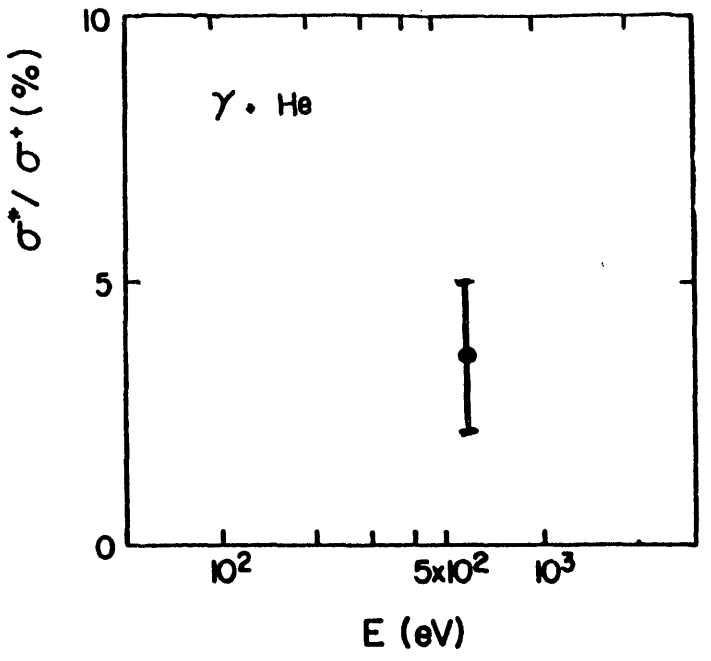

Figure 6. *All existing data above 300 eV photon energy for the ratio σ^{++}/σ^{+} before 1990. Data point from T.A. Carlson, Phys. Rev. 156, 143 (1967).*

Samson considers photoioinzation as being analogous to e^- ionization of He^+ [J.A.R. Samson, Phys. Rev. Lett. 65, 2861 (1990)]. This suggestion leads to a very low ratio $\boldsymbol{R}=\sigma^{++}/\sigma^{+}$ at 2.8 keV photon energy, and no asymptotic value. Thus, he obtains $\boldsymbol{R}$ = 1.2% at 2.8 keV, and $\boldsymbol{R}$ = 0.3% at 10 keV.

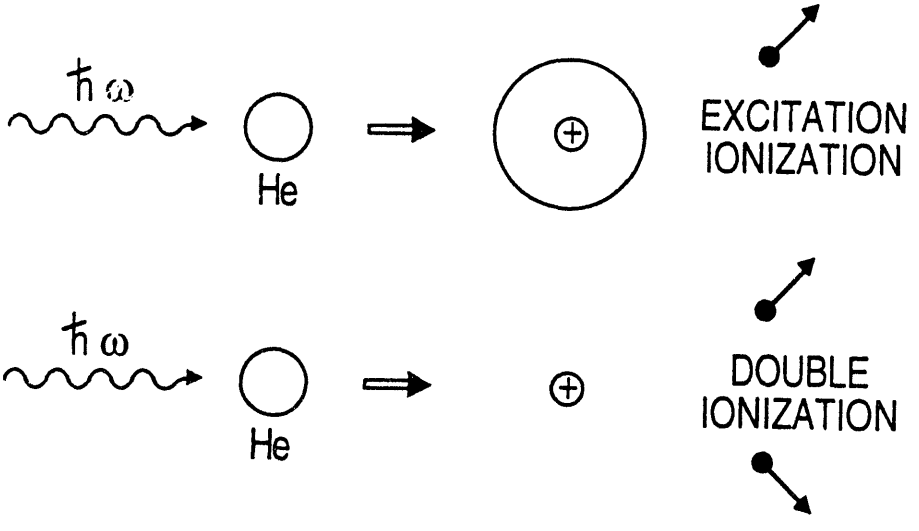

Figure 7. *Comparison of electron and photon ionization.*

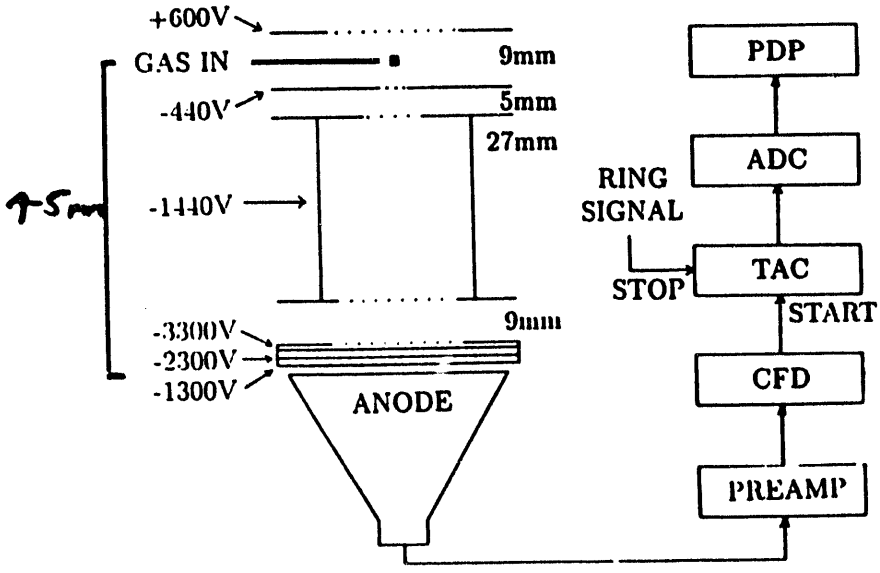

Figure 8. *Time-of-flight spectrometer used in experiments at X24A and X26C at NSLS, and at BESSY.*

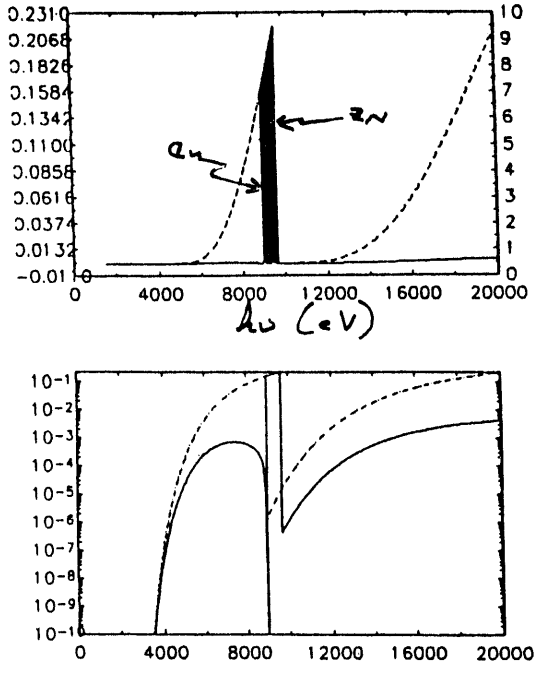

Figure 9. *Ross balanced filters*

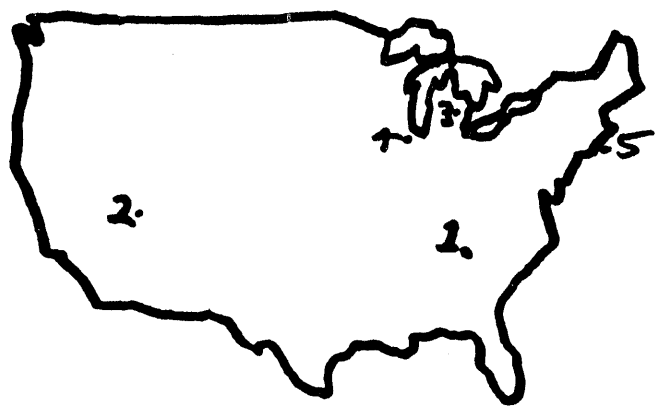

Figure 10. *Geographical distribution of authors: (1) N. Keller, R.D. Miller, I.A. Sellin, J. Levin (also at NIST), U. Tennessee, ORNL; (2) D.W. Lindle, UNLV; (3) N. Berrah, UWM (also ANL); (4) Y. Azuma, H.G. Berry, ANL; (5) B. Johnson, D-H. Lee, BNL.*

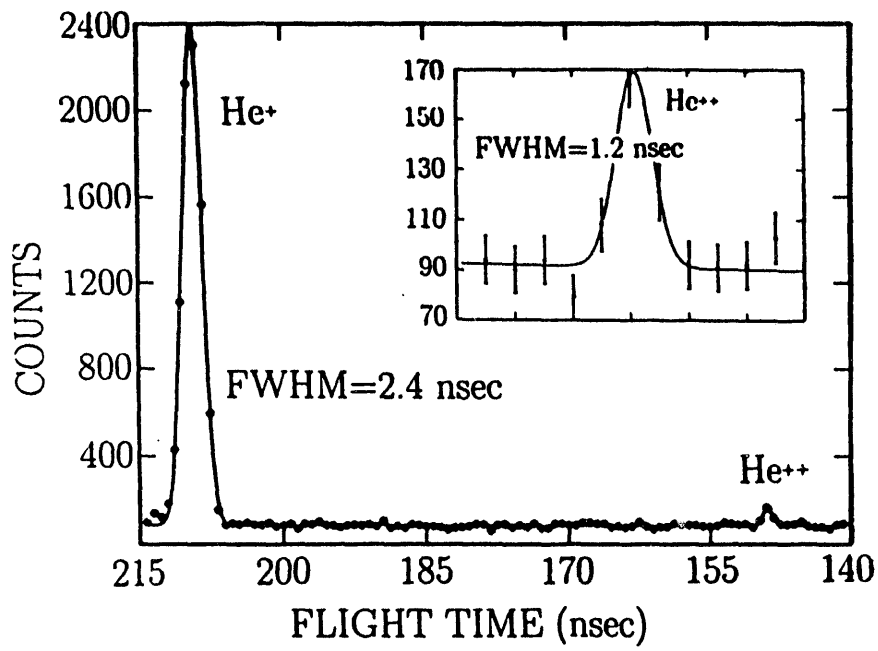

Figure 11. *Time-of-flight spectrum at 2.8 keV.*

The experiments utilize single bunch mode of the storage ring because:

1. No need to detect electrons: => fewer biases, since the two electrons have much different
2. Can use static fields, no pulsed electronics => narrower peaks

BUT only a few days of beam time available each year.

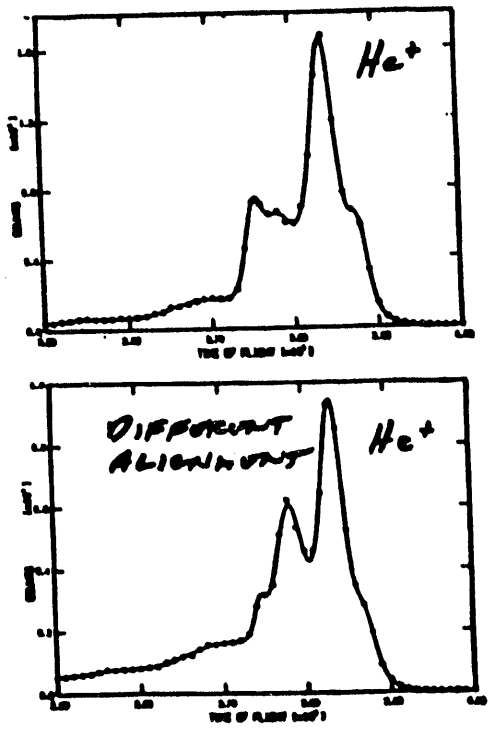

Figure 12. *Example of spurious production*

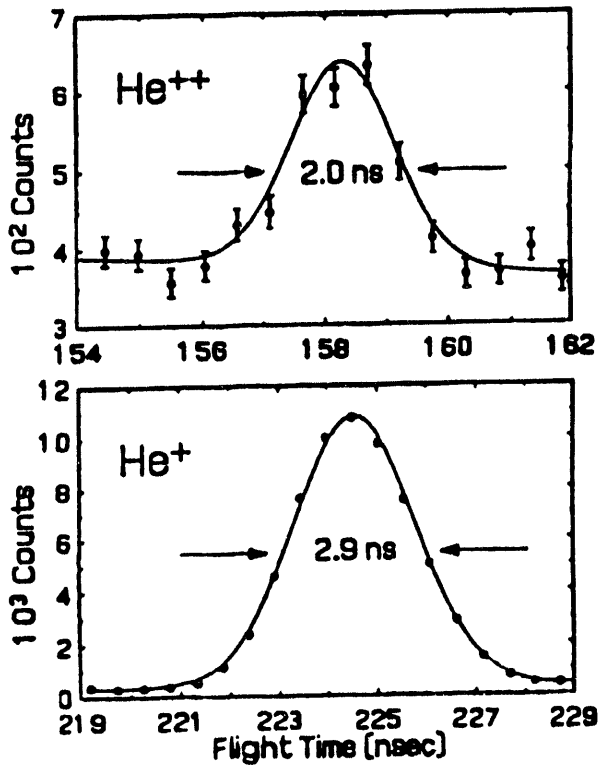

Figure 13. Observed peaks at 3.3 keV

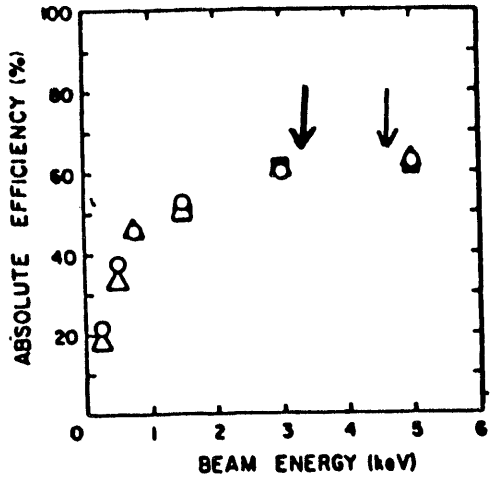

Figure 14. *Multichannelplate efficiency: For He^+, H^+, and O^+ ions, from Gao et al Rev.Scient.Instrum. 55, 1758 (1984)*

We obtained values for the production ratio He^{++}/He^+ = 1.6±0.3% at 3.2 keV per charge (Feb. 1991), and 1.6±0.5% at 4.7 keV per charge (Sept. 1991).

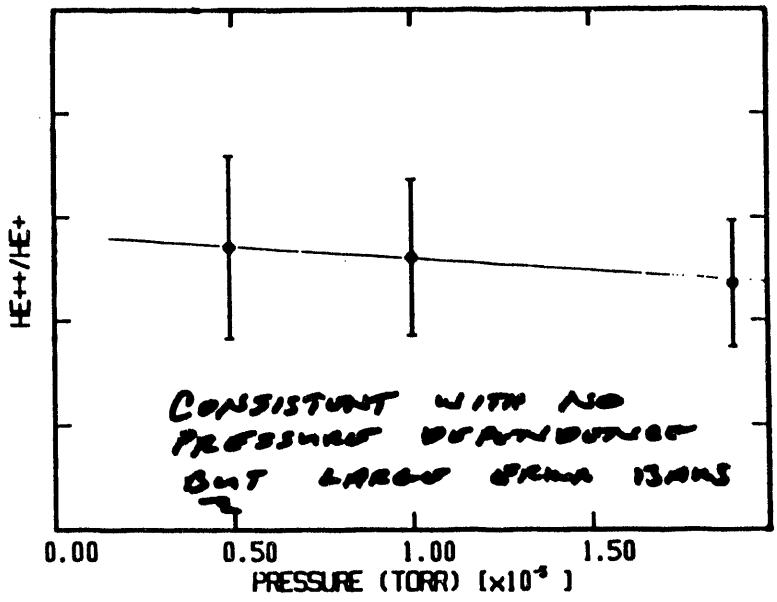

Figure 15. *The background pressure dependence. The results are consistent with no pressure dependence.*

The pressure dependence results can be compared with the results at threshold of Holland et al, J. Phys B 12, 2465 (1989): the flight times are 200 ns for these experiments (10 μs for Holland et al), and a flight length of 4.5 cm (50 cm for Holland et al).

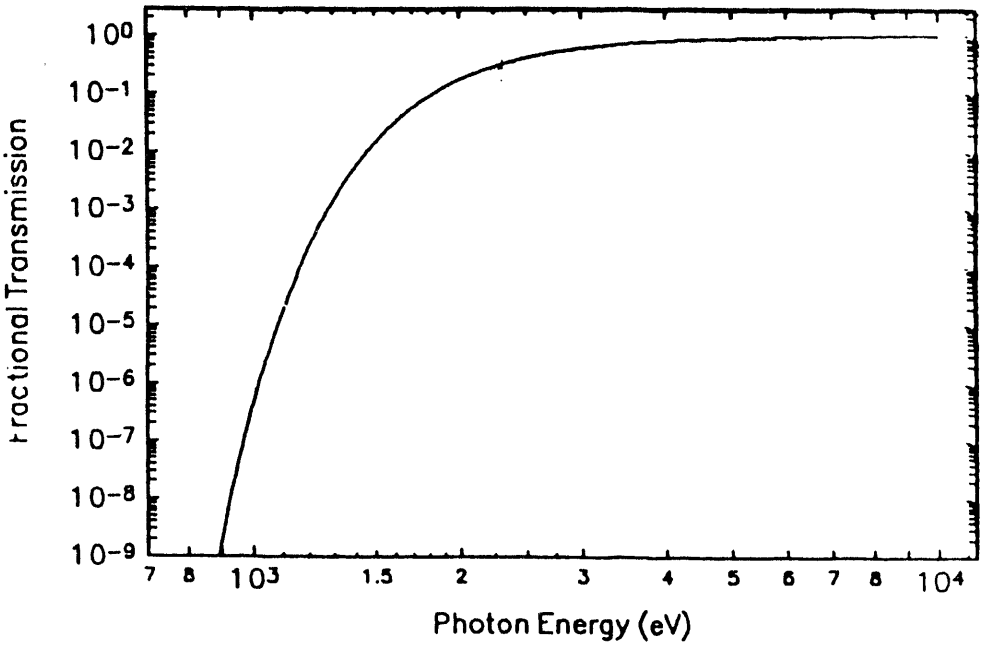

Figure 16. Theoretical transmission through a 5 mil beryllium window.

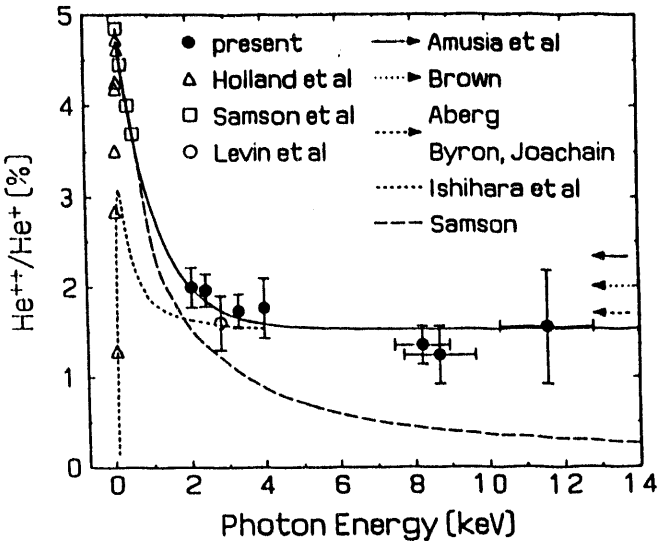

Figure 17. *Comparison of the experimental results of Levin et (1993) and other experiments and theories for the production* ratio σ^{++}/σ^{+}.

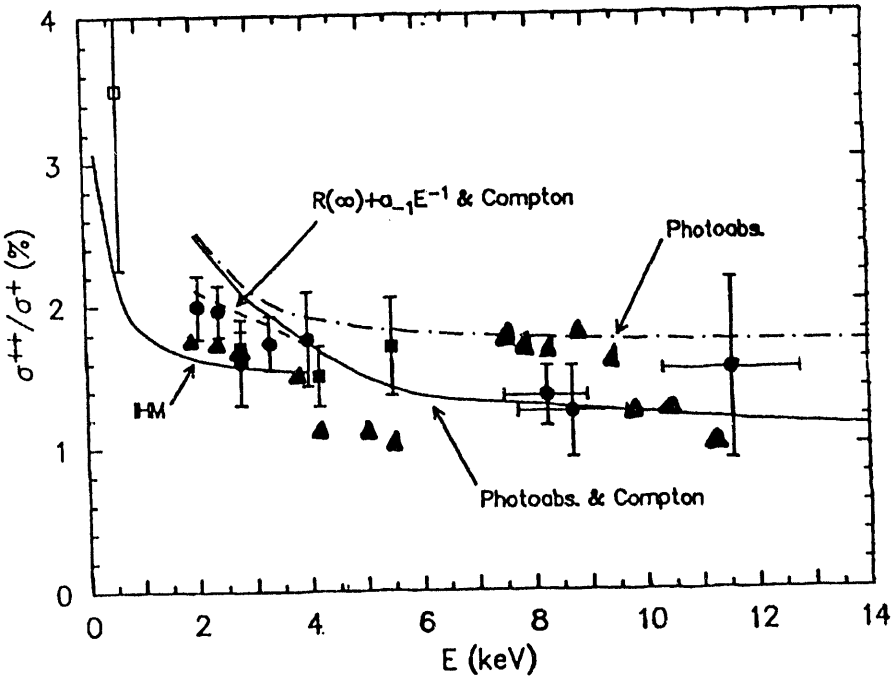

Figure 18. *The presently known experimental data for the production* ratio σ^{++}/σ^{+}. *Levin et al 1991, 1993; Samson and Bartlett; Sagurton et al, Bull. Am. Phy. Soc. 38, 1147 (1993)*

Compton scattering of photons from electrons bound in light elements

P. M. Bergstrom, Jr.

Department of Physics and Astronomy, University of Tennessee, Knoxville, Tennessee 37996 and Oak Ridge National Laboratory, Oak Ridge, Tennessee 37831

Abstract

A brief introduction to the topic of Compton scattering from bound electrons is presented. The fundamental nature of this process in understanding quantum phenomena is reviewed. Methods for accurate theoretical evaluation of the Compton scattering cross section are presented. Examples are presented for scattering of several keV photons from helium.

Samson, Greene and Bartlett[1] have recently noted that experiments measuring the ratio of double to single ionization by single photon impact on helium[2] are dominated at several keV by Compton scattering. Andersson and Burgdörfer[3] have estimated the contribution of Compton scattering to this ratio; relying on photoionization and shakeoff data. We discuss the nature of the bound Compton scattering and consider methods to obtain total cross sections for this process.

Compton scattering has been a valuable test of the most fundamental ideas of modern physics. Arthur Holly Compton observed that radiation scattered from atoms consists of essentially two components; the first at the wavelength of the incident radiation, corresponding to classical scattering, and the rest at a wavelength which varies with scattering angle. The inelastically scattered component may be roughly understood as scattering from free stationary electrons. The kinematics of Compton scattering from free stationary charges is readily determined from relativistic energy and momentum conservation under the further assumption that the radiation is quantized according to Planck's law and that these light quanta (or photons) and the target interact. The energy of the scattered radiation is uniquely determined by the energy of the incident radiation and by the scattering angle as

$$\omega_c = \frac{\omega_i}{1 + \frac{\omega_i}{mc^2}(1 - cos\theta)} \qquad (1)$$

This result (actually the analogous result for the shift in wavelength) was derived independently and published nearly simultaneously by Compton[4] and Debye[5] and depends on a quantal or particlelike description of radiation.

Shortly after the development of the wave mechanical description of atomic phenomena, DuMond[6] suggested that Compton scattering could be used to distinguish between various atomic models. While radiation scattered from atoms approximately satisfies Eq.(1) , the free Compton line (peak) which is observed in the spectrum of scattered energies at fixed angle is somewhat broadened. Dumond related this broadening to the momentum distribution of the bound electrons. He tried a number of different trial momentum distributions for the different electronic states, finding agreement between the observed spectrum, for scattering of Mo K_α radiation from beryllium, and a model that used the free atom wave mechanical predictions for the inner shell electrons and the free electron Sommerfeld model for the valence electrons.

DuMond's relationship between the momentum distribution of the bound electrons and the Compton scattering cross section has since been more rigorously established within the impulse approximation[7-11]. This relationship makes Compton scattering a unique tool for investigating all aspects of the bound charge distribution, including correlations. In the remainder of this paper, we discuss the nature of the Compton scattering process and methods for calculating cross-sections. We concentrate on the accurate, efficient evaluation of the cross-section for scattering of high energy photons from helium.

The lowest order amplitude for Compton scattering may be obtained by evaluating the diagrams of Fig. 1 within external field quantum electrodynamics. Such calculations have recently been accomplished[12,13]. As a result, it is now possible to understand the region of validity of simpler, more approximate approaches. The features of the scattered photon spectrum, at fixed scattering angle, are apparent in the nonrelativistic Kramers Heisenberg Waller (KHW)[14] matrix element. In the Coulomb gauge the KHW matrix element is written

$$M_{KHW} = (\epsilon_1 \cdot \epsilon_2^*) \langle f | e^{i(k_1 - k_2)\cdot r} | i \rangle - \sum_n \frac{\langle f | e^{-ik_2\cdot r} (\epsilon_2^* \cdot p) | n \rangle \langle n | e^{ik_1\cdot r} (\epsilon_1 \cdot p) | i \rangle}{E_n - (E_B + \omega_1 + i\varepsilon)} \quad (2)$$
$$- \sum_n \frac{\langle f | e^{ik_1\cdot r} (\epsilon_1 \cdot p) | n \rangle \langle n | e^{-ik_2\cdot r} (\epsilon_2^* \cdot p) | i \rangle}{E_n - (E_B - \omega_2)}$$

where ϵ_1 and ϵ_2 are the polarization vectors for the incident and scattered photons, $\mathbf{k}_1$ and $\mathbf{k}_2$ are the incident and scattered photon momenta, ω_1 and ω_2 are the incident and scattered photon energies, | i>, |f> and |n> are the electron wave functions and where E_B is the binding energy of the scattering electron. The first term A^2 or seagull term) of the KHW matrix element accounts for the Compton peak. The remaining terms, called the **p•A** or pole terms, give divergent behavior for soft scattered photons in all shells and resonant behavior in the outer atomic shells. *S* matrix calculations contain all three features. Fig. 2 presents a case, the scattering of 279 keV photons from the L3 subshell of lead, where all three features are observed. The dominant features are the angle dependent Compton peak in the hard photon region of the spectrum and the nearly isotropic resonance at the K-L3 characteristic energy. The divergent soft scattered photon spectrum is also seen.

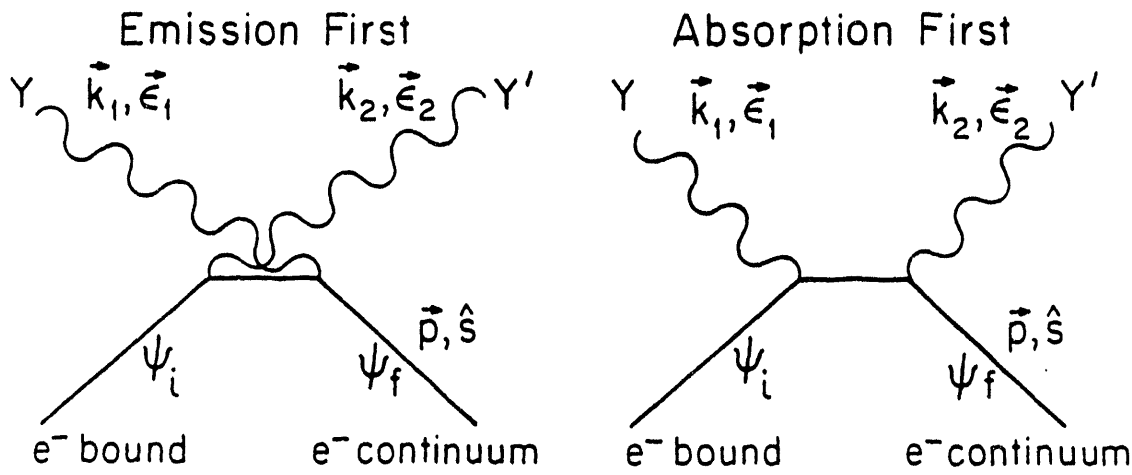

Figure 1. *Diagrams representing the S matrix amplitudes which must be evaluated to obtain the Compton scattering matrix element.*

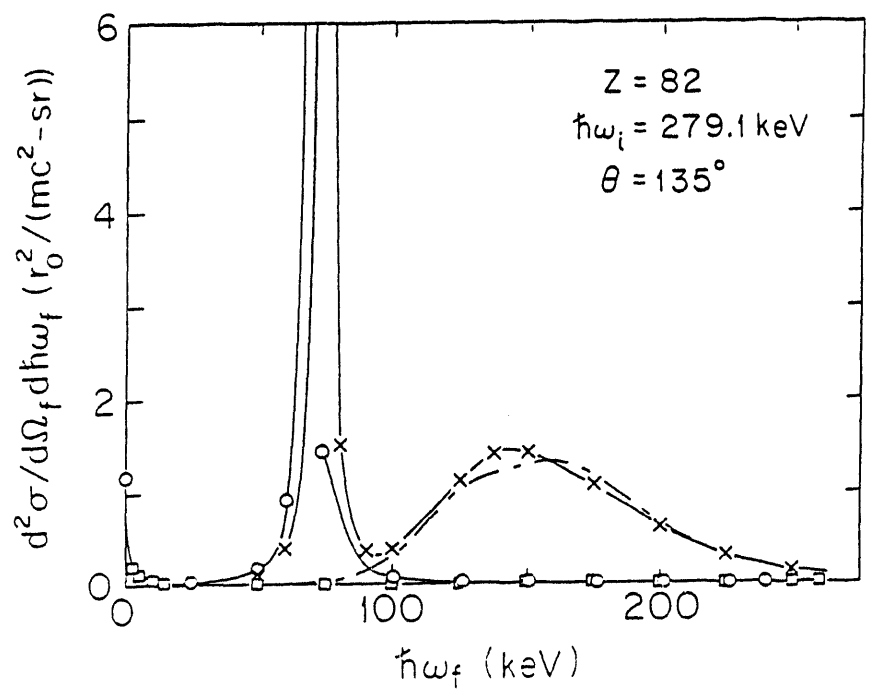

Figure 2. *Comparison of various nonrelativistic calculations with the it S matrix calculation (solid line) for the scattering of 279 keV photons from the L3 subshell of lead.*

The validity of the A^2 approximation in describing the peak region of the double differential cross section, for high photon energies, has been discussed by Eisenberger and Platzmann[7]. Comparing their experimental data for the scattering of 17.4 keV photons from helium, they found that the Compton peak is well described using only this term. The validity of the A^2 approximation in scattering from the K shell for any incident photon energy and scattering angle may be simply understood in terms of the underlying kinematics. We illustrate this in Fig. 3. The maximum scattered photon energy, the kinematic limit for the process, is determined by energy conservation to be the incident photon energy minus the binding energy of the scattering electron. In order for the Compton peak to be observable, it must shift to kinematically allowed energies. The shift for bound electron scattering is approximately equal to the free Compton shift to lower energies plus the Compton defect ($\approx E_B$ / 6) to higher energies. Bergstrom et al[13] have derived the following expression for the incident photon energy at which the center of the peak is observable for any scattering angle

$$\omega_1 > \sqrt{\frac{7}{3(1-\cos\theta)}}\frac{E_B}{Z\alpha}. \tag{3}$$

For incident photon energies that satisfy Eq. (3), the A^2 term is usually dominant and approximations derived from it are adequate.

The most common A^2 treatments involve direct evaluation of the matrix element or the impulse approximation discussed above. It is evident from Eq. (2) that a direct evaluation of the A^2 term necessarily involves retaining higher multiples as the usual electric dipole approximation vanishes. In Fig. 4, the A^2 approximation to the cross section singly differential in scattered photon angle is given along with the multipole contributions for the scattering of 12 keV photons from the K shell of helium. The need for many multipoles to accurately describe the spectrum is clear, particularly near the the scattered photon energy of 11.46 keV, which corresponds to the energy predicted by Eq. (1) when $\theta = 180$ degrees. Another interesting feature is the possibility of ejection of the electron into an s state. This zero-zero transition, strictly forbidden in a nonrelativistic formalism for single photon processes, is possible because Compton scattering is a two photon process and the angular momentum of the incident photon can be completely transferred to the scattered photon. Based on the spectrum we can also understand the energies of electrons ejected by the Compton scattering process (in the region of the Compton peak). According to this spectrum, the ejected electron energies (obtained as $E_f = \omega_1 - \omega_2 - E_B$) are low relative to photoionized electrons for the same energy incident photon.

The impulse approximation may be derived from the A^2 term under the further assumption that the final electron state may be represented by a plane wave. We then have

$$\frac{d^2\sigma}{d\omega_2 d\Omega_2} = \alpha^2\left(\frac{1+\cos^2\theta_2}{2}\right)\frac{\omega_2}{\omega_1}\frac{1}{k}J_{n\ell}(p_z), \tag{4}$$

where

$$J_{n\ell}(p_z) = \frac{1}{2}\int_{p_z}^{\infty} dp \frac{I_{n\ell}(p)}{p}. \tag{5}$$

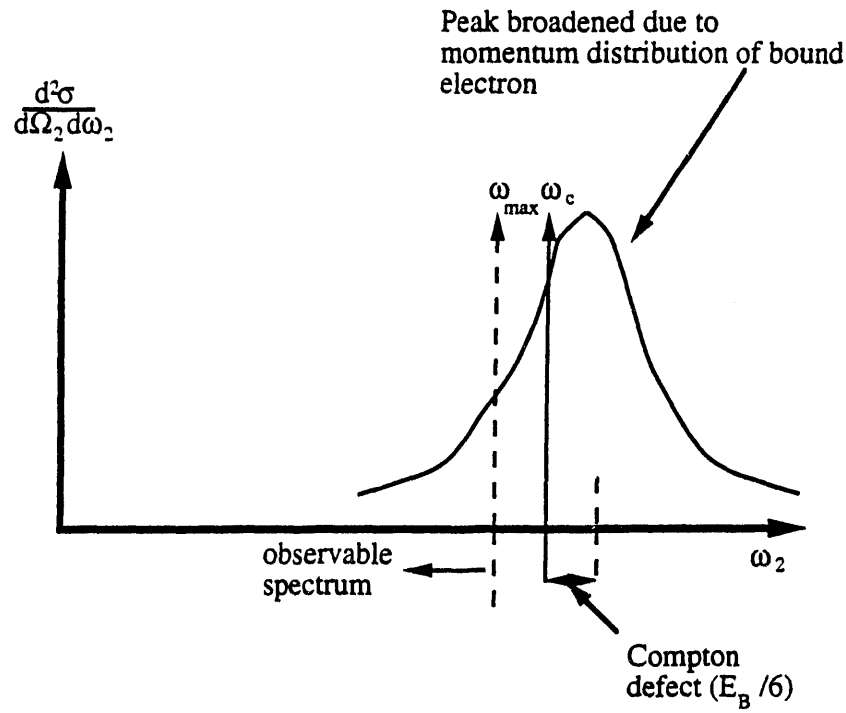

Figure 3. *Cartoon illustrating the kinematic factors that determine the validity of the A^2 approximation.*

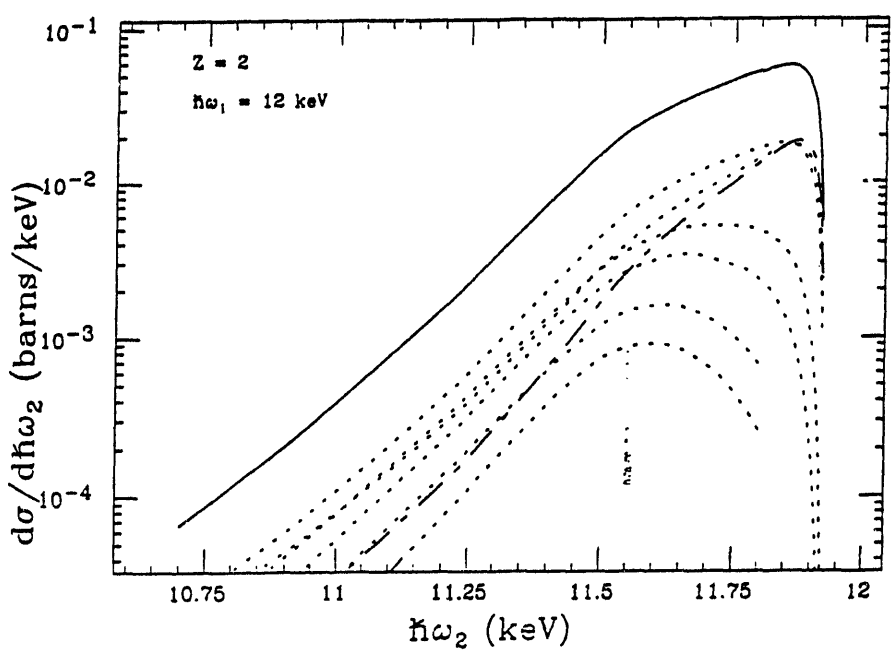

Figure 4. *Scattered photon spectrum for the scattering of 12 keV photons from helium (solid curve). Also shown are the multipole contributions (dots, except at $l = 0$ is chain dashed curve).*

$J_{nl}(p_z)$ is called the Compton profile of the scattering state with quantum numbers n and l, where

$$p_z = \frac{E_i(\omega_1 - \omega_2) - \omega_1\omega_2(1 - cos\theta_2)}{k}. \tag{6}$$

This variable is the projection of the momentum of the bound electron on the direction of the photon momentum transfer. Here

$$I_{nl} = |\chi_{nl}(p)|^2 p^2. \tag{7}$$

Tabulations of Hartree-Fock Compton profiles are available for all atoms[10]. In Fig. 5 we present a comparison of a direct evaluation of the A^2 term and the impulse approximation of it to the full S-matrix treatment for the scattering of 8 keV photons from helium. As expected, from Eq. (3), both treatments based on the A^2 term are valid here.

In order to define any cross section for Compton scattering, that has been integrated over scattered photon energies, the question of the soft photon divergence in the **p•A** term must be addressed. The standard program for handling infrared divergences in QED relies on the fact that for sufficiently soft photon energies a divergent radiative process is indistinguishable from a corresponding radiationless process. Therefore, the full amplitude for the radiationless process must be written as the sum of the lowest order amplitude for that process, the amplitudes for radiative corrections to that process and the amplitudes for all radiative processes indistinguishable from the radiationless process. The infrared divergence in the radiative process is cancelled by a corresponding divergence in the radiative corrections to the radiationless process. The radiationless process which corresponds to Compton scattering in the limit of soft scattered photons is photoeffect. Therefore, the full ionization amplitude, which is finite, is written order by order in the fine structure constant as

$$M = M_{pe} + [M_{rc}(\delta) + M_{ird}(\delta)] + \cdots \tag{8}$$

where M_{pe} is the lowest order photoeffect amplitude, M_{rc} are the lowest order radiative corrections to photoeffect, and M_{ird} is the Compton scattering amplitude for scattered photon energies $< \delta$. The full amplitude M must be independent of choice of δ. Gavrila and coworkers[15-19] have evaluated both M_{rc} and M_{ird} and have explicitly demonstrated this cancellation. The effects of this procedure on total photon absorption by hydrogen has recently been investigated by Bergstrom et al[13]. They found that the finite correction of this procedure to the full absorption cross section is small. This means that the total ionization cross section may be accurately approximated by adding the lowest order cross section for photoionization to the A^2 cross section for Compton scattering.

In the A^2 approximation, the singly differential cross-section, observing only the direction but not the energy of the scattered photon is often written in terms of the incoherent scattering factor S(x) (where x is the momentum transfer) as

$$\frac{\mathrm{d}\sigma}{\mathrm{d}\Omega_2}(\omega_1,\theta_2) = S(x)\left(\frac{d\sigma}{d\Omega_2}\right)_{KN}. \tag{9}$$

Here we have written the cross section in terms of the Klein Nishina cross section for scattering from free stationary electrons

$$\left(\frac{\mathrm{d}\sigma}{\mathrm{d}\Omega_2}\right)_{KN} = \frac{\alpha^2}{2}\left(\frac{\omega_2}{\omega_1}\right)^2\left\{\frac{\omega_1}{\omega_2}+\frac{\omega_2}{\omega_1}-sin^2\theta_2\right\}. \tag{10}$$

The incoherent scattering factor has been tabulated for all elements by Hubbell et al[21]. Their tabulated values for helium are the configuration interaction calculations of Brown[22] and therefore contain correlation effects. The calculations of Brown are in excellent agreement with the results of Kim and Inokuti[23]; the latter also contain correlation effects, having been obtained from variational wavefunctions. As it is derived by summing over all final states of the system (other than the ground state), the incoherent scattering factor must be understood to include all inelastic scattering process. Compton scattering is the dominant contribution at high photon energies. Another approach to obtain this singly differential cross section (angular distribution) is to integrate an A^2 approximation to the Compton scattering doubly differential cross section over scattered photon energy. In Fig. 6 we present the scattered photon angular distribution calculated within the incoherent scattering factor approximation, and by integrating the doubly differential cross sections obtained within the A^2 and the impulse approximations for the scattering of 10 keV photons from the helium ground state. The incoherent scattering factor is slightly larger than the direct evaluation of the A^2 term, reflecting the contributions of other scattering processes included in the incoherent scattering factor approximation such as Raman scattering, ionization excitation and double ionization. Total cross sections for Compton scattering are then simply obtained by integrating these singly differential cross sections over the scattering angle. The nonrelativistic limit is the classical Thomson cross section.

We have reviewed results pertinent to Compton scattering of keV photons from helium. Simple and acurate methods for calculating cross sections have been given. A discussion of the validity of these approximations has also been presented.

Acknowledgements. I would like to thank the organizers of the workshop and Argonne National Laboratory for the opportunity to attend a very worthwhile event. I also thank those with whom I have investigated the Compton scattering process, Ken-Ichi Hino, Joseph Macek, Richard Pratt, Tihomir Surić and Krunoslav Pisk.

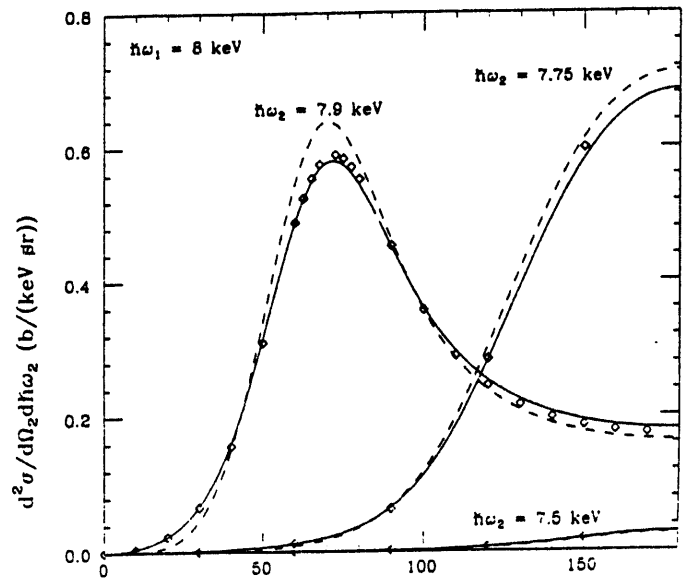

Figure 5. *Comparison of the full A^2 result (solid line) and the impulse approximation with the relativistic it S matrix calculation (diamonds) for the scattering of 8 keV photons from the helium ground state.*

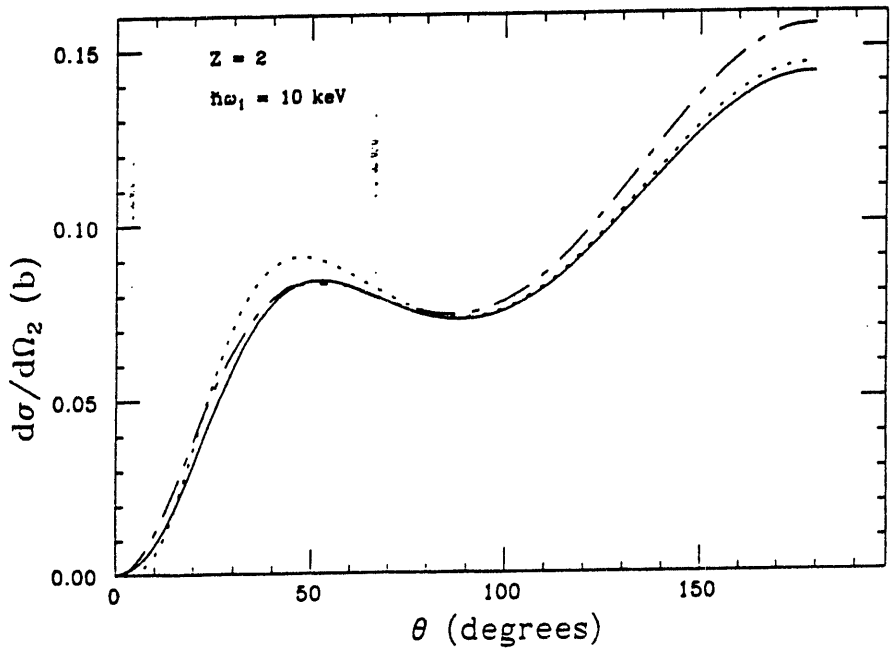

Figure 6. *Comparison of the scattered photon angular distributions for the scattering of 10 keV photons from helium within the incoherent scattering factor (chain dashed curve), A^2 (solid curve), and impulse approximations (dots).*

References

1. James A. R. Samson, Chris H. Greene and R. J. Bartlett, Phys. Rev. Lett. **71**, 201 (1993).
2. J. C. Levin, D. W. Lindle, N. Keller, R. D. Miller, Y. Azuma, N. Berrah Mansour, H. G. Berry, and I. A. Sellin, Phys. Rev. Lett. **67**, 968 (1991); J. C. Levin, I. A. Sellin, B. M. Johnson, D. W. Lindle, R. D. Miller, N. Berrah, Y. Azuma, H. G. Berry and D. -H. Lee, Phys. Rev. **A 47**, R16 (1993).
3. Lars R. Andersson and Joachim Burgdörfer, Phys. Rev. Lett. 71, 50 (1993).
4. Arthur H. Compton, Phys. Rev. 21, 483 (1923); **22**, 409 (1923).
5. P. Debye, Physik. Z. **24**, 161 (1923).
6. J. W. M. DuMond, Phys. Rev. **33**, 643 (1929).
7. P. Eisenberger and P. M. Platzmann, Phys. Rev. **A 2**, 415, (1970).
8. P. Eisenberger and W. A. Reed, Phys. Rev. **B 9**, 3237 (1974).
9. S. Manninen, T. Paakkari, and K. Kajante, Philos. Mag. **29**, 167 (1974).
10. F. Biggs, L. B. Mendelsohn, and J. B. Mann, At. and Nuc.Data Tab. **16**, 201 (1975).
11. Roland Ribberfors, Phys. Rev. **B 12**, 2067 (1975); ibid., 3136 (1975).
12. T. Surić, P. M. Bergstrom, Jr., K. Pisk and R. H. Pratt, Phys. Rev. Lett. **67**, 189 (1991).
13. P. M. Bergstrom, Jr., T. Surić, K. Pisk and R. H. Pratt, Phys. Rev. **A 48**, 1134 (1993).
14. H. A. Kramers and W. Heisenberg, Z. Physik **31**, 681 (1925); I. Waller and D. R. Hartree, Proc. Roy. Soc.(London) **A 124**, 119 (1929).
15. M. Gavrila, Lett. al Nuov. Cim. **5**, 180 (1969); Phys. Rev. **A 6**, 1348 (1972); **A 6**, 1360 (1972); Rev. Roum. Phys. **19**, 473 (1974).
16. A. Costescu and M. Gavrila, Rev. Roum. Phys. **18**, 493 (1973).
17. M. Gavrila and M. N. Tugulea, Rev. Roum. Phys. **20**, 209 (1975).
18. James McEnnan and Mihai Gavrila, Phys. Rev. **A 15**, 1537 (1977).
19. D. J. Botto and M. Gavrila, Phys. Rev. **A 26**, 237 (1982).
20. O. Klein and Y. Nishina, Z. Physik. **52**, 853 (1929).
21. J. H. Hubbell, Wm. J. Veigele, E. A. Briggs, R. T. Brown, D. T. Cromer, and R. J. Howerton, J. Phys. Chem. Ref. Data **4**, 471 (1975).
22. R. T. Brown, J. Chem. Phys. **55**, 353 (1971).
23. Yong-Ki Kim and Mitio Inokuti, Phys. Rev. **165**, 39 (1968).

Electron ionization and the Compton effect in double ionization of helium

James Samson
Department of Physics, University of Nebraska, Lincoln Nebraska

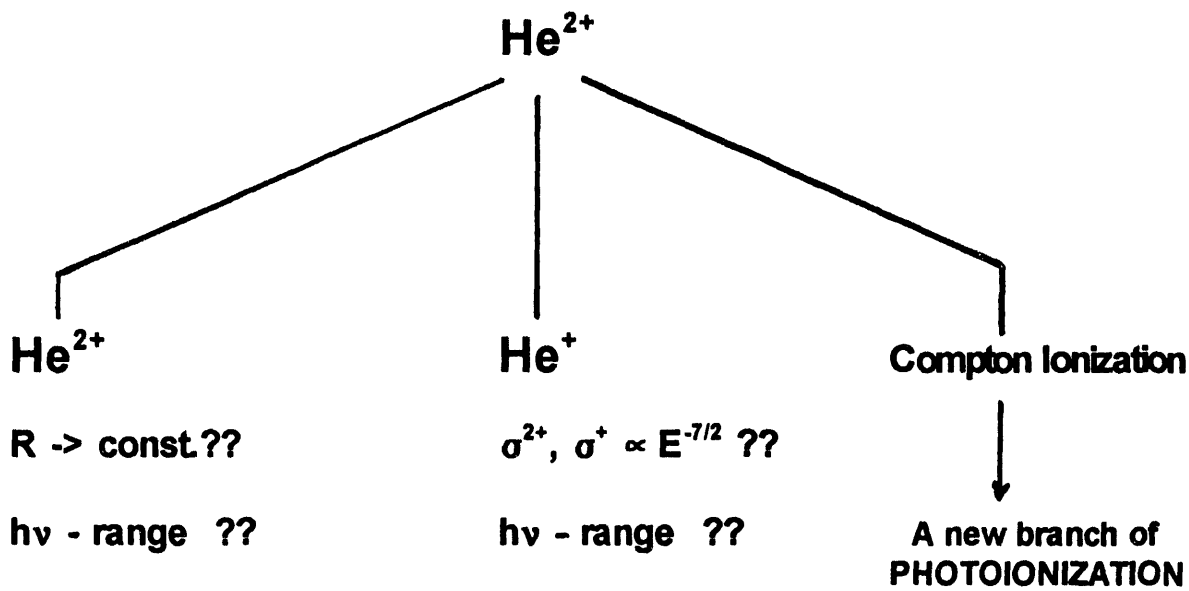

WHAT ARE THE IMPORTANT CORRELATION PROCESSES??

GSC, SO, TS1 (INTERNAL E⁻ COLLISIONS)

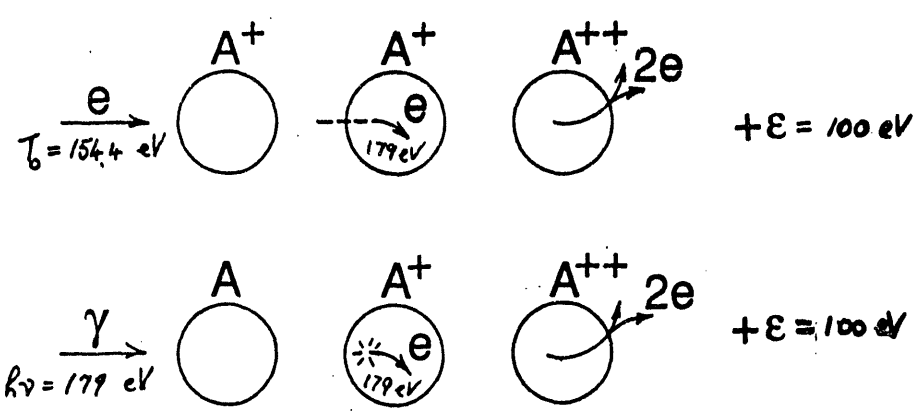

$\sigma_\gamma^{2+} / \sigma_\gamma$ (tot) = σ_e^{+} / const.

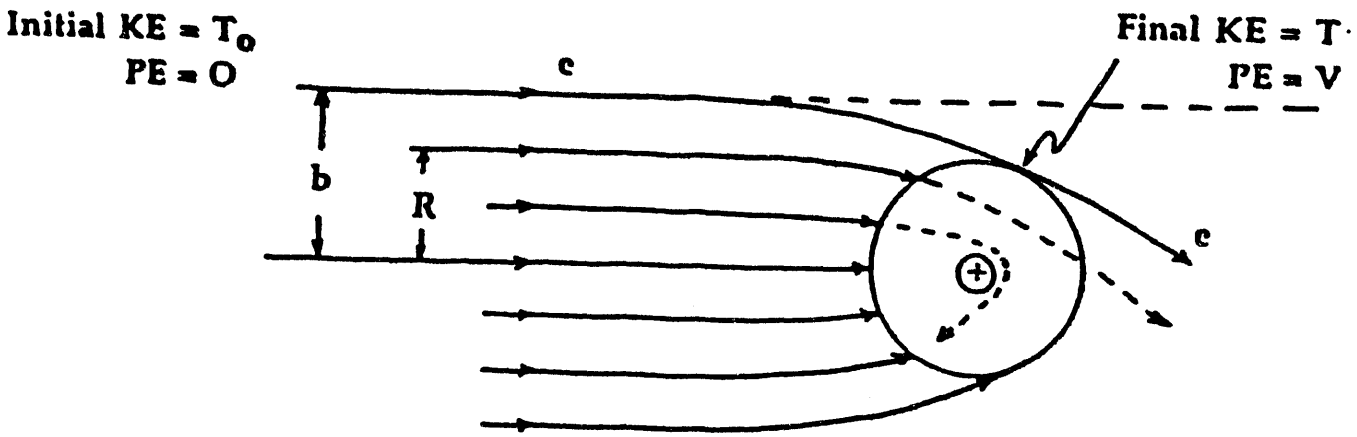

Figure 2. *Schematic diagram for electron impact on an ion showing the impact parameter b for an electron of initial kinetic energy T_0 that can just enter a zone of radius R.*

From the conservation of energy and angular momentum we find that

$$b^2 = R^2\,(1\text{-}V/T_0), \qquad (1)$$

where V is the potential energy of the electron at a distance R from the ionic nucleus. Thus, equating σ_e(abs) to πb^2, Eq.(1) becomes

$$\sigma_\gamma^{2+}/\sigma_\gamma(\text{tot}) = \sigma_e^{+}/k(1\text{-}V/T_0)\,, \qquad (2)$$

where k is a constant that is proportional to πR^2.

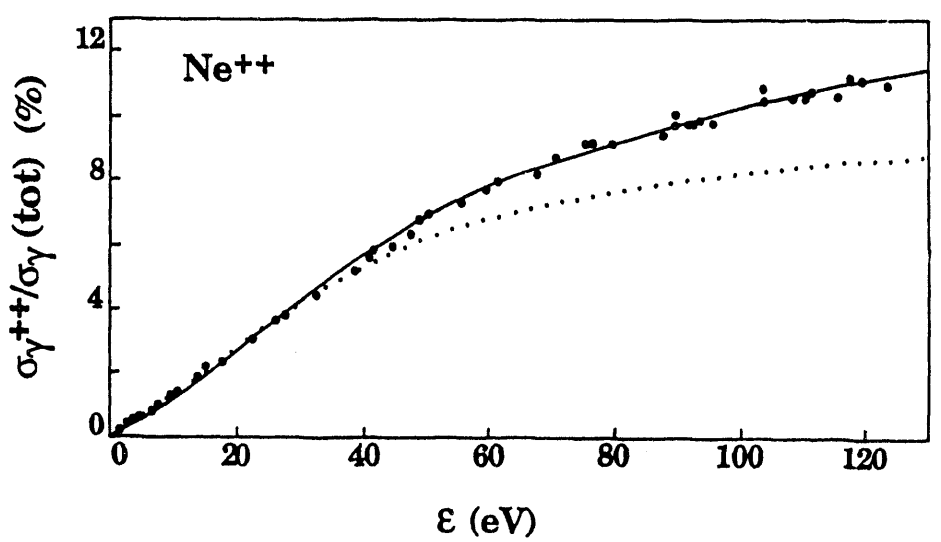

Figure 3. *Neon charge state production ratio*

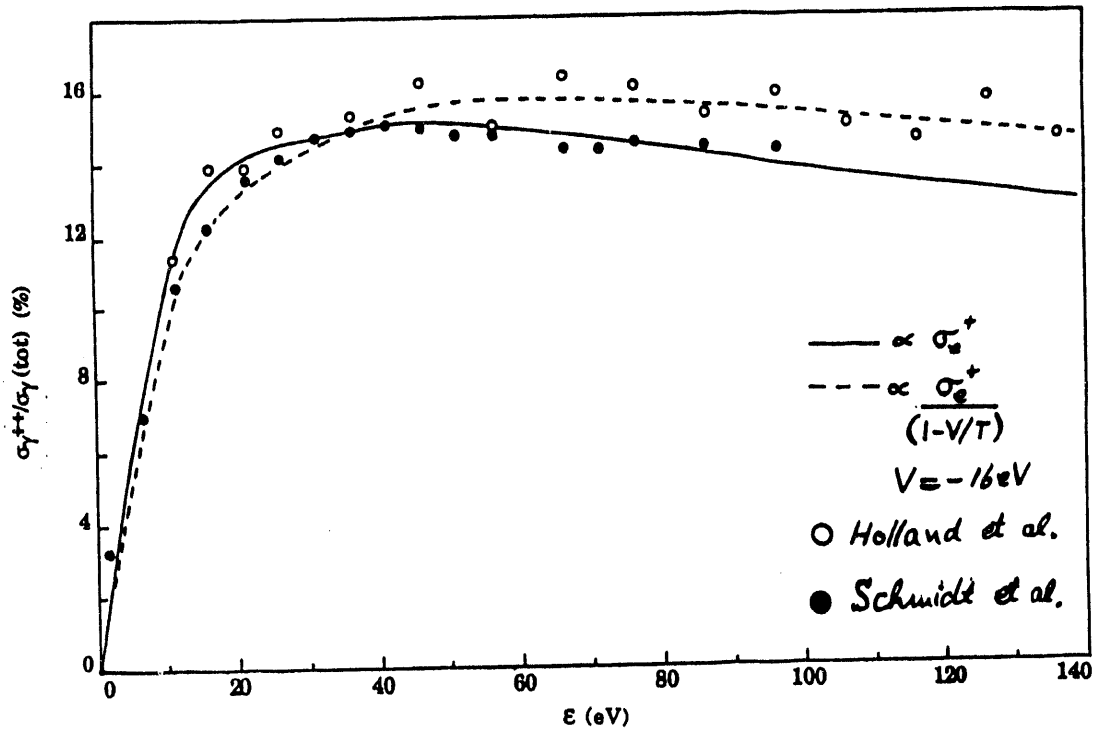

Figure 4. *Helium charge state production ratio at low energies.*

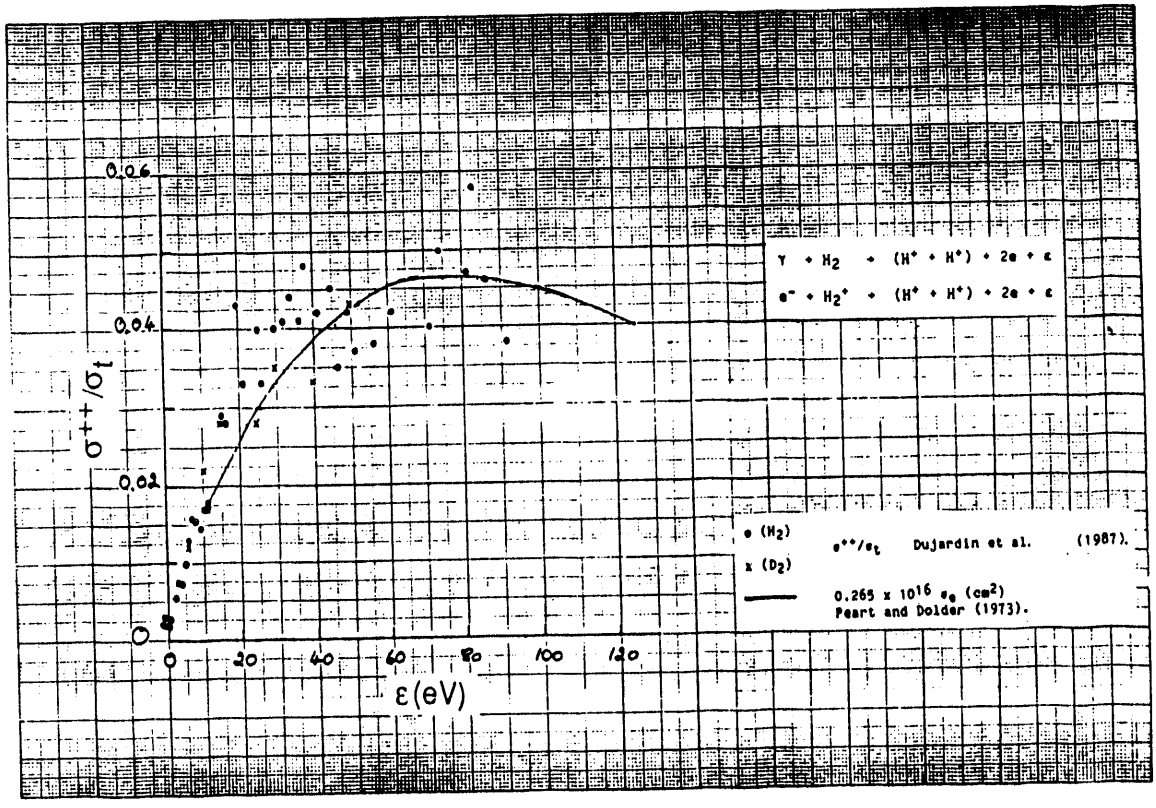

Figure 5. *Helium charge state production ratio; comparison with the theory of Peart & Dolder.*

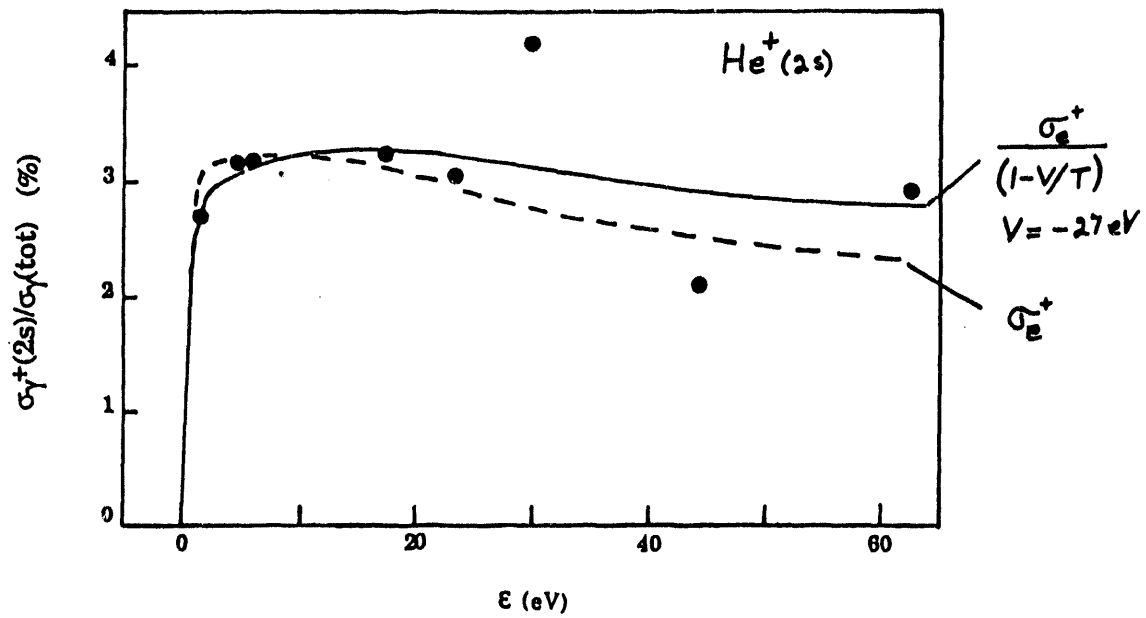

Figure 6. *Helium single ionization compared with electron ionization.*

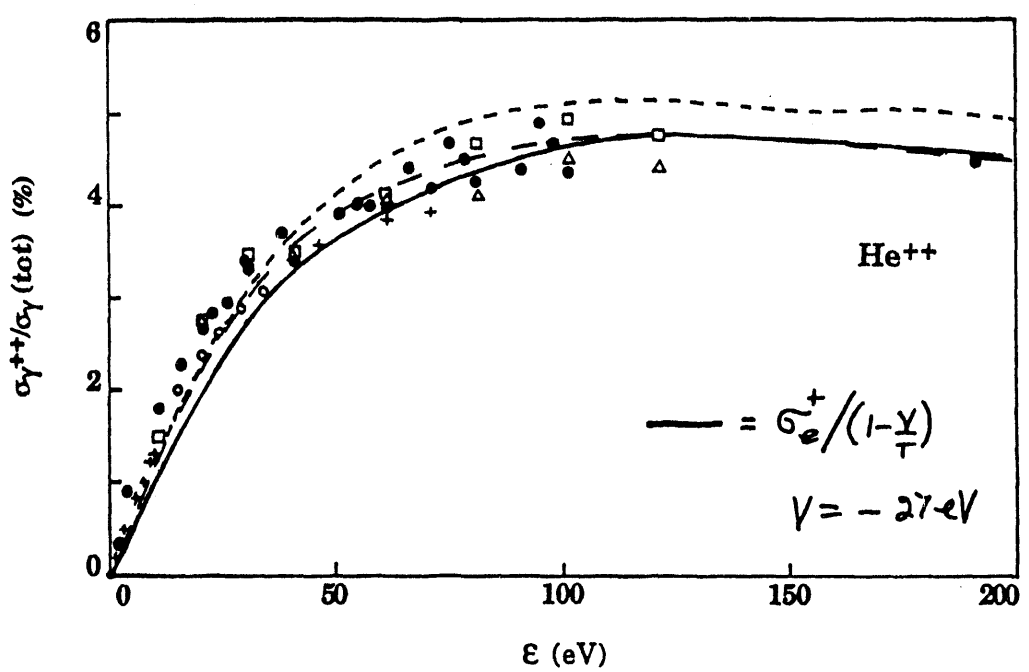

Figure 7. *Helium double ionization compared with electron ionization.*

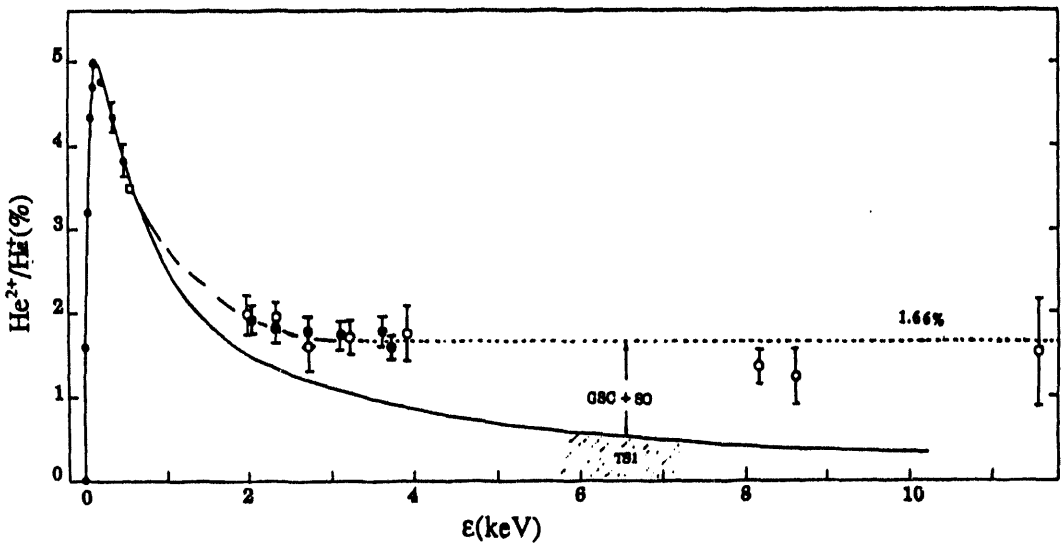

Figure 8. *Measured helium charge state ratio at high energies.*

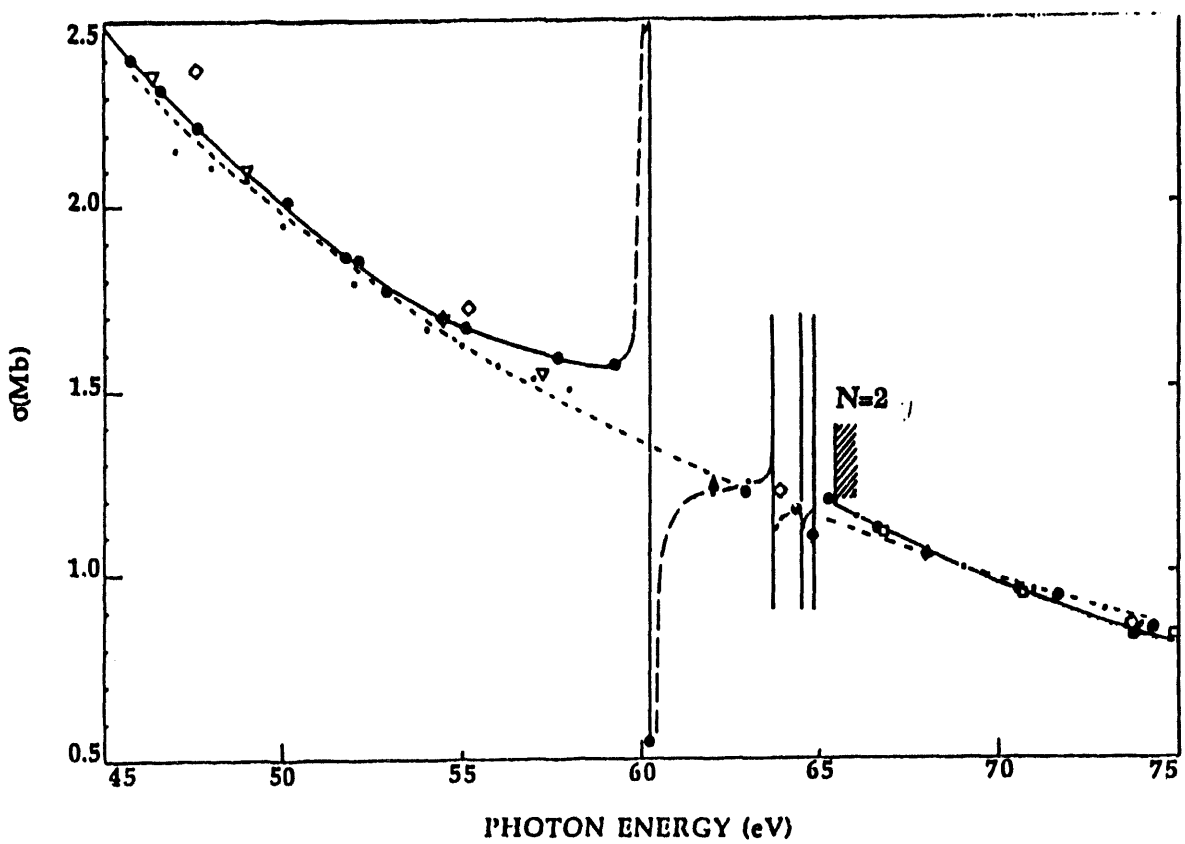

Figure 9. **Photoionization cross sections of He between 45 and 75 eV. Experimental: ●, present data; ——, best fit to data; – – – –, Marr and west (1976); •, Chan et al (1991); △, Morgan and Ederer (1984); □, Watson (1972); Theory: ▽, Altick and Moore (1966); ◆, Wendin (1971); ◇, Amusia et al (1976); — — —, Burke and McVicar (1965) and Fisher and Idrees (1990).**

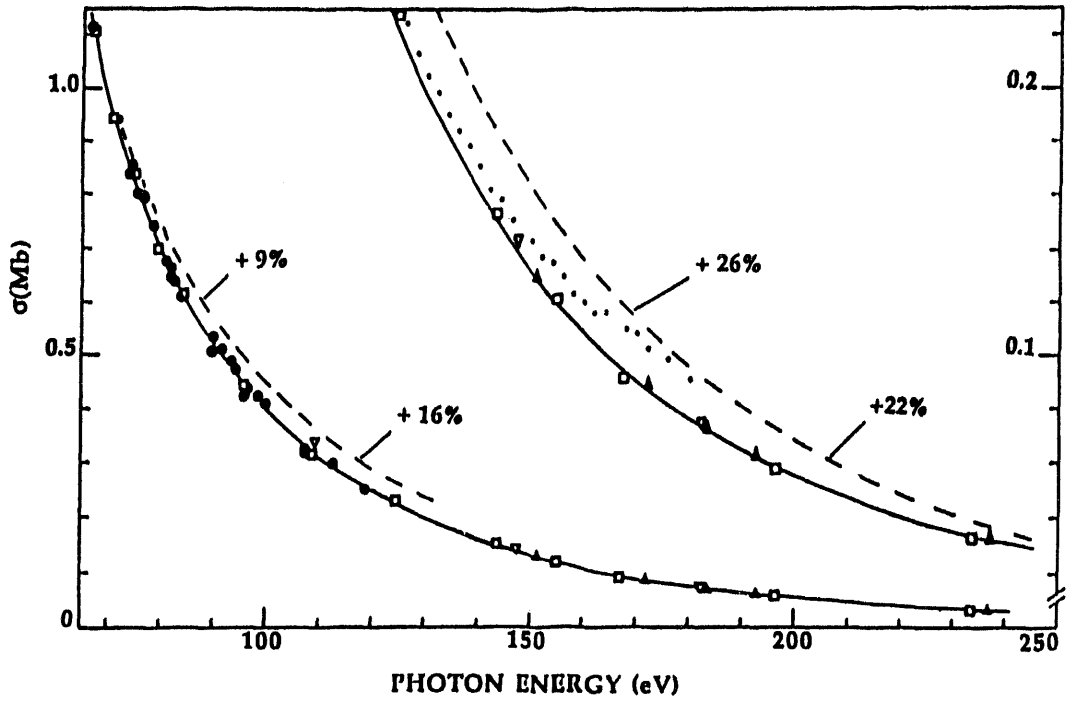

Figure 10.

Photoionization cross sections of He between 70 and 250 eV. ●, present data; —— best fit to data; □, Watson (1972); ▽, Henke (1967); ▲, Denne (1970); – – –, Marr and West (1976); •, Chan et al (1991). The percent values represent the deviation between the present results and the compilation of Marr and West.

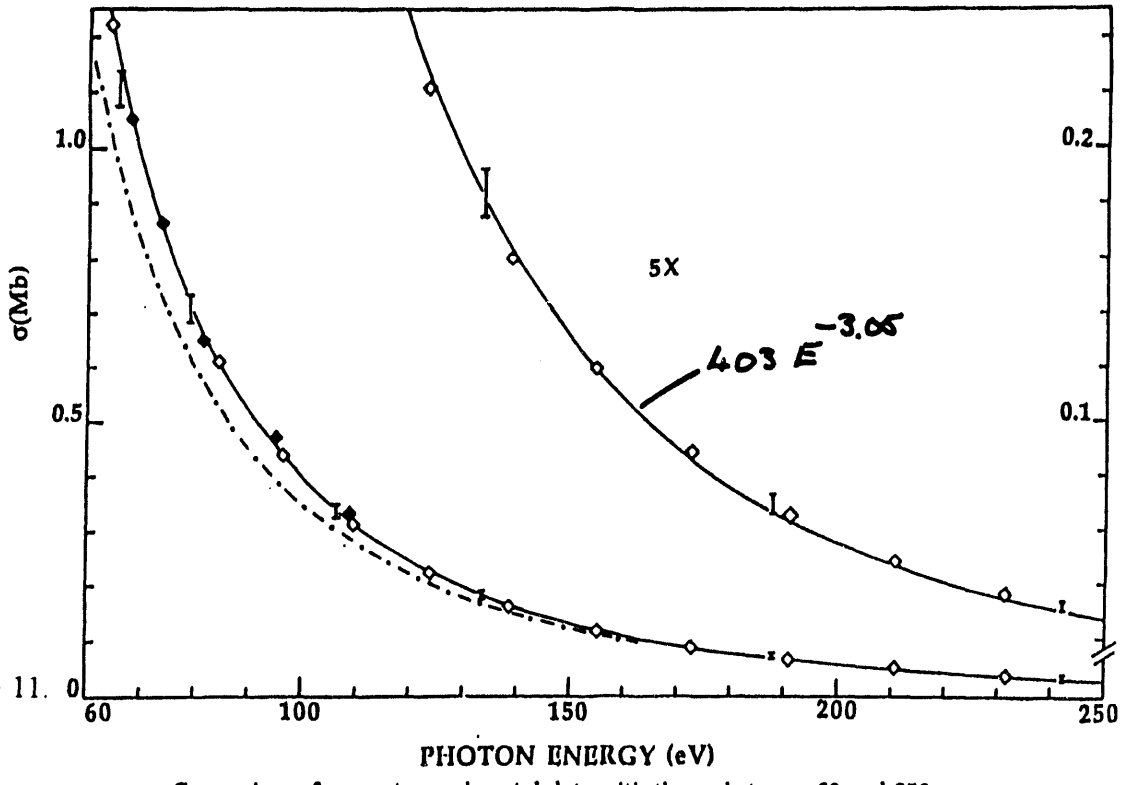

Figure 11.

Comparison of present experimental data with theory between 60 and 250 eV. ——, present results. Theory; ◆, Wendin (1971); ◇, Amusia et al (1976); I, Bell and Kingston (1971); – · – · –, Reilman and Manson (1979).

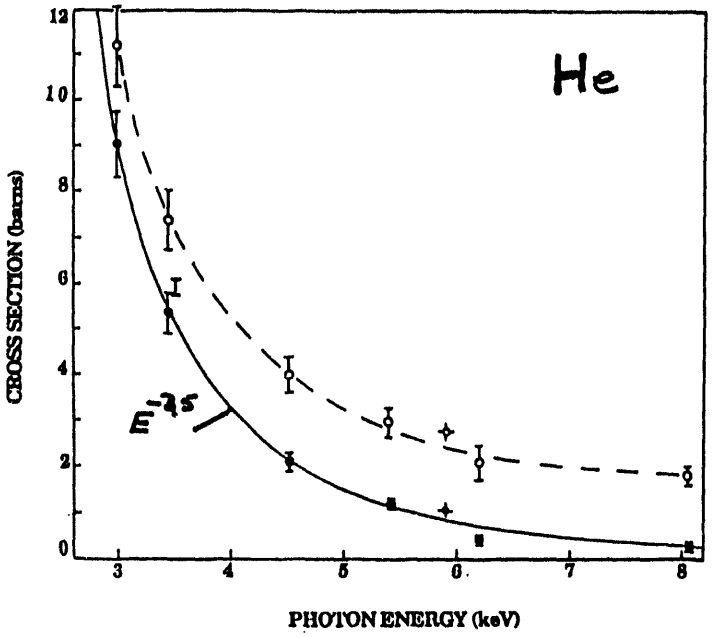

Figure 12.

6. Attenuation and Photoionization data derived from the experimental results of Bearden (1966) and McCrary et al (1970). O and ●, Bearden; ⊹ and ✦, McCrary et al. The dashed line helps to view the attenuation data. The solid line is a best fit to the photoionization data and can be represented by the equation σ(barns) = 410 E(keV)$^{-3.5}$. Theory: Σ, calculated data in the length (upper cap) and velocity (lower cap) approximation at 3.5 keV, Bell and Kingston (1971).

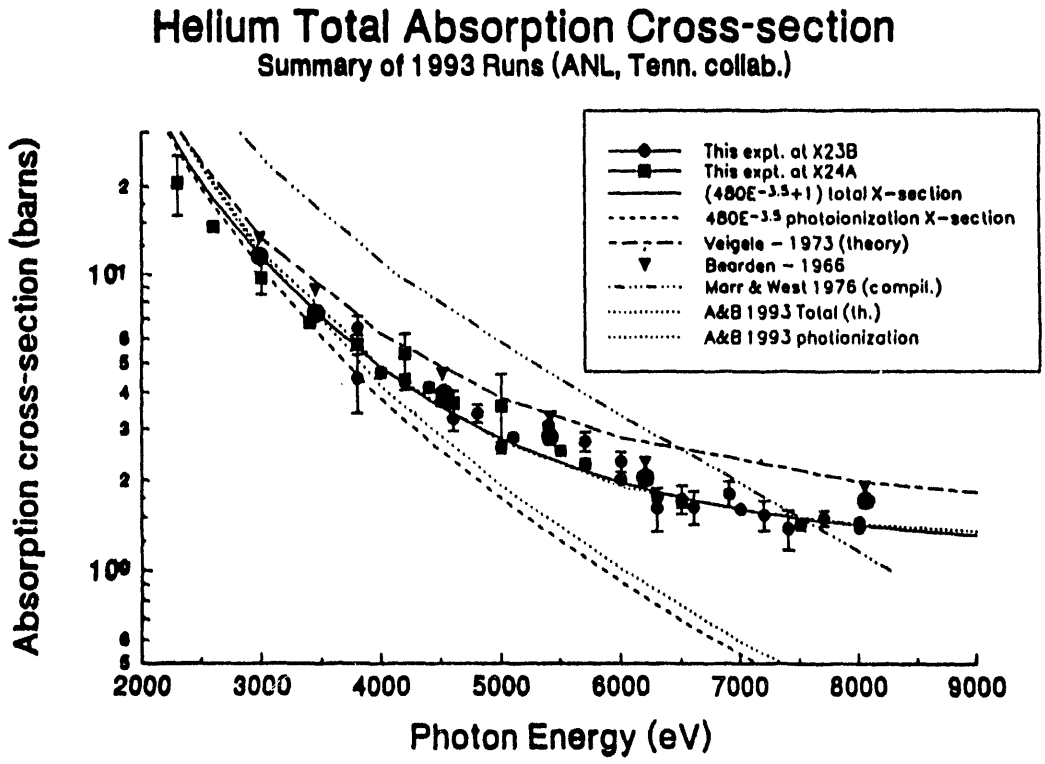

Figure 13. *Measured total absorption cross-section; Azuma et al, preliminary data.*

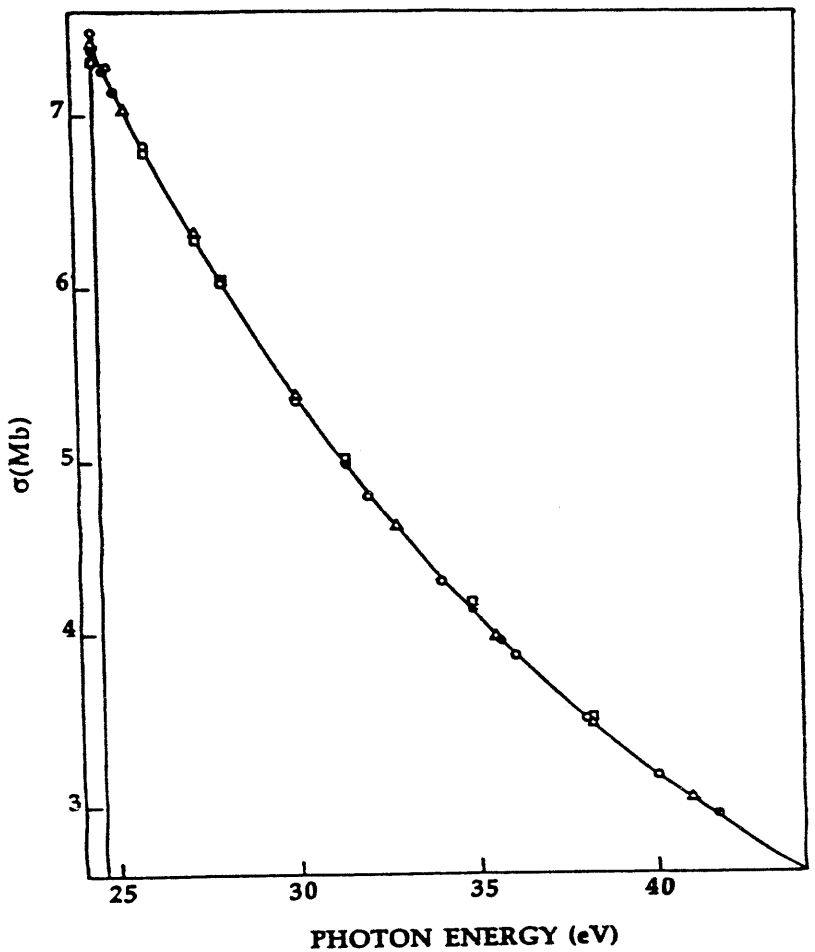

Comparison of present experimental data with theory between 24.6 eV and 44 eV. —— present results. Theory; □, Bell and Kingston (1971); ●, Stewart (1978); ○, Fernley (1987); Δ, Tang et al (1992).

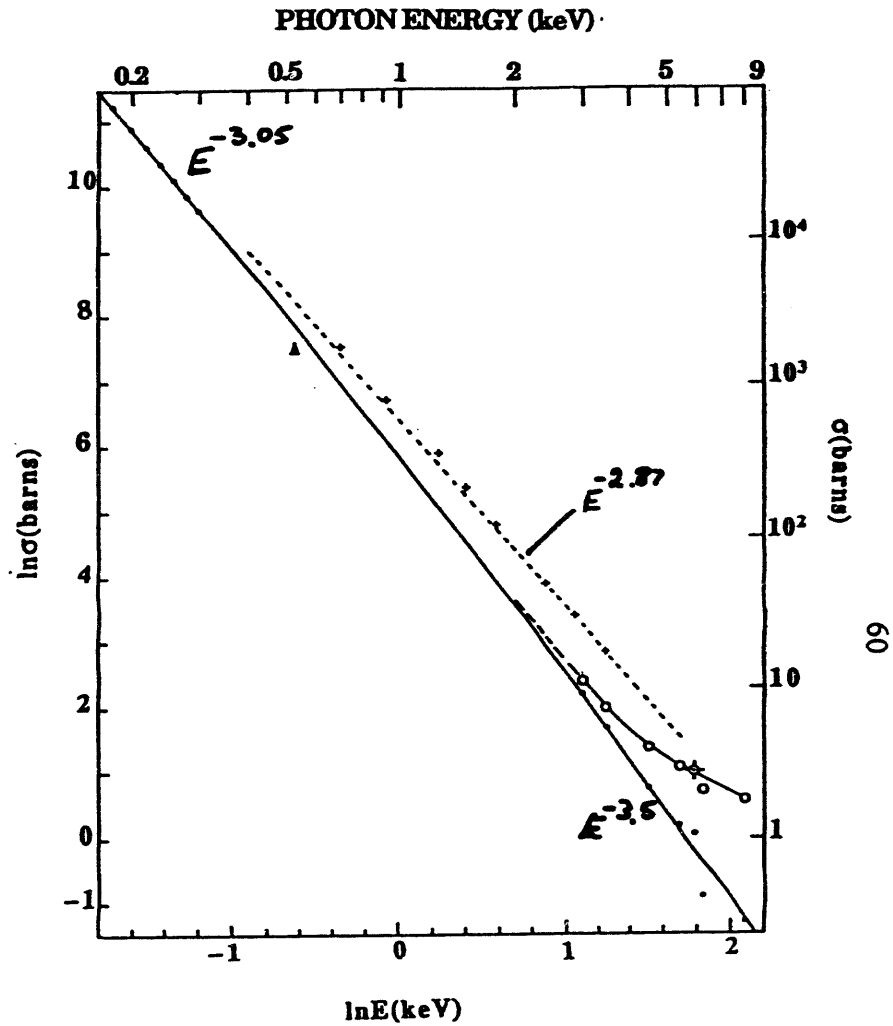

Predicted photoionization cross sections (solid line) between 200 eV and 8 keV. Small dots at low energy, present data; small dots at high energy, derived from Bearden (1966) and McCrary et al (1970); ▲, Denne (1970); Attenuation data: – – – Marr and West (1976); +, Allen (1935); ⊹ McCrary et al; O, derived from Bearden (1966).

Elimination of Two Atomic Electrons by a Single High Energy Photon

M. Ya. Amusia

Argonne National Laboratory, USA and the A.F. Ioffe Physical-Technical Institute, Russia

I. Introduction

The theoretical investigation of one photon - two electron photoionization of atoms have taken its second breath. Being initiated about thirty years ago, it was abandoned for a long time due to almost complete lack of experimental data, and, correspondingly, due to lack of interest from the community. Now the situation is changing rapidly. Intensive radiation from synchrotrons and storage rings permits to study the double electron photoionization by single photons in a very broad frequency region - from the threshold of this process up to very high in atomic scale energies.

For a long period it was almost a general belief, that the high but not relativistic frequency region of this process is theoretically clear and may be described using the lowest order perturbation theory in interelectron interaction. Therefore, most intriguing seemed to be the low and intermediate energy region, where higher order terms become decisively important. Just there, starting from the threshold, different rather sophisticated corrections, such as dynamical polarization of the target by the incoming photon or strong repulsion of two photoelectrons could modify the expected in the lowest order of perturbation theory cross section not only qualitatively but even quantitatively.

However it became clear recently, that double photoionization is not that simple even at high photon energies. After analyzing the new experimental data [1], it was demonstrated [2] that a rather big contribution to double photo`nization is coming from a process, in which two outgoing photoelectrons are accompanied by a continuous spectrum photon, i.e. in Compton-effect. Surprisingly enough, it appeared that the ratio of the double - to single charged ion yields is, at least for helium, energy independent, and equal to about 1.6% in the photon frequency region from 1 up to 12 kev. This observation is puzzling, leading to the conclusion that in this case the discussed ratio is the same whenever double and single charge ions are produced via photoionization or Compton effect. All this stimulates the theoretical investigation of the double-charged ion production in the high energy region.

2. Mechanism of two-electron photoionization - high energy region

Double electron photoionization is a process in which the direct interaction between atomic electrons manifests itself most transparently. Without this interaction the process is impossible

and therefore it cannot be described in the framework of any self consistent independent-electron approximations.

While at least for He the ratio of the double to single ionization cross sections is small, the first order perturbation theory in interelectron interaction seems to be a good starting point. Therefore the amplitude of the process under consideration in the language of the many-body theory may be represented by four diagrams:

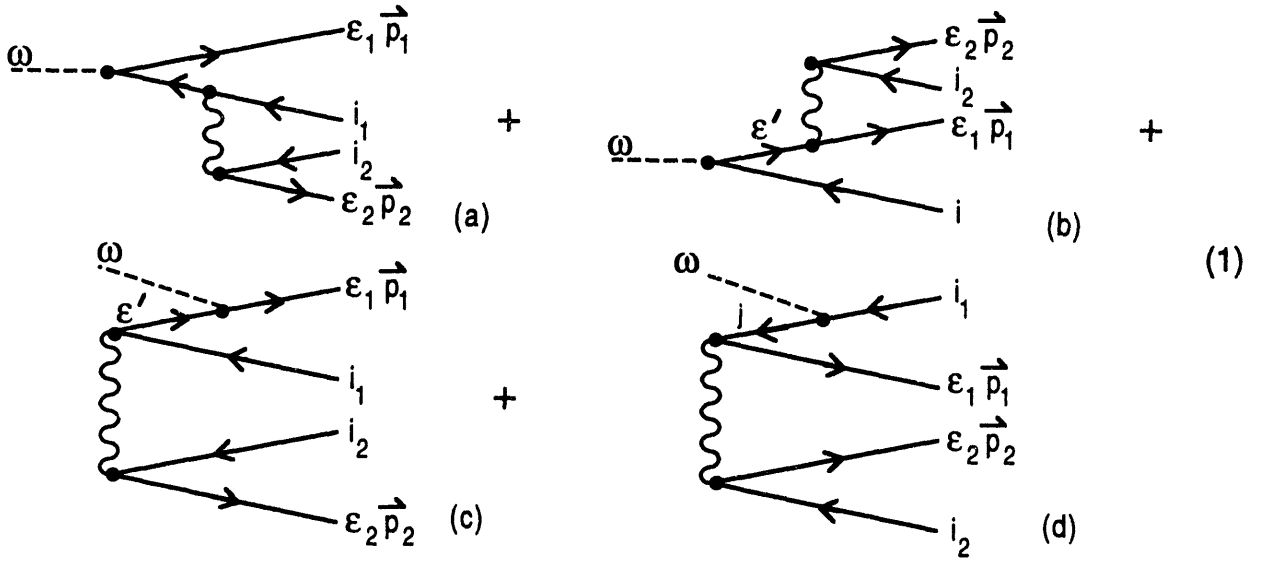

Here the line directed to the right (left) stands for an electron (vacancy) described by a Hartree-Fock one particle wave function, the wavy line represents the Coulomb interelectron interaction, and the dashed line describes a photon [3].

While time is considered to increase from the left to the right, diagrams (1) present the physical process of double ionization as developing in time. It is said, that (1a,b) describes the final state electron correlations or interaction, while (1c,d) are due to ground (or initial) state correlations. The diagram (1a), if the created vacancy j is sufficiently deep, so as it can decay by emitting one of the outer electrons, represents an Auger decay contribution. Otherwise, except for cases with i equal to i_1 (or i_2), the process presented by (1a) is called quasi-Auger decay. If j is equal to i_1 (or i_2) the diagram (1a) describes the shake off process, i.e. ionization of the second electron due to instant alteration of the self consistent field acting upon all atomic electrons after the elimination of the j electron. Diagram (1b) represents the direct knock out of the second electron by the first one.

For helium and helium-like ions in their ground states it is rather accurate to substitute the self-consistent field acting upon electrons by the pure Coulomb one with an effective charge $Z_{eff}=Z-\eta$, $\eta \approx 0.25$, Z being the nuclear charge.

For photon energies $\omega << \alpha^{-1}Z$, $\alpha=1/137$ being the fine structure constant, the dipole approximation for photon-electron interaction is valid, and the interaction operator is defined by one of the three

forms:[1]

"length":	$\mathbf{r}$	a	
"velocity":	∇	b	(2)
"acceleration":	$-Z_{eff}\mathbf{r}/r^3$	c	

Note, that the precise dipole interaction operator is the same for "length" and "velocity" forms, as given by (2a,2b), respectively. However, in "acceleration" form the precise dipole operator is

$$d_{acc} = -Z\mathbf{r}/r^3 \qquad (3)$$

But for He and He-like ions the difference between (3) and (2c) is small.

3. Some results of calculations

In the above described approximation it is possible to estimate the contribution of different terms of (1) into the total double photoionization cross section σ^{++}. While the total magnitude of σ^{++} is the same for r and ∇ operators, the contribution of different terms of (1) depends upon the choice of the operator, or is "gauge noninvariant". For the ∇ form and ω>>I, I being the target ionization potential, one has the following contributions, collected in the Table 1 [4]:

Table 1. Contributions to double-electron photoionization cross section

Diagram	$p_1>>p_2$	$p_1\sim p_2$	$p_1<<p_2$
a	$\omega^{-7/2}$	$\omega^{-17/2}$	$\omega^{-13/2}$
b	$\omega^{-9/2}, e'\sim p_1, p_2$	$\omega^{-9/2}, m\sim R^{-1}$	$\omega^{-13/2}$ any ϵ'
c	$\omega^{-7/2}, e'\sim R^{-1}$	$\omega^{-9/2}, m\sim p_1$	$\omega^{-13/2}$ $\epsilon'\sim R^{-1}$
d	$\omega^{-13/2}$	$\omega^{-11/2}$	$\omega^{-13/2}$

For pure dipole photons in He and He-like ions in the ground states only s-holes exist, so the contribution of (1d) is zero. For elimination of two s-electrons, one has at ω>>I

$$\frac{\sigma^{++}(\omega)}{\sigma^{+}(\omega)} = \frac{a}{Z_{eff}^2}, \qquad (4)$$

where "a" is a constant, equal to 0.092. Note, that in the ∇-form the main contribution is coming

---

[1]The Atomic system of units is used throughout this paper: $e=\hbar=m=1$

from ground state correlations (1c) and shake off (1a).

If at least one of the eliminated electrons is a p-electron, the ratio (4) is rapidly increasing, as ω/I. The experiment, which would prove this statement is rather complicated, but the results promise to be interesting. A long-living 1s2p triplet state can be created by laser beam, acting upon He 1s2s ^3S quasi-stable state.

Contributions of different parts of the spectral region to $d\sigma^{++}/d\epsilon$ and σ^{++} were calculated in the framework of the described above model. The results are collected in the Table 2 [4]:

Table 2. Contributions of different spectral regions to $d\sigma^{++}/d\epsilon$ and σ^{++}

Spectral region	Contribution to ds^{++}/de	Contribution to s^{++}
$\epsilon_1 \sim \omega$, $\epsilon_2 \sim I^{++}$	$\sim \sigma^+/I^{++}$	$\sim \sigma^+$
"Edge" region		$(0.092\ \sigma^+/Z^2_{eff})$
$\epsilon_{1,2} >> I^{++}$	[a] $\omega << cR^{-1}$	[a]
$\epsilon_1 \epsilon_2 \leq (\omega + cR^{-1})(\omega/c^2)^{1/2}$	$\sim (\sigma^+/\omega)(I^{++}/\omega)^{1/2}$	$\sim \sigma^+(I^+/\omega)$
	[b] $\omega \geq c^2$	[b]
	$\sim \sigma^+/\omega$	$\sim \sigma^+$
		$(0.59\sigma^+/Z^2_{eff})$

It is seen, that the main contribution is coming from the "edge" region, which determines also the angular distribution: one of the photoelectrons, the slow one, is an s-electron, while the other is a p-electron. The contribution of equal energy fast photo-electrons region to the total σ^{++} cross section is suppressed, because two unbound electrons cannot absorb a dipole photon. Nevertheless, if one considers this part of the spectrum, he will observe electrons which are strongly angular correlated, their total momentum being small.

Nondipole effects in the energy distribution of photoelectrons are already considerable at ω=137 I^+, what is illustrated in Fig. 1 [4]. Indeed, a maximum appear just in the middle of distribution, i.e. for ϵ_1, ϵ_2. This prediction is waiting for its experimental verification.

Of some, but perhaps pure academical interest is the study of photoionization at relativistic energies, $\omega \sim c^2$, where, as is seen in Fig. 1 again a minimum appears at $e_1=e_2$. However the maximas in intermediate region become more and more important with growths of ω [5]. Although the cross sections, both σ^{++} and σ^+, are very small, their ratio is increasing, reaching the value $0.59/Z^2$, i.e. by a factor of 6 bigger than in the nonrelativistic region. This ratio is increasing rather fast being equal to $0.37/Z^2$ at $\omega=2c^2$.

However, the entire process with ω growing is no more a pure photoionization: it starts to be accompanied by secondary photon emission and then by electron-positron pair creation.

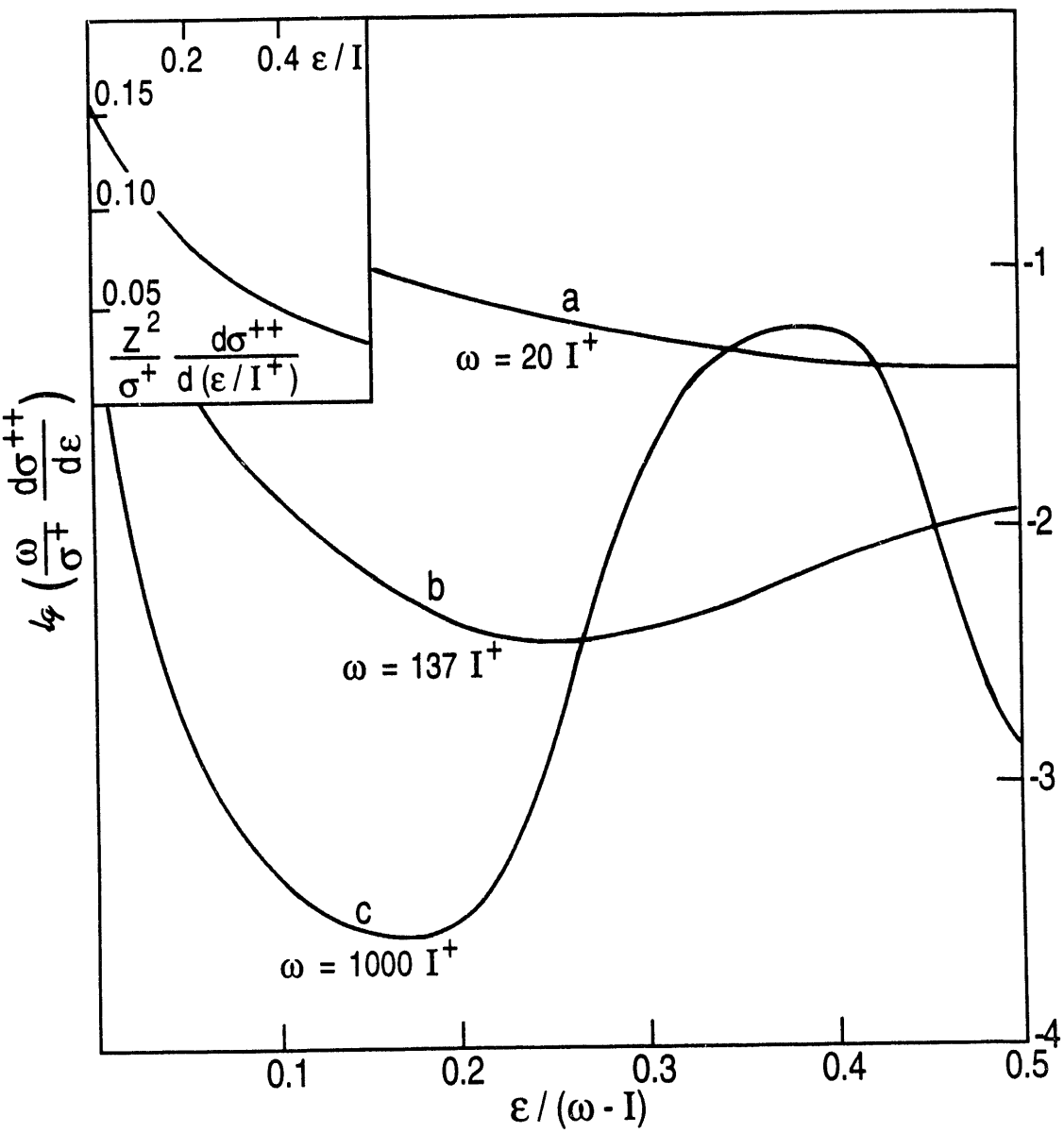

Fig. 1. *Energy distribution of photoelectrons in double ionization of He and He-like ions.*

4. Improvement of the model

As it is seen from Table 1, the main contribution to σ^{++} is coming from that part of the energy distribution, where one electron is slow while the other is fast. It was demonstrated also, that the intermediate electron in (1c) is predominantly slow. Therefore its interaction with the second electron must be taken into account nonperturbatively, substituting the first order contribution (1a) (1c) by a precise ground state wave function. It should be kept in mind, that a reasonably accurate variational wave function can be rather inaccurate for calculating the photoionization: different space regions are giving an important contribution to double electron photoionization cross section and to ground state energy. Rather complicated is to obtain the final state wave function, which would take into account the interaction of outgoing electrons with the vacancies and between each other. Of course, for sufficiently fast photo electrons the lowest order Born approximation is valid but the corresponding small parameter is the quantity $p(I/\omega)^{1/2}<<1$, which is decreasing slow. For instance, one has $p(I/\omega)^{1/2} = 0.16$ for helium at such a high frequency as 10 kev.

If corrections to the initial and final state wave functions are taken into account non-self consistently, the results of calculation become "gauge noninvariant", i.e. different in the "length", "velocity" and "acceleration" forms. Most fundamental is the length form, coming from the expression of photon-electron interaction ΔU:

$$\Delta U = \boldsymbol{j}\boldsymbol{A} = \mathbf{v}\boldsymbol{A} = \mathbf{r}\boldsymbol{A} \qquad (9)$$

where $\boldsymbol{j}(\mathbf{r})$ is the electron current and $\boldsymbol{A}$ is the vector potential of the electromagnetic field. But for all local many-body Hamiltonians with interparticle interaction depending only upon the interparticle distance all three forms - "length", "velocity" and "acceleration" - are equivalent.

If interparticle interaction V is taken into account perturbatively, the forms $\mathbf{r}$, ∇ and ∇ are equivalent if all terms of the photoionization amplitude in a given order of V are taken into account. If, however, the interelectron interaction is included nonperturbatively even partly, the "gauge invariance" can be restored only if some other corrections in V will be included also nonperturbatively.

Namely, if the one-electron potential is calculated in Hartree approximation, $\mathbf{r}$ and ∇ forms are equivalent, but ∇ is not. Its equivalence can be restored if the matrix elements of the photon-electron interaction are calculated not in single-electron approximation but in Random Phase Approximation (RPA). If the one-electron potential is taken in Hartree-Fock approximation, $\mathbf{r}$, ∇ and ∇ are nonequivalent. To restore the equivalence Random-Phase Approximation with Exchange (RPAE) must be used to calculate the photon-electron matrix element interaction instead of one-electron approximation. So, if in diagrams (1) the one-electron (vacancy) states are Hartree-Fock ones, the photon-electron interaction must be taken into account in RPAE, i.e. include an infinite system of diagrams:

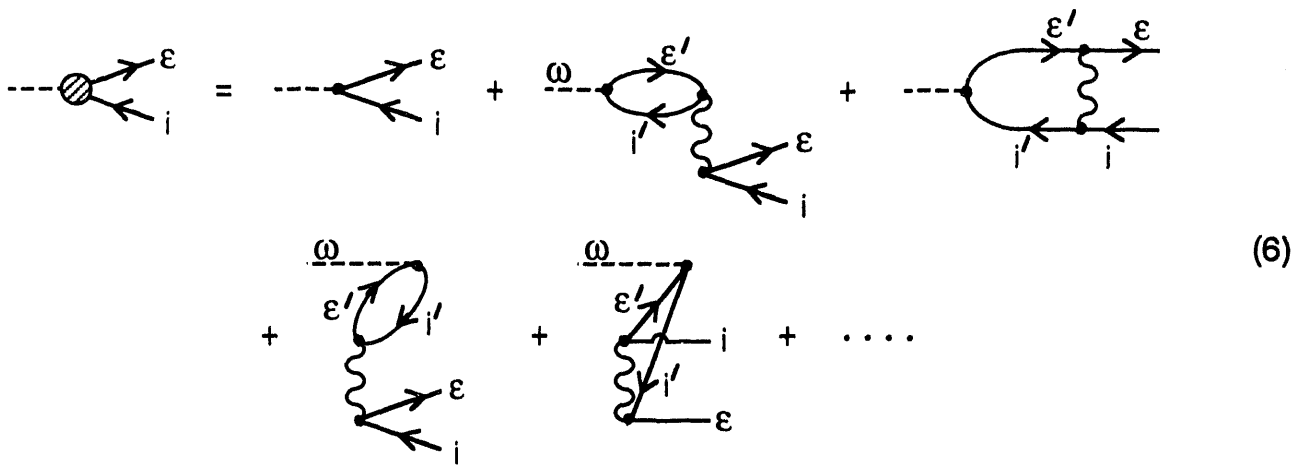

(6)

The vertex (6) when being a part of a more complicated diagram like that describing double electron photoionization (1), can violate the energy conservation law, having $\epsilon+I_i \neq \omega$.

So, it is known how to establish "length", "velocity", and "acceleration" forms equivalence when the double electron photoionization is studied using perturbation theory approach. However each diagram's contribution is not "gauge invariant". For example, in high energy limit in the "velocity" form the main contribution is coming from (1a) and (1c), while in the "length" form the contributions of (1b) and (1c) are much bigger and therefore have almost to compensate each other.

For atoms more complex than He higher order corrections are important not only to restore the "gauge invariance". For example, if energy transferred to the second electron is close to intermediate multielectron sub-shell (like $4d^{10}$) ionization potential, the modification of the interelectron interaction due to virtual excitation of this subshell must be taken into account. This is exemplified by the following diagram (compare to (1c)).

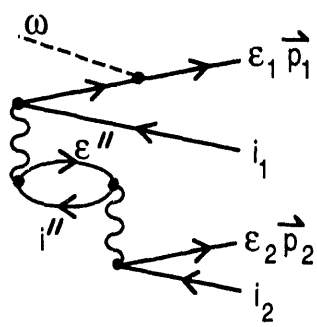

(7)

Atoms heavier than helium are very interesting objects for investigating double electron photoionization: for them the σ^{++}/σ^{+} ratio is much bigger reaching for example 0.6 just below the $4d^{10}$ ionization threshold in Xe.

For noble gases an important and not completely clear similarity exist between calculated in

RPAE with Hartree-Fock thresholds photoionization cross sections of the subvalent ns^2 subshells and the double electron photoionization cross sections, which is illustrated by Fig. 2, where rather complicated curves, presenting double photoionization cross section frequency dependence are depicted together with the cross section σ^+ for ns^2-subshells.

Recently it became clear that for multielectron atoms slow electron in double ionization are formed not directly, as it is described by (1), but to large extent via a higher order mechanism, mainly that including the satellite excitation [6], which is exemplified for Ar by (8).

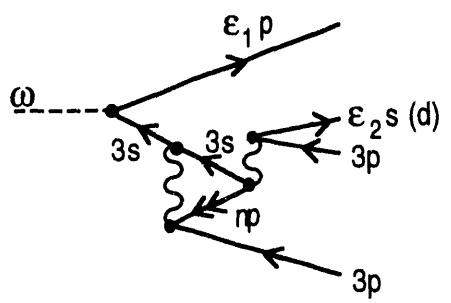

(8)

The intermediate state in (8) - $\epsilon_1 p, np; 3s^{-1}3p^{-6}$ - is a satellite state $np3p^{-1}$ in an ion with a vacancy 3s. However, this satellite excitation can decay by autoionization of a 3p electron, thus leading to double-ionization. The demonstration and account of the role of higher order diagrams require much more efforts of both the experimentalists and the theorists.

5. Multiple photoionization near inner shell thresholds

For complex atoms the increase of photon energy leads to the opening of new channels connected with intermediate and inner shell ionization. The subsequent Auger decays result in multiple charge ion production. The Auger-processes are accompanied by shake off, direct knock-out and the interference of them. As a result, the total ion charge yield is increasing and the upper degree of ionization is higher than what could result from pure step-by-step Auger decay.

Entirely, the calculation of a given charge ion yield as a function of frequency is a complicated problem. However the increase of the cross section of multiple ionization near inner or intermediate shell thresholds can be described or parameterized rather easy.

Indeed, close to the inner shell i threshold two simplest diagrams are singular, namely those given in (9):

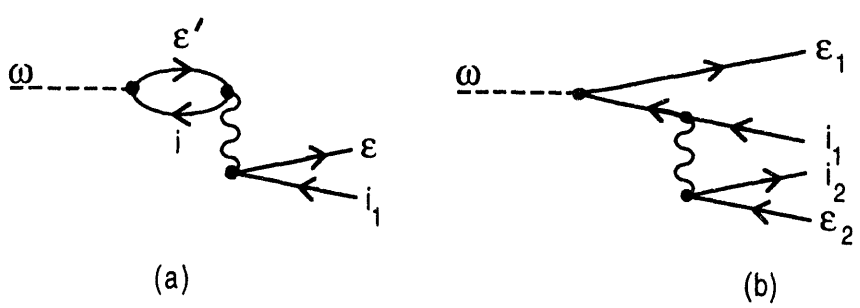

(9)

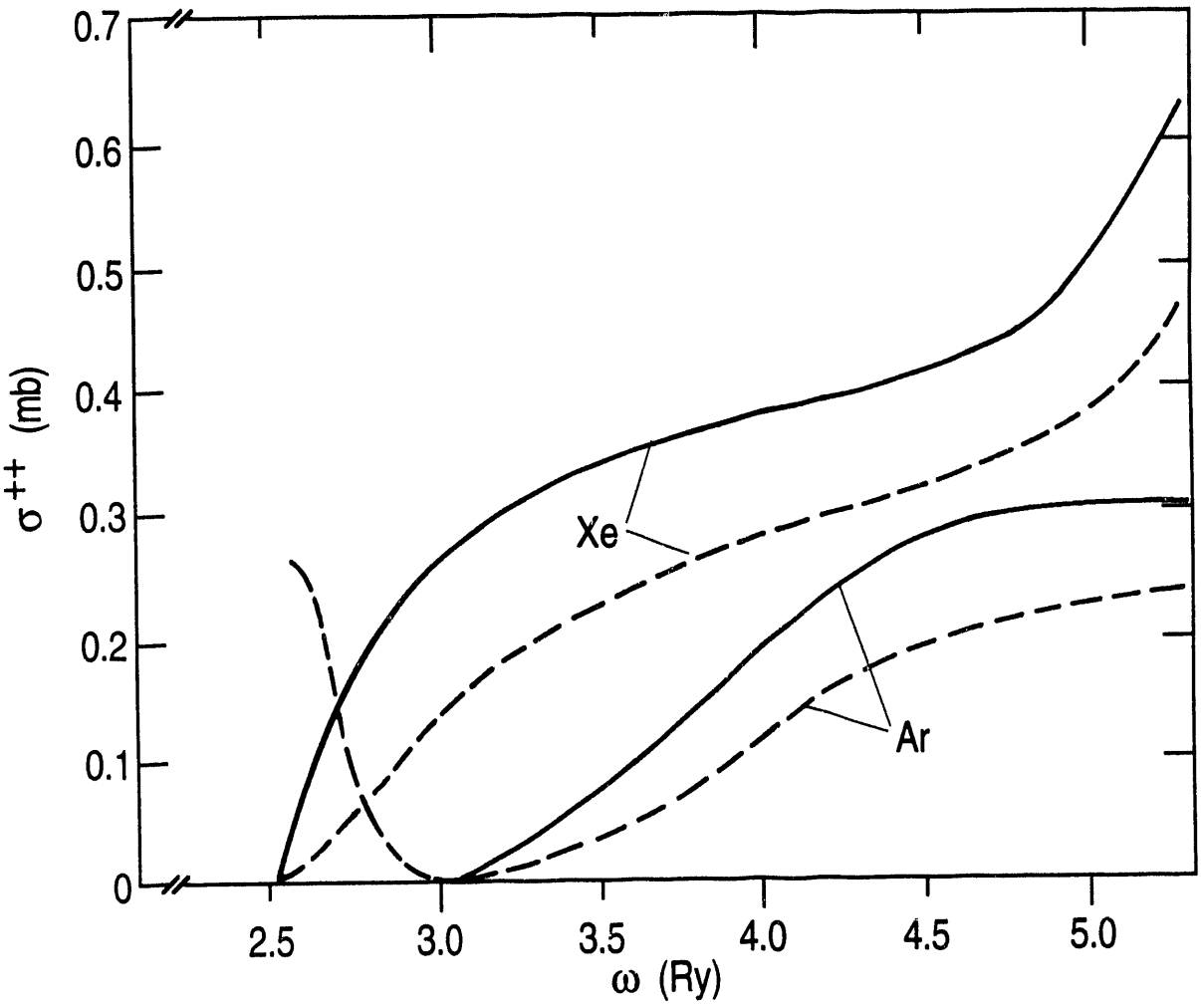

Fig. 2. *Double electron photoionization cross section of Ar and Xe*
solid lines - σ^{++} *dashed lines* - σ^{γ}_{ns2}, $3s^2$ *for Ar and* $5s^2$ *for Xe.*

The diagram (9a) is not increasing the ion yield anywhere except the proximity of i-shell ionization threshold. On contrary, (9b) for w above the threshold describes the contribution of Auger-process which leads to increase of the degree of ionization above i-shell threshold. This same mechanism leads to increase of ion production well below the i-shell threshold, where it can be called quasi-Auger process. Assuming that the cross section of i-shell photoionization $\sigma_i(\omega)$ depends weakly upon w near threshold, the contribution of (9b) can be presented as:

$$\Delta\sigma(\omega) = \left[\frac{1}{2} + \frac{1}{\pi}\mathrm{arctg}\frac{2(I_i - \omega)}{\Gamma_i}\right]\sigma_i(I_i)\ , \qquad (10)$$

where Γ_i is the total width of the vacancy i and I_i is its ionization potential. Note, that the contribution of the second term in (10) is quite noticeable well below i-shell threshold. The increase of the cross section of the (+n) ion production below i-threshold is given by the formula:

$$\Delta\sigma^{+n}(\omega) = \frac{1}{2\pi}\frac{\Gamma_i}{I_i - \omega}\sigma_i^{+n}(I_i) \ . \tag{11}$$

Here $\sigma_i^{+n}(I_i)$ is the contribution of the inner-shell ionization to (+n) ion production above i-shell threshold.

The expression for the mean charge, produced in ionization, as a function of photon frequency is also quite simple:

$$N_i(\varepsilon) = \frac{N_i^- \varepsilon + N_i^+ \beta}{\varepsilon + \beta} \ . \tag{12}$$

Here $\epsilon=2(I_i-\omega)/\Gamma_i$ and $\beta=\frac{1}{\pi}\frac{\sigma_{i+1}(I_i)}{\sigma_i(I_i)}$. In (11) N_i^- (N_i^+) is the mean ion charge well below (above) the i-threshold and $\sigma_{i+1}(I_i)$ is the biggest cross section of the outer (compared to i) subshell. The mean ion charge $N_i(\epsilon)$ is defined in (12) as

$$N_i(\varepsilon) = \sum_{n=1} n\sigma^{+n}(\varepsilon) \Big/ \sum_{n=1} \sigma^{+n}(\varepsilon) \tag{13}$$

The summation in (13) is performed over all possible degrees of ionization, starting from n=1.

Expression (12), just as (10) or (11), can be directly compared with the experimental data and used to parametrize the experimentally observed dependences. These expressions are much more general than the simple diagram (9a), employed at the first step of their derivation. The results of calculations, with the help of (12), for Ar 1s-threshold vicinity, along with the experimental data [7] are presented in Fig. 3.

The agreement with experiment can be considerably improved if one uses N^- as an adjustable parameter or observed quantity, which is illustrated by the dashed curve in Fig. 3.

Note, that $N_i(e)$ is much smoother than $\Delta\sigma(\omega)$, which is seen from (10)-(12) as well as from the experiment.

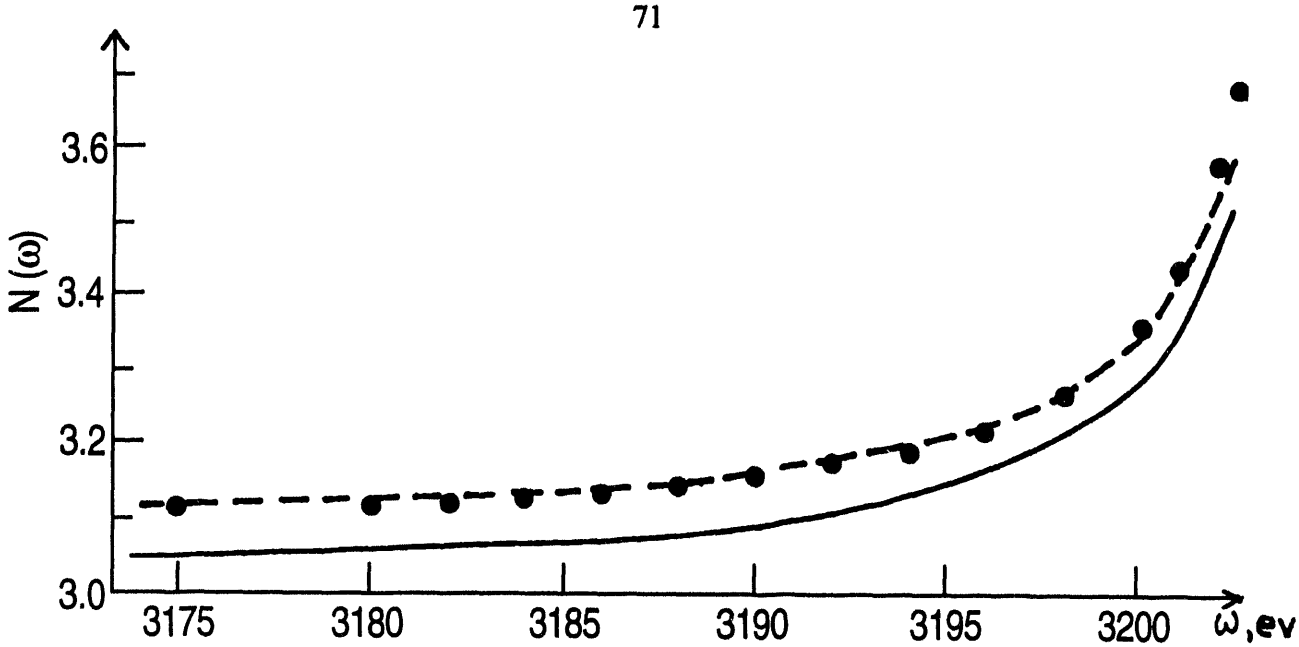

Fig. 3. *The mean charge of ions produced in Ar photoionization. solid line - calculations, dots - the experiment [7] dashed line - calculated curve shifted to experimentally observed N.*

6. Double ionization accompanying Compton-effect

With increase of ω the single and double photoionization cross sections are decreasing very fast, because the required recoil from the nucleus continues to grow up to rather high photon energy $\omega \sim c^2/2$. Therefore the Compton cross section σ_c starts to be important, although being of higher order in the fine structure constant as compared to the photoionization cross section $\sigma_{ph}(w)$. The following relation can be used to estimate the frequency at which they are equal

$$\sigma_c \approx \frac{8\pi}{3c^4} = \sigma_{ph}(\omega) \tag{14}$$

with $\sigma_{ph}(w)$ given in hydrogen-like approximation by:

$$\sigma_{ph}(\omega) = 0.1729 \frac{Z_{eff}^5}{\omega^{7/2}} . \tag{15}$$

Here Z_{eff} is the effective nuclear charge. For He the equation (14) leads to $\omega \approx 5.25$ kev. At higher frequencies Compton effect becomes absolutely dominating. Contrary to photoionization, this process can proceed on unbound electrons, their energy being increased by ΔE:

$$\Delta E \approx \frac{\omega^2}{c^2}(1-\cos\phi) + \vec{p}_1(\vec{k}_1 - \vec{k}_2) . \tag{16}$$

Here $\mathbf{p}_1 \sim 1$ is the initial state atomic electron momentum, $\mathbf{k}_1(\mathbf{k}_2)$ are initial (final) photon momenta. If DE is bigger than one-electron ionization potential, Compton scattering is accompanied by ionization. If DE is bigger than the energy, required to eliminate two electrons off the atom, double charged ions can be produced in Compton scattering. The important role of this process in connection with two-electron ionization was recognized and emphasized only recently [2].

In order to describe double electron ionization in Compton process, let us use the diagrams (see (1)) of lowest order in interelectron interaction.

The operator, describing the photon-electron interaction is given by:

$$\Delta H = \frac{1}{2c^2} A^2 + (\frac{1}{c}\vec{p}\vec{A})^2 . \qquad (17)$$

Therefore, two groups of diagrams appear - that with first term of (17) and that with the second term of (18) i.e. diagrams (19) and (20), respectively.

The double ionization caused by the term $A^2/2c^2$ is presented by:

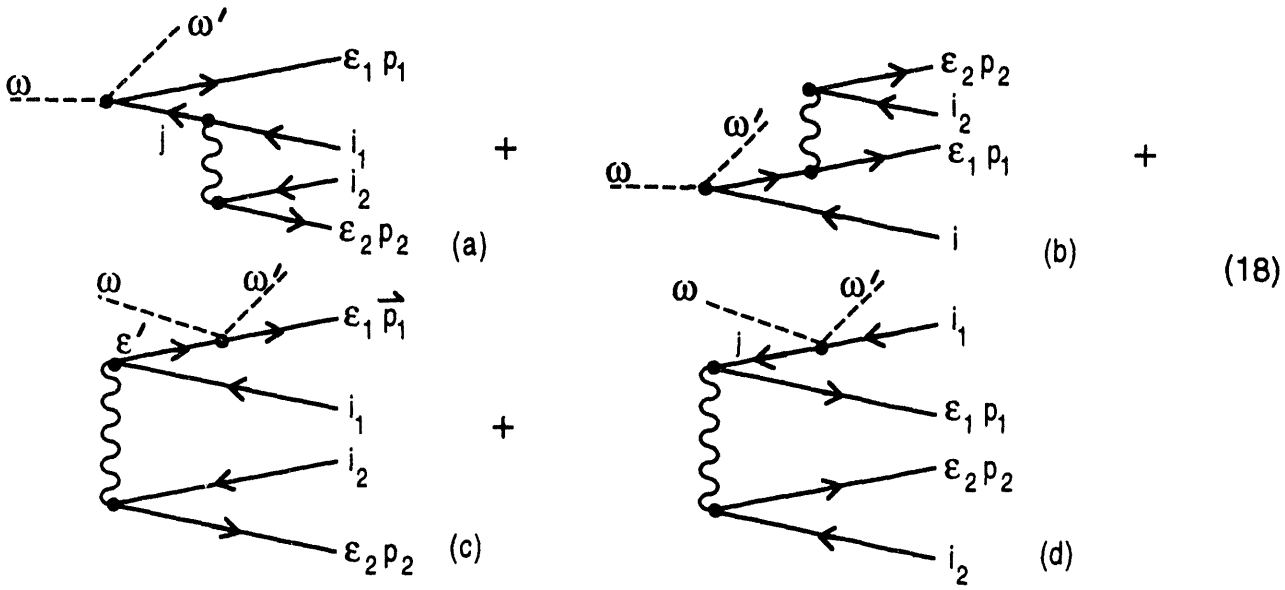

These are the so-called sea-gull diagrams. For He in its ground state $i_1=i_2=1s$.

The second group, with $\left(\frac{1}{c}\vec{p}\vec{A}\right)^2$ operator, includes more different diagrams originating from (1).

But having in mind that the Compton effect is accompanied by energy transfer to the atom which is much less than ω or ω', only diagrams with comparatively small virtually and small energy transferred via Coulomb interelectron interaction must be considered as potentially important.

These are the following:

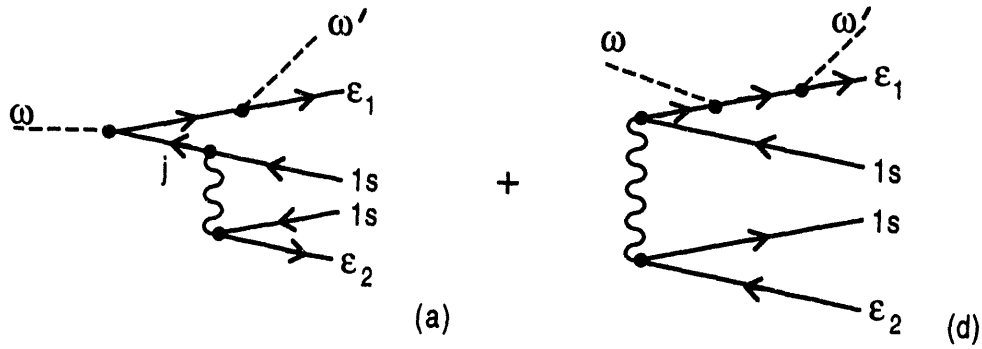

(19)

Examples of diagrams, which contributions are small due to big energy transfer via Coulomb interaction are given by:

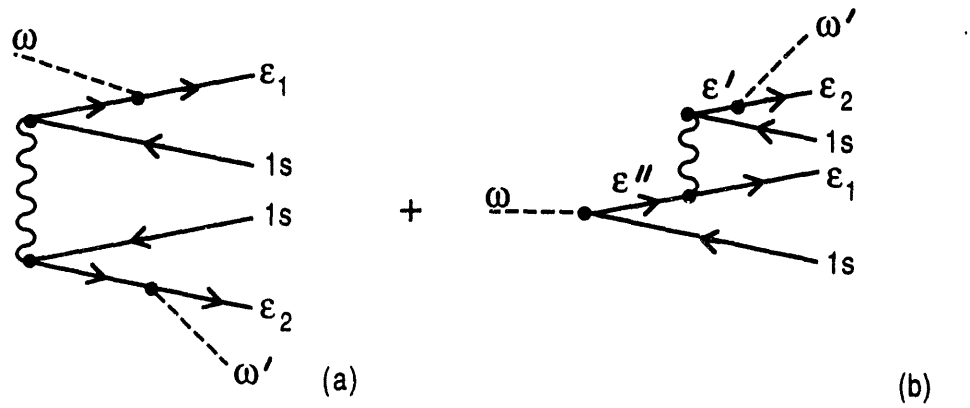

(20)

It is seen, that the photoabsorption or Compton scattering diagrams which give the main contribution to the double ionization amplitude looks similar:

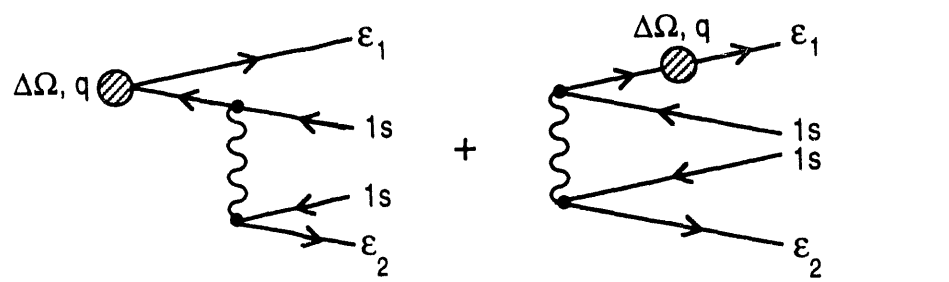

(21)

where the dashed circle presents the "external field-atomic electron" interaction operator. One-electron ionization is given by the following diagram:

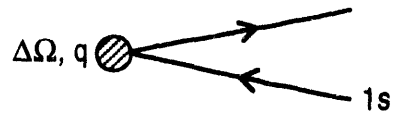

(22)

where $\Delta\omega$, q is the energy and momentum transferred from the external field to the atom. So, if $\Delta\omega$ is sufficiently high, the ratio σ^{++}/σ^{+} becomes independent upon the specific structure of the external ionizing field and equal to the corresponding value for photoionization.

A rather general discussion about the σ^{++}/σ^{+} ratio for different external fields, including that of a fast charged particle, took place long ago [5] and is supportive to our conclusion. Indeed, it is emphasized in [5], that for any external field action, i.e. for any "virtual" photon exchange the ratio σ^{++}/σ^{+} is the same as for photoionization. However, while $A^2/2c^2$ terms are equivalent to an external field, being similar to the fast electron action upon an atom, the $\left(\frac{1}{c}\vec{p}\vec{A}\right)^2$ operator, which leads to virtual electron excitation as an intermediate state, is not.

The entire problem of Compton scattering as a mechanism for double electron ionization requires quantitative theoretical analysis as well as further experimental investigation. Having quite different from that for a single photon ratio of the transferred energy to the transferred momentum, Compton-effect will help to discover new and interesting features of the double-ionization process. Being in essence similar to the fast electron by the relation between transferred energy and momentum, the Compton-effect differs from that process by the lack of the second Borh corrections. So, Compton-effect will lead to double ionization process which is different from that caused by either a single photon or a fast electron.

7. The investigation of secondary photon emission in coincidence with double charged ion production

The investigation of double ionization in coincidence with secondary photon emission would be very interesting. As a target for the first step of such research program He atom is convenient. The observation in coincidence of an α-particle and a secondary photon would prove that the double ionization is accompanied by photon emission. It is of interest to study the cross section of this process as a function of incoming photon energy, starting from several kev and up to several dozens of kev. Of interest is the consideration of the threshold region and the onset of this process as well as the region of high energy transferred to the atom.

For a given incoming energy it is interesting to study the cross section in a broad region of secondary photon frequency - from the double charged ion formation threshold down to lower frequencies. The results will give information on the target atom wave function in the ground

and excited states, including continuum. By studying the cross section of this process as a function of the ionized electrons kinetic energy, the information can be obtained on the role of electron motion in that Compton scattering which leads to double ionization. This information is essential in order to be able to understand at what energy and to which extent the double electron ejection takes place as if the pair of electrons would be unbound but correlated, and where the atomic binding is essential.

8. Concluding remarks

While the investigation, both experimental and theoretical, of double electron ionization of atoms by single photons was initiated more than two decades ago, the lack of high intensity sources of electromagnetic radiation almost completely stopped this activity. Without experimental support the theoretical work was also terminated. Now the situation is changing rapidly. Many publications considering double electron photoionization in high, medium and low energy region appeared recently and are on the way. Unexpectedly, the double electron photoionization became connected with Compton effect, making all the domain even more exciting and interesting. It is desirable to pay much more attention also to other than He targets, from H^- to heavier and more complicated atoms.

The investigation in this field are of great importance for understanding of the atomic structure and of the role of electron correlation in atoms.

References

1. J.C. Levin, D.W. Lindle, N. Keller, R.D. Miller, Y. Azuma, N. Berrah Mansour, H.G. Berry and I.A. Sellin, Phys. Rev. Lett. 67, 968 (1991).*
2. J.A.R. Samson, C.H Green and R.J. Bartlett, Phys. Rev. Lett. 71, 201 (1993).
3. M. Ya. Amusia and M.P. Kazachkov, Phys. Lett. A28, 1, 27 (1968).
4.. Ya. Amusia, E.G. Drukarev, V.G. Gorshkov and M.P. Kazachkov, J. Phys. B: Atom. Molec. Phys. 8, 1248 (1975).
5. E.G. Drukarev and F.F. Karpeshin, J. Phys. B: Atom. Molec. Phys. 9, 3, 339 (1976).
6. U. Becker and R. Wehlitz, Physica Scripta T41, 127 (1992).
7. J. Doppelfeld, N. Anders, B. Esser, F. von Busch, H. Scherer and S. Zinz, J. Phys. B: Atom. Mol. Opt. Phys. 26, 445 (1993).

---

*See also references and discussions in the talk of Y. Azuma at this workshop.

Double Photoionization of He at intermediate energies*

Nora Berrah

Physics Department, Western Michigan University, Kalamazoo, MI 49008

Abstract

The ratio of double-to-single ionization of He has been measured between 280 and 1210 eV to investigate its behavior in this partially unexplored region. These measurements, compared with the most recent theories of Pan and Kelly (private communication) and of Hino [Phys. Rev. **A 47**, 4845 (1993)], show the importance of including not only ground state but also final state correlations, in contrast to the high-energy behavior discussed by Dalgarno and Sadeghpour [Phys. Rev. **A 46**, R3591 (1992)] where consideration of final-state correlations proves inessential. Our intermediate-energy results also appear to indicate the importance of including higher-order effects in the theory.

---

1. Motivations:

(a) Need for experimental test, *in a three-body system*, of the spread in theoretical values for the process:

$$h\nu + He \dashrightarrow He^{+} + e^{-}$$

$$\dashrightarrow He^{++} + e^{-} + e^{-}$$

(b) Test the validity of theories that attempt to describe e^{-} - e^{-} correlations in a two-electron system.

(c) How does the ratio of double to single photoionization behave at intermediate energies?

(d) What is the relationship between e^{-} - e^{-} correlation in double photoionization and in the double ionization by charged particles?

2. Double photoionization of He at low energies (threshold - 400 eV)

3. Double photoionization of He at intermediate energies (280 - 1210 eV)

4. Angular distribution of He satellites $He^{+}n\ell$ (n=2-7)

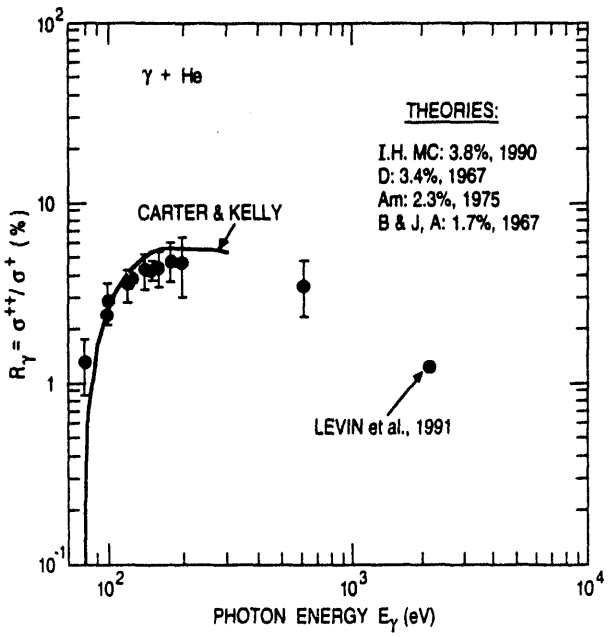

Figure 1. *Measurements of σ^{++}/σ^+ in helium; Data: T.A. Carlson, Phys. Rev.* ***156****, 142 (1967); V.A. Schmidt, N. Sander, H. Kuntzemuller, P. Dehtz, F. Wuilleumier and E. Källne, Phys. Rev.* ***A13****, 1748 (1976); D.M.P. Holland, K. Codling, J.B. West and G.V. Marr, J. Phys.* ***B12****, 2465 (1979).*

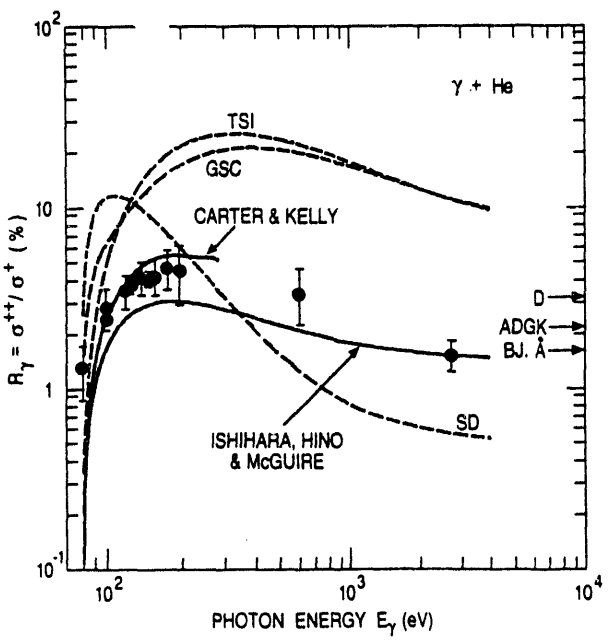

Figure 2. *Ratio of σ^{++}/σ^+ in helium versus photon energy; Ishihara, Hino and McGuire, Phys. Rev.* ***A44****, R6980 (1991).*

e-e correlation has also been studied using photoelectron spectroscopy of double photoionization of helium:

"Studies of Electron Energy and Electron Angular Distributions in the Double Photoionization of Helium", R. Wehlitz, F. Heiser, O. Hemmers, B.L. Anger, A. Menzel and U. Becker, Phys. Rev. Lett, **67**, (1991).
"Energy- and Angle-resolved Double Photoionization in Helium"; O. Schwarzkopf, B. Krassig, J. Elmiger and V. Schmidt, Phys. Rev. Lett, **70**, (1993).
"Angular Distribution of Electrons Following Double Photoionization", F. Maulbetsch and J.S. Briggs, Phys. Rev. Lett, **68**, (1992).

Double ionization of helium **by collision with fast projectiles** (ions, protons, antiprotons...)

Electron impact of He with He^+; J.A. Tanis et al, Phys. Rev. A, (1991).
Electron impact of He with U^{90+}; H. Berg et al, Phys. Rev. A, (1991).
Electron impact of He with p; B. Skogvall and Schieviets, Phys. Rev. Lett, (1990).
Electron impact of He with e^-; James Samson, Phys. Rev. Lett, (1990).
Electron impact of He with p and p^-; John Reading et al, Phys. Rev. Lett, (1989).

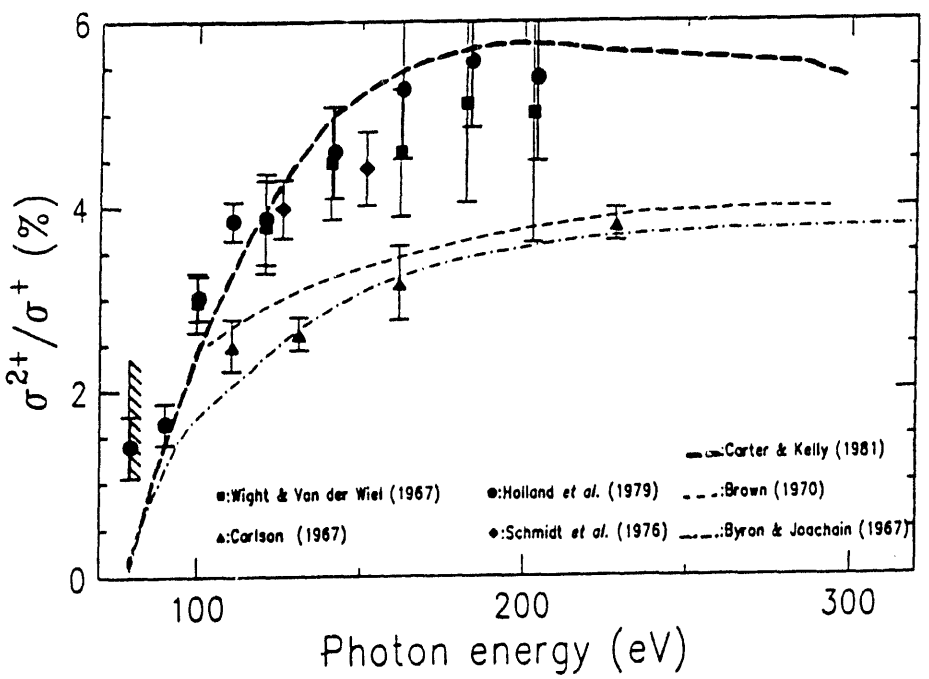

Figure 3. *Double photoionization of helium at low energies*

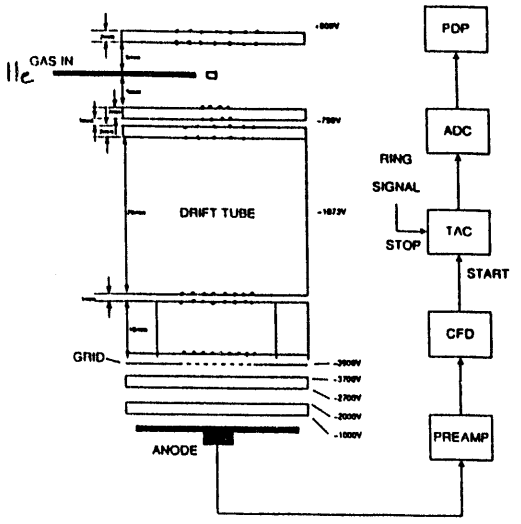

Figure 4. *Schematic of the time-of-flight apparatus.*

From Dietz et al, re high flux toroidal gratings: parameters: major radius = 116,000 mm; minor radius = 483 mm; dimension of ruled area = 100 x 30 mm^2; divergence behind exit slit < 2.6 mrad.

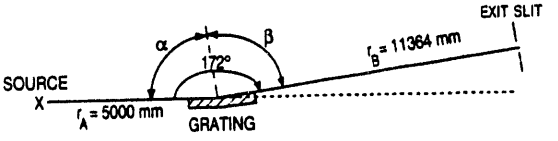

Figure 5. *Optical layout of the Fritz-Haber-Institut (FHI) high-energy toroidal grating monochromator (HE-TGM).*

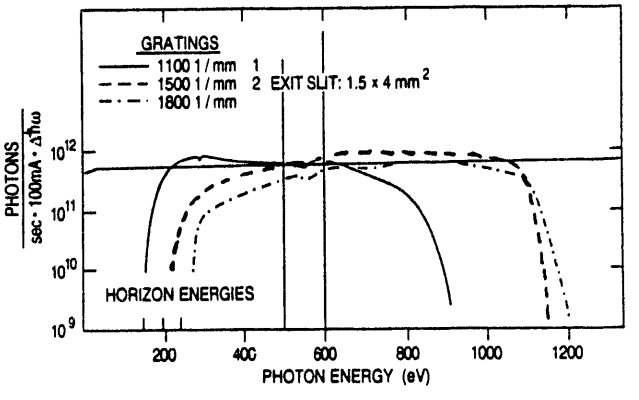

Figure 6. *Experimental photon flux measured for the METRO mode of the storage ring BESSY. The curves are obtained by recording the photo yield from a freshly-evaporated gold film and making appropriate corrections. TRhe calculated values of the horizon energies are indicated on the photon energy axis.*

POSSIBLE PROBLEMS:

(1) Higher order effects due to the monochromator
(2) Stray light contributions due to the monochromator or beamline or...

SOLUTIONS:

(1) For stray light: Use appropriate filters in the photon beam before the interaction of the target with the photons. The effect is of the order of 25%.
(2) For Higher orders: Quantify the effect by taking measurements above the edge of the appropriate filter and correct for it.
To be safe add an error of 5% to account for remaining stray light and higher orders. Kossman et al J. Phys. **B22**, L411 (1989); Holland et al J. Phys. **B12**, L411 (1979)

5. Conclusions

Efforts to reduce the experimental error bars are in progress.

We plan to extend the present measurements up to 2.8 keV for a complete comparison with the various theories.

6. Future Directions

Study electron-electron energy sharing with the electron-electron angular correlations.

The story of He is not finished yet!!!

More fun to come both experimentally and theoretically.

This work was completed in part at the Fritz Haber Institut der Max Planck Gesselschaft, Berlin, Germany, with Franz Heiser, Ralf Wehlitz, Scott Whitfield and Uwe Becker. Collaborators were Jon Levin, NIST, Maryland, and Ivan A. Sellin, UT/ORNL.

---

*Work supported in part by the U.S. Department of Energy, Office of Basic Energy Sciences, Division of Chemical Sciences.

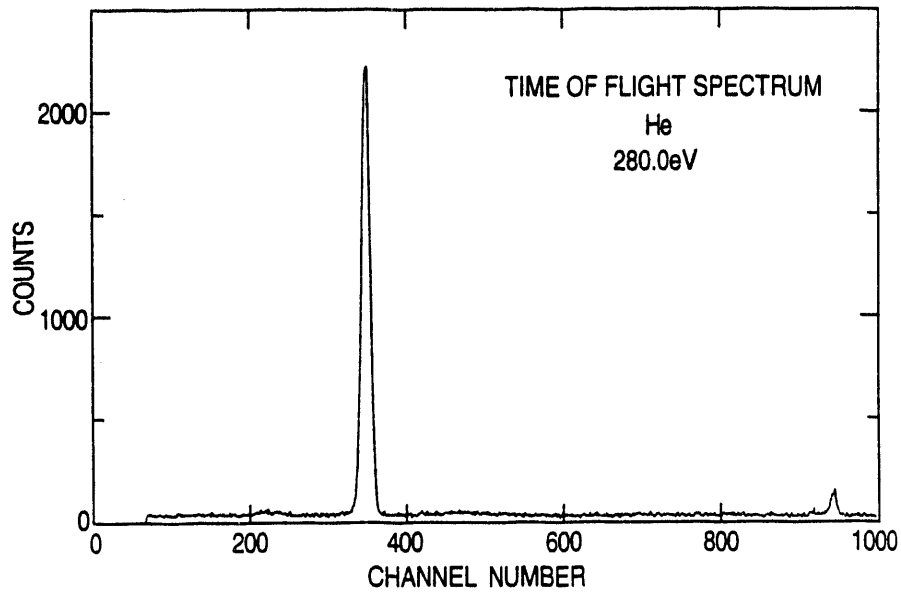

Figure 7.

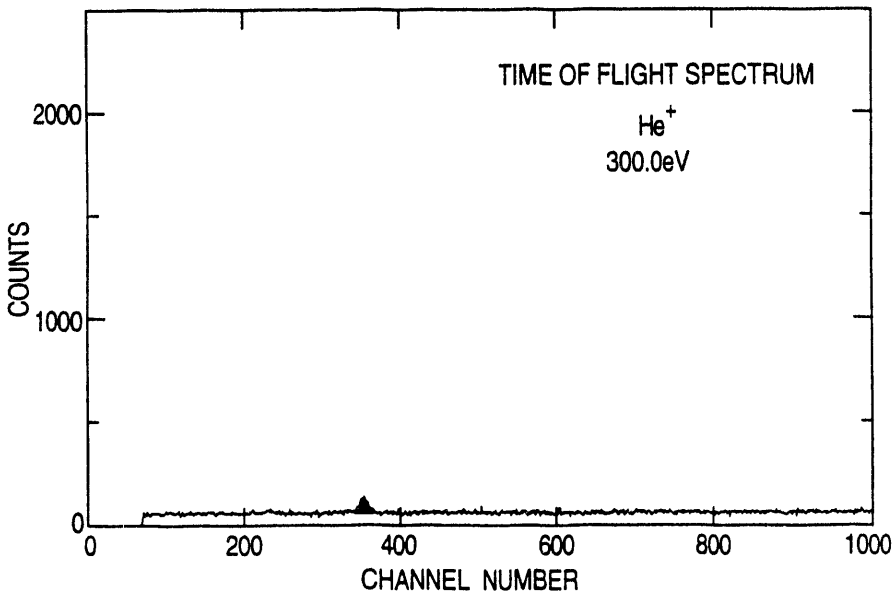

Figure 8.

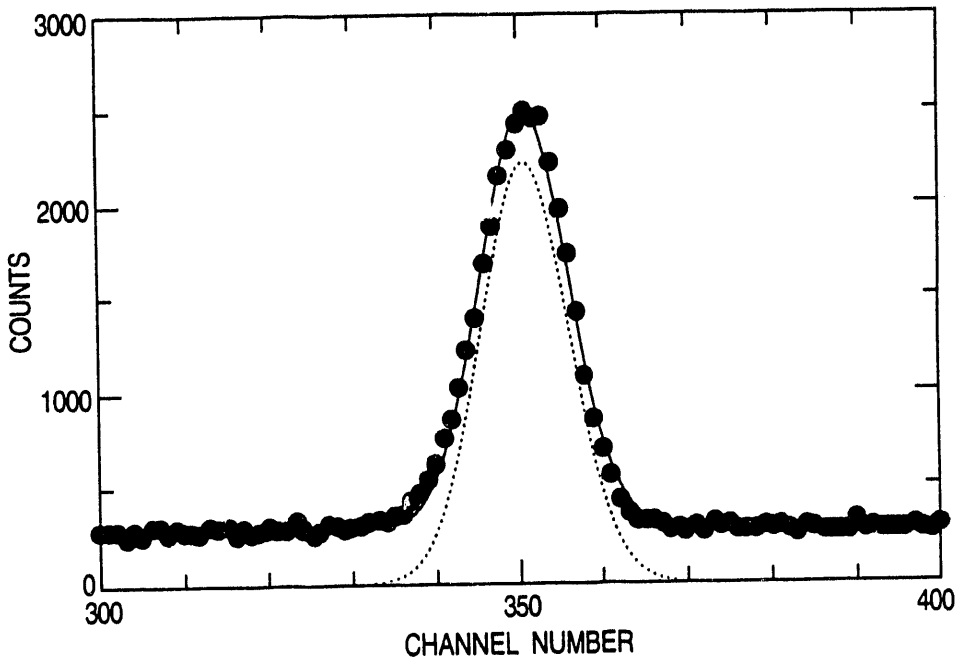

Figure 9.

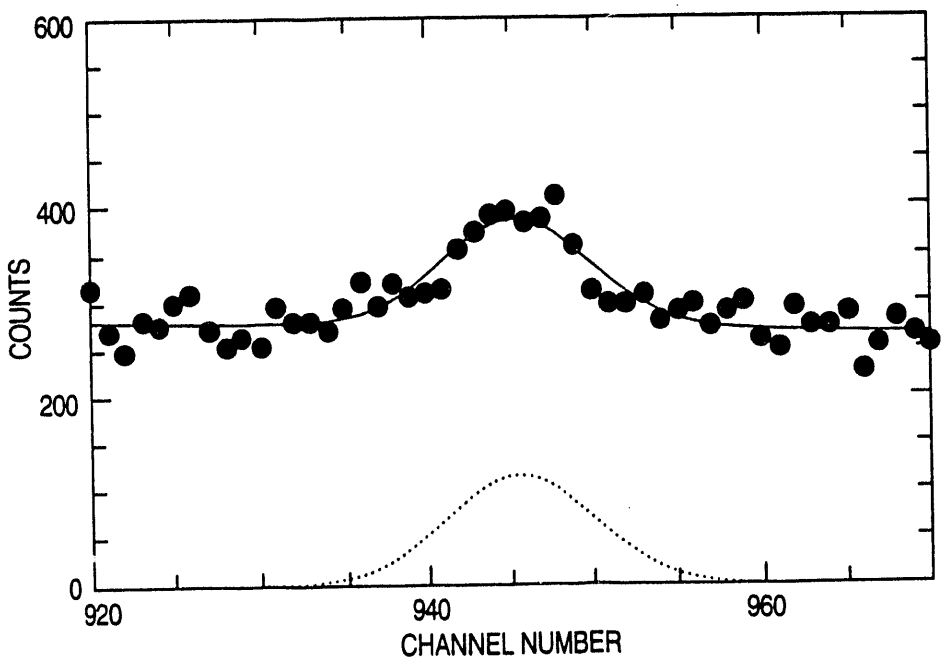

Figure 10.

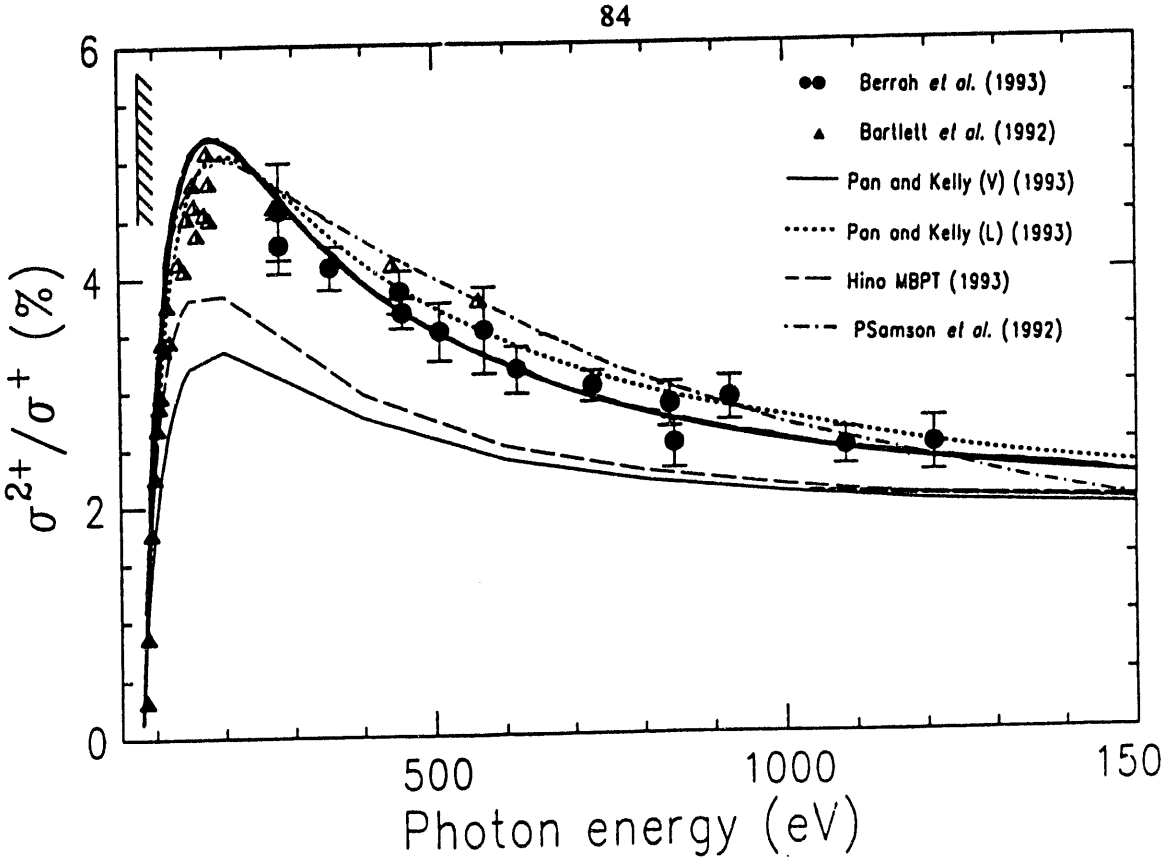

Figure 11. *Experimental and theoretical results for the charge state ratio at low energy.*

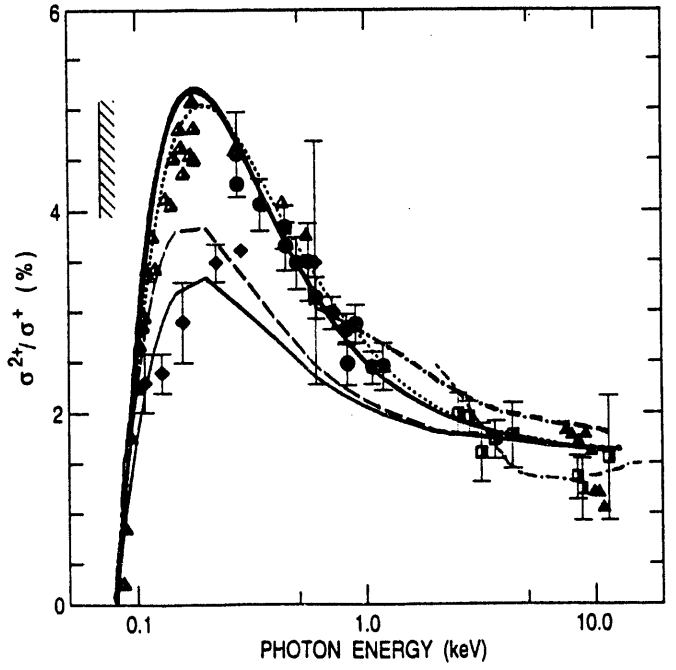

Figure 12. *Experimental and theoretical results for the charge state ratio up to 12 keV.*

Double Photoionization: Gauge Dependence, Coulomb Explosion, and ...

H. R. Sadeghpour, Zhuang Fan, and A. Dalgarno

Harvard-Smithsonian Center for Astrophysics, 60 Garden St., Cambridge, MA 02138 USA

Abstract

The high-luminosity synchrotron beams capable of stripping both electrons from helium at keV energies, provide experimenters [1-3] with the opportunity to test theoretical predictions [4-14]. The helium atom makes an ideal candidate for the experimental and theoretical studies due to its "cleanliness", and because it is a truly three-body neutral atomic system.

The physics involved in photoionization by high-energy photons is different from that in the low-energy photoabsorption process. Briefly, above the threshold for double escape, 79 eV for He, the configuration space available for photoabsorption is confined within a volume of radius $r \sim 1/k$, where $k=\sqrt{[2(\omega - E_0)]}$ is the momentum kick to the photoelectrons. As the frequency of the photons is increased, the configuration space shrinks to a smaller volume near the nucleus. The implications of this shrinking effect are three-fold: a) the phase-space for X-ray absorption will be small and dominated by the asymmetric sharing of photon energy by the two electrons, b) the electron-electron correlation in the final state will play a diminishing role with increasing photon energy, and c) the choice of the gauge for the electric dipole operator will be of importance for the correct description of the asymptotic double photoionization rate.

That an asymptotic limit of the single photoionization oscillator strength of helium exists was demonstrated by several authors [4-8] who showed that the continuum oscillator strength for exciting $He^+(n)$ states behave as

$$\frac{df_n^+}{d\epsilon} \sim C(ns)(2\epsilon)^{-7/2}, \qquad (1)$$

where ϵ is the energy available to the photoelectron in atomic units and $C(ns)$ are proportionality constants whose values are given by [4,7]

$$C(ns) = \frac{512\pi Z^2}{3} | < \Psi(r_1, r_2)|\delta(r_2)|u_{ns}(r_1) > |^2, \qquad (2)$$

where Z is the nuclear charge, $u_{ns}(r)$ is the usual hydrogenic radial wavefunction, and $\Psi(r_1, r_2)$ is the initial ground wavefunction for the two-electron atom or ion. In obtaining Eqs. (1) and (2), Stewart and Dalgarno [7] stressed that using the length of form of the dipole operator (they used the acceleration form) gave an incorrect $\epsilon^{-3/2}$ dependence of the oscillator strength with photon energy, if a Born final-state wavefunction is used.

Two remarks are in order regarding Eq. (2). Firstly, the problem is restricted to the *s*-manifold of $He^+(nl)$ states, as the higher angular momentum states contribute an additional factor of ϵ^{-l} to Eq. (1). Secondly, Eq. (2) is a mathematical confirmation of the shrinking volume effect in X-ray photoabsorption. As the hard photon "collides" with the atom, the full two-electron wavefunction collapses onto the nucleus, releasing a photoelectron with almost all of the photon energy and angular momentum, leaving the other photoelectron with little energy and zero angular momentum.

The asymptotic contribution from double plus single photoionization is obtained by invoking a sum rule as [7]

$$C \equiv \sum_n C(ns) + \int_0^\infty C(\epsilon' s)d\epsilon' = \frac{512\pi Z^2}{3} < |\Psi(r_1, 0)|^2 > . \qquad (3)$$

Equation (3) is particularly useful in that only a "good" representation of the initial state wavefunction is needed to calculate accurately the sum. The recent results by Samson *et al.* [15] (in this volume) gives a value for C = 346, approximately 10% larger than the asymptotic value of C=309.15.The ratio of the double-to-single ionization cross section is given asymptotically by

$$R = \frac{C}{\sum_n C(ns)} - 1. \qquad (4)$$

The ratio obtained for He, H^-, and Li^+, are respectively, 1.67, 1.50, and 0.87 [11].

This simple asymptotic analysis gives results in complete accord with *ab initio* calculations. Ishihara *et. al* [10] considered this agreement to be "fortuitous" because the asymptotic calculation ignores a certain many body perturbation (MBPT) process, known as the two-step one (TS1). In TS1, final state correlation between two electrons occurs when one outgoing electron interacts with the other electron en route to double escape. A possible resolution of this dilemma was offered in the form of the dependence of the MBPT diagrams on the choice of the gauge of the dipole operator. In short, it can be shown that the TS1 diagram has a different asymptotic behavior depending on the form of the dipole operator used. Specifically, the TS1 diagram acquires an extra inverse power of energy dependence in the acceleration gauge ($\epsilon^{-9/2}$). The *point* to be made here is that despite the independence of the final outcome on the gauge of the operator, individual amplitudes contributing to the final outcome exhibit characteristically

different behaviors with energy.

We have calculated the double-to-single photoionization ratio of helium at all energies by writing the final state wavefunction as an uncorrelated symmetrized product of hydrogenic function for $He^+(ns)$, $u_{ns}(r)$ with charge Z, and the Coulomb continuum electron, $f_{\epsilon p}(r)$ with unit charge, to calculate the asymptotic oscillator strengths in the acceleration gauge

$$\frac{df_n^+}{d\epsilon} = \frac{2}{3\omega^3} | < \psi_\epsilon(r_1, r_2) | d_1 + d_2 | \Psi(r_1, r_2) > |^2, \tag{5}$$

where ω is the photon energy in atomic units. The correlated ground state wave function is of the multi-configuration Hartree Fock (MCHF) type from C. Fischer, with 21 configurations [16]. All continuum oscillator strengths for exciting $He^+(ns)$ levels up to n=18 were calculated. The results are shown in Fig. 1(a) as functions of $1/n$ and ω. It is evident that at higher energies, the oscillator strengths tend to follow the n^{-3} trend more faithfully than at lower energies. At the limit $1/n = 0$, the total excitation plus ionization oscillator strength for ejecting a zero-energy electron and an $\epsilon = \omega - E_0$ electron with $l = 1$ angular momentum is obtained. Also shown in Fig. 1(b) is the dependence of these same oscillator strengths on energy and n. As a function of energy, the oscillator strengths approach the asymptotic (Born) limit set by Eq. (1), shown as the horizontal lines in Fig. 1(b). The excitation-ionization ratio is then found to have a limiting value of 8.93% as the asymptote [17].

The asymptotic procedure outlines above for atomic systems can also be extended to double ionization of molecular species such as H_2. Expressions similar to Eqs. (2) and (3) can be given as [18]

$$C(n\ell\sigma) = N | < \Psi(\mathbf{r}_1, \mathbf{r}_2) | \delta(\mathbf{r}_{2a}) + \delta(\mathbf{r}_{2b}) | \psi_{n\ell\sigma}(\mathbf{r}_1) > |^2, \tag{6}$$

where $N = 256\pi/3$, and r_{2a} and r_{2b} are, respectively, the position vectors from electron 2 to centers a and b, and

$$C = N < \Psi(\mathbf{r}_1, \mathbf{r}_2) | \delta(\mathbf{r}_{2a}) + \delta(\mathbf{r}_{2b}) | \Psi(\mathbf{r}_1, \mathbf{r}_2) > . \tag{7}$$

$\Psi_{n\ell\sigma}(r_1)$ are the electronic wave functions of H_2^+ in prolate spheroidal coordinates at the equilibrium internuclear separation $R = R_e$. For the ground state wave function of H_2, we employed the correlated wavefunction of James and Coolidge [19]. Only transitions in which the final state of H_2^+ has Σ symmetry participate in the photoionization process in the limit of high energies. The final asymptotic ratio of 2.25 for H_2 is compared with its united atom limit of 1.67% for He.

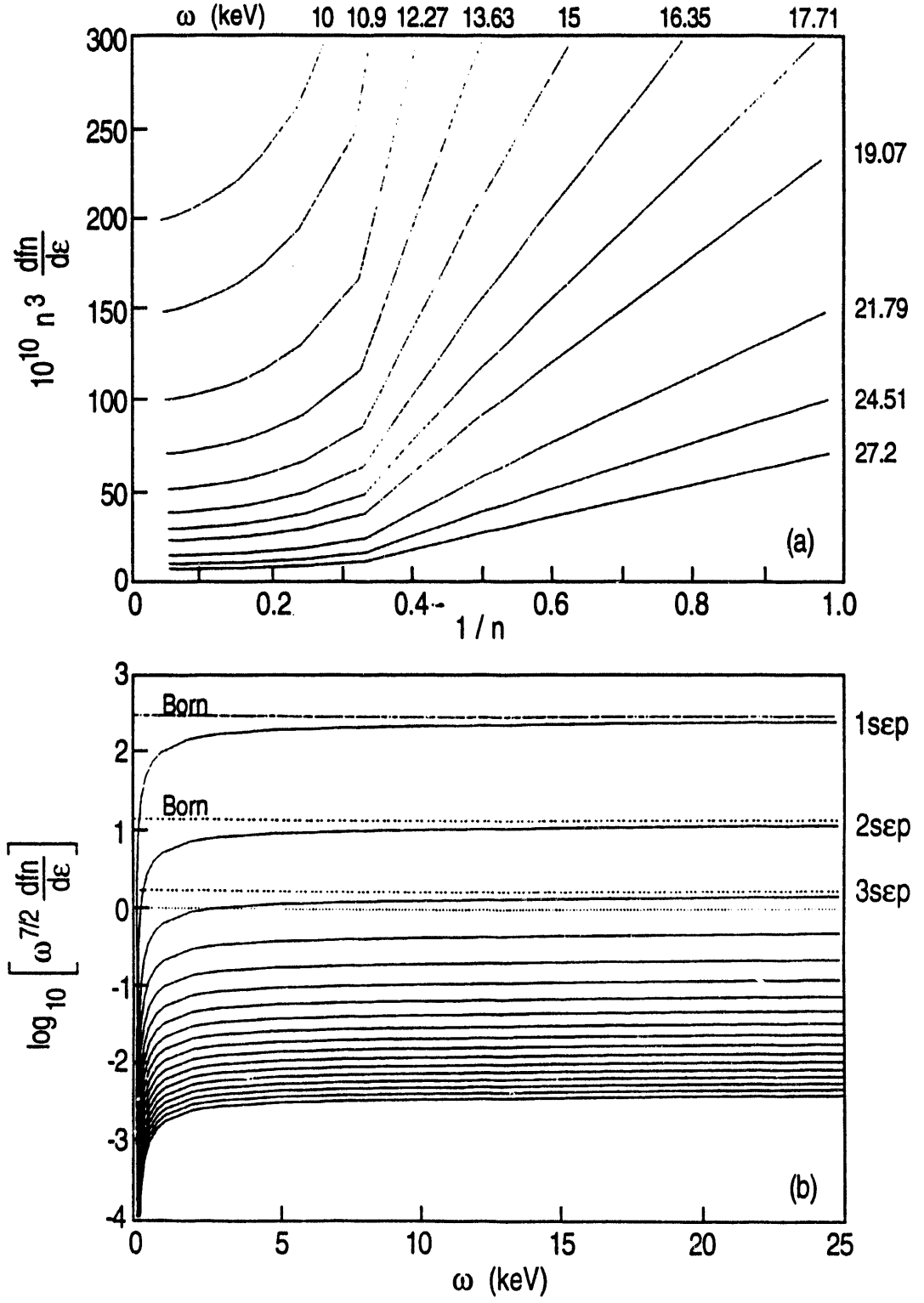

Figure 1. *Continuum oscillator strengths for helium.*

Interesting opportunities still await exploration in this field. In the Coulomb explosion case in H_2, the experimental signature for double photoionization is the release of two equal-momentum protons. In the case of H^-, the large continuum oscillator strength in the H(n=2) manifold causes the H^- case to become an anomaly in the helium isoelectronic series. In addition, the double ionization of metastable states of helium can provide a check on the effect of the correlation, not only in the final state, but also in the initial state configuration.

This work was supported by the US Department of Energy, Division of Chemical Sciences, Office of Basic Energy Sciences, Office of Energy Research. We thank C. Fischer for access to her MCHF wavefunction.

References

[1] J. C. Levin *et al.*, Phys. Rev. Lett. **67**, 968(1991).
[2] J. C. Levin *et al.*, Phys. Rev. **A 47**, R16(1993).
[3] Y. Azuma *et al* (To be published).
[4] P. K. Kabir and E. E. Salpeter, Phys. Rev. **108**, 1256(1957).
[5] F. W. Byron and C. J. Joachain, Phys. Rev. **164**, 1(1967).
[6] T. Åberg, Phys. Rev. **A 2**, 1726(1970).
[7] A. Dalgarno and A. L. Stewart, Proc. Phys. Soc. Lon. **76**, 49(1960).
[8] M. Ya. Amusia *et al* J. Phys. **B 8**, 1248(1975).
[9] R. L. Brown and R. J. Gould, Phys. Rev. **D 1**, 2252(1970).
[10] T. Ishihara, K. Hino, and J. H. McGuire, Phys. Rev. **A 44**, R6980 (1991).
[11] A. Dalgarno and H. R. Sadeghpour, Phys. Rev. **A 46**, R3591(1992).
[12] L. R. Andersson and J. Burgdörfer, Phys. Rev. Lett. **71**, 50(1993).
[13] K. Hino, Phys. Rev. **A 47**, 4845(1993).
[14] Z. Teng and R. Shakeshaft, Phys. Rev. **A 47**, 3487(1993).
[15] J. R. Samson *et al* (To be published).
[16] C. F. Fischer (private communication).
[17] Z. Fan, H. R. Sadeghpour, and A. Dalgarno (to be published).
[18] H. R. Sadeghpour and A. Dalgarno, Phys. Rev. **A 47**, R2458(1993).
[19] H. M. James and A. S. Coolidge, J. Chem. Phys. **1**, 825(1993).

Single and Double Ionization by high energy photon impact

Lars Andersson and Joachim Burgdörfer

Department of Physics, University of Tennessee, Knoxville, TN
and Oak Ridge National Laboratory, Oak Ridge, TN

1. Photoabsorption at high energies

2. Compton scattering

3. Intermediate energies

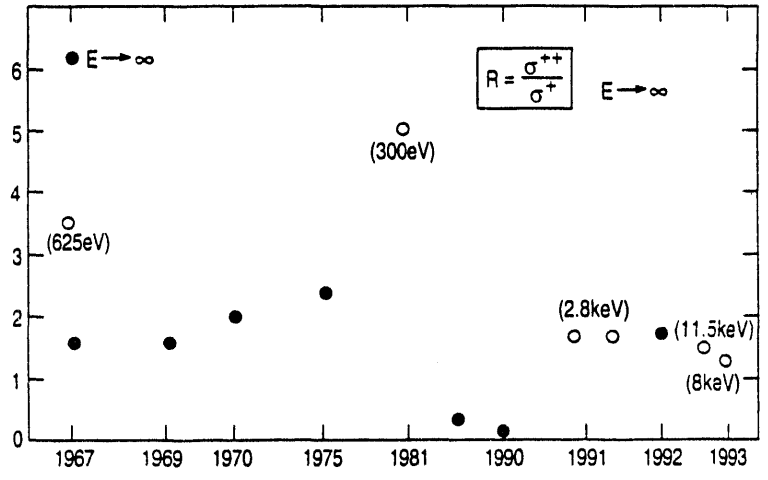

Figure 1. *Chronological development of the ratio of single to double ionization: References: 1967: Carlson; Byron and Joachaim; 1969: Aberg; 1970: Brown and Gould; 1975: Amusia et al; 1981: Carter and Kelly; 1990: Samson; 1991: Ishihara et al; 1992: Dalgarno and Sadeghpour; 1993: Levin et al, Bartlett and Samson.*

- Does a (non-relativistic) high energy limit exist?
- Behavior at finite energies?
- Relativistic corrections?
- Experimentally accessible?
- Connection to charged particle ionization?

Photoabsorption cross-section (acceleration gauge)

$$\frac{df^A(kLM,nlm)}{dE} = \frac{2k}{\omega^3}\left|\langle kLM,nlm\left|(\nabla_1 V+\nabla_2 V)_z\right|i\rangle\right|^2,$$

Final state (excitation - ionization)

$$\Psi^{(-)}_{k,nlm}(\mathbf{r}_1,\mathbf{r}_2) = \frac{1}{\sqrt{2}}\left[\Phi_{nlm}(\mathbf{r}_1)\,\Phi^{(-)}_{\mathbf{k}}(\mathbf{r}_2)\,D^{(-)}_{\mathbf{k}_{12}}(\mathbf{r}_{12}) + \mathbf{r}_1 \leftrightarrow \mathbf{r}_2\right]$$

Coulomb distortion factor

$$D^{(-)}_{\mathbf{k}_{12}}(\mathbf{r}_{12}) = \exp(-\pi\alpha/2)\Gamma(1-i\alpha)\,{}_1F_1[i\alpha,1,-i(k_{12}r_{12}+\mathbf{k}_{12}\cdot\mathbf{r}_{12})]$$

$$\frac{df^A(kLM,nlm)}{dE} = \frac{2k}{\omega^3}\left|\langle kLM,nlm\left|(\nabla_1 V+\nabla_2 V)_z\right|i\rangle\right|^2,$$

$$\Psi^{(-)}_{k,nlm}(\mathbf{r}_1,\mathbf{r}_2) = \frac{1}{\sqrt{2}}\left[\Phi_{nlm}(\mathbf{r}_1)\,\Phi^{(-)}_{\mathbf{k}}(\mathbf{r}_2)\,D^{(-)}_{\mathbf{k}_{12}}(\mathbf{r}_{12}) + \mathbf{r}_1 \leftrightarrow \mathbf{r}_2\right]$$

$$D^{(-)}_{\mathbf{k}_{12}}(\mathbf{r}_{12}) = \exp(-\pi\alpha/2)\Gamma(1-i\alpha)\,{}_1F_1[i\alpha,1,-i(k_{12}r_{12}+\mathbf{k}_{12}\cdot\mathbf{r}_{12})]$$

$$\sigma_s = \sigma^+_{ph} + \sigma^{++}_{ph} = \sum_{LM}\sum_{lm}\left[\sum_n \sigma^+_{ph}(kLM,nlm) + \int_0^{\infty(\omega-I_2)} dE'\,\frac{d\sigma^{++}_{ph}(kLM,k'lm)}{dE'}\right.$$

Evaluation by closure

$R = \sigma^{++}/\,\sigma^{+} \quad = \quad (\sigma_s - \sigma^{+})/\,\sigma^{+}$

The CDW Approximation (VPS, BBK)

Three body breakup amplitude

$T_{123} \approx T_{12}^{c}\ T_{13}^{c}\ T_{23}^{c}$, where T_{ij}^{c} (i or j=3) is the two-body Coulomb amplitude, and T_{12}^{c} is the e-e amplitude. These lead to

==> Electron scattering "on the way out"

==> Gamov singularity at threshold $\approx \exp(-2\pi/v)$

==> Validity only at high energies

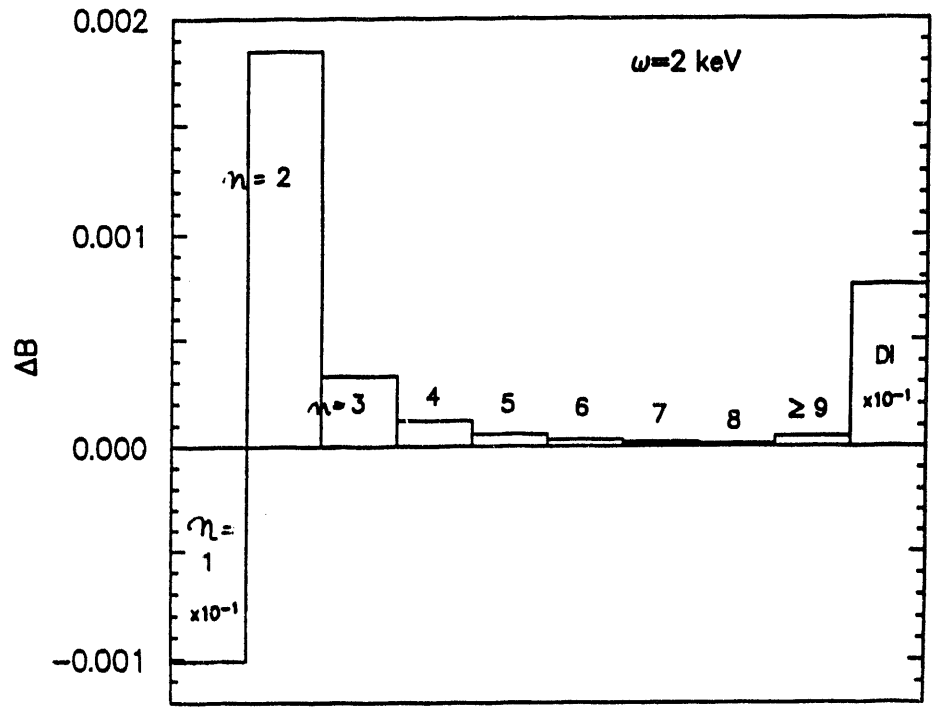

Figure 2. *Effect of final state correlation.*

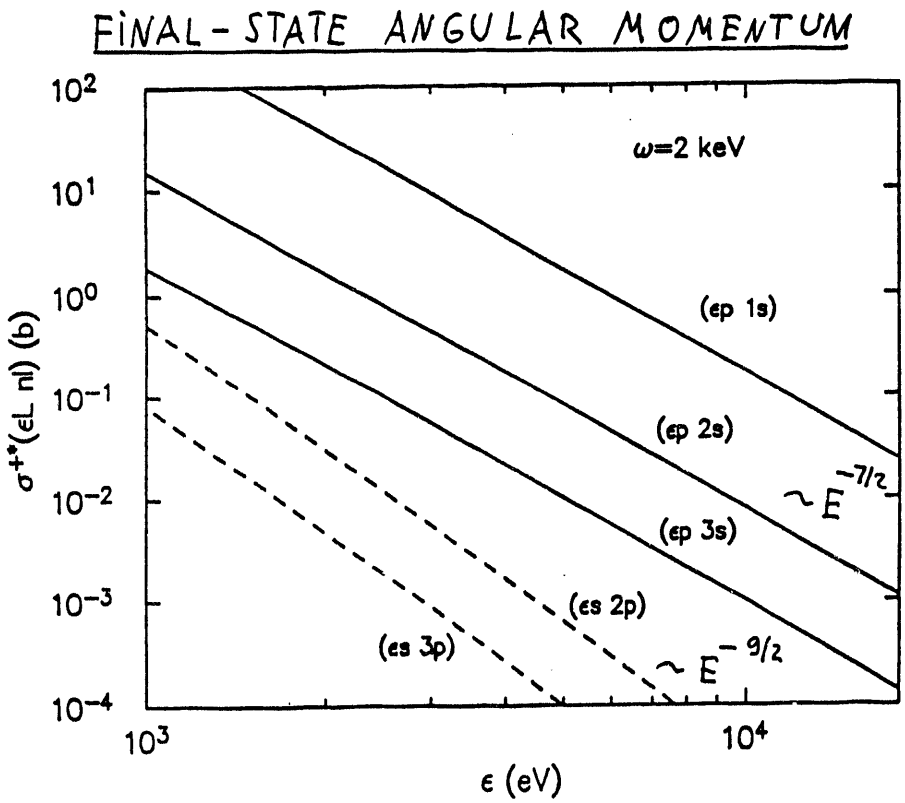

Figure 3. *Final state angular momentum.*

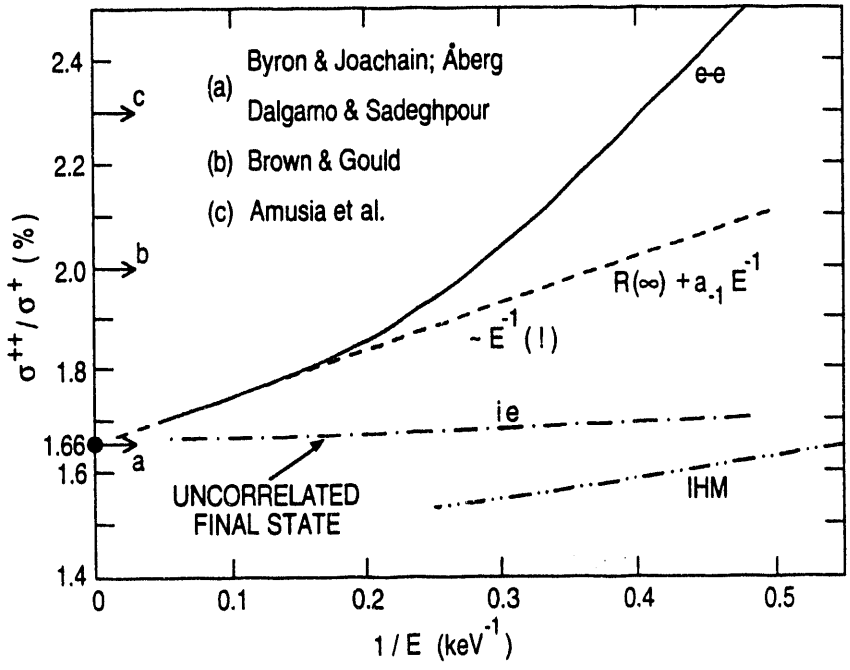

Figure 4. *Asymptotic photoabsorption cross section.*

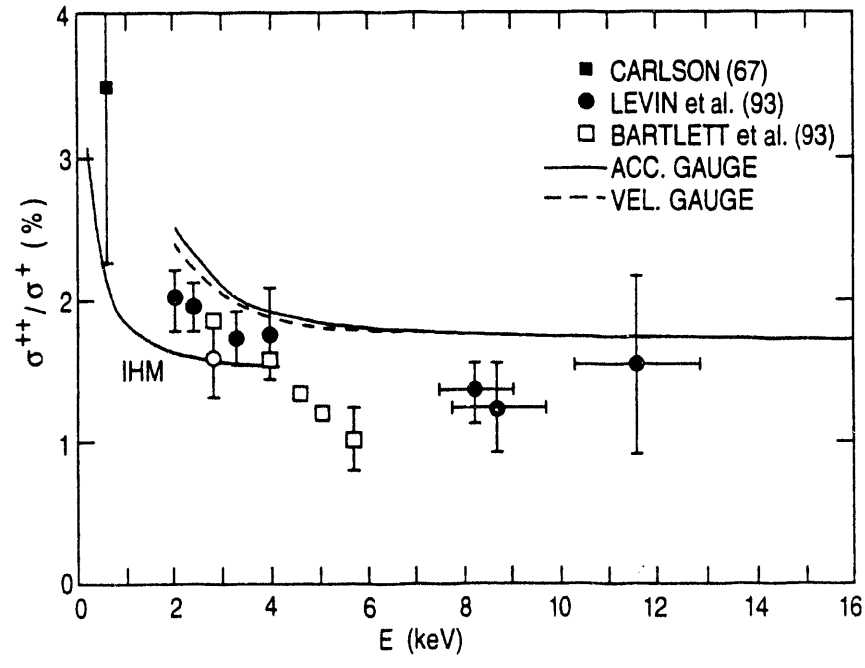

Figure 5. *High energy photoabsorption: comparison with experiment.*

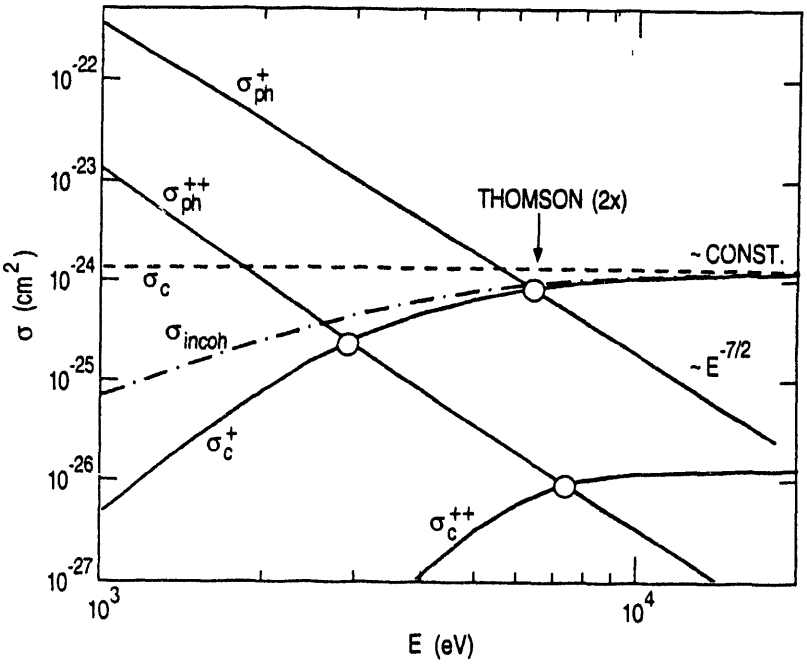

Figure 6. *Photoabsorption and Compton cross sections.*

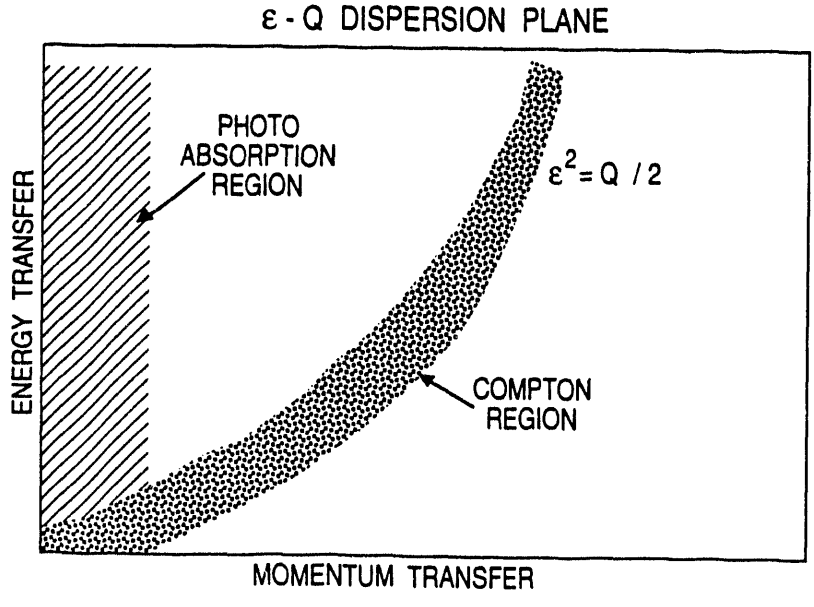

Figure 7. *The Compton and photoabsorption cross sections in the dispersion plane.*

The effect of Compton scattering on the double to single ionization ratio in helium

Roger J. Bartlett
in collaboration with M. Sagurton, J.A.R. Samson and Z.X. He

Los Alamos National Laboratory, Los Alamos, New Mexico

Introduction

Early measurements were made from threshold up to about 600 eV, and were used to test the validity of the internal scattering model by comparison with electron impact ionization. At high energies, theories predict an asymptotic limit of the ionization ratio. At what energy is this ratio reached and what is its value?

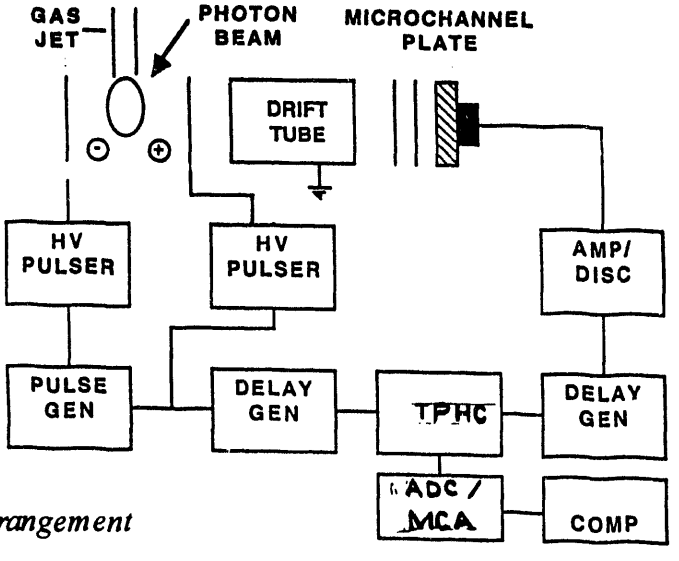

Figure 1. *Experimental arrangement*

Experimental pitfalls are:

- Low energy stray light: eliminated by transmission filters (Ni and Al).
- Low energy electrons generated by photons striking solids: eliminated by the use of baffles and magnetic fields.
- Detector discrimination for the different ion states: eliminated by post acceleration of 5400 volts.

The equation for the ionization ratio is

$$R = (\sigma_{pe}^{2+} + \sigma_{co}^{2+}) / (\sigma_{pe}^{+} + \sigma_{co}^{+})$$

where $\sigma_{pe}^{+,2+}$ are the single and double photoabsorption cross sections and $\sigma_{co}^{+,2+}$ are the single and double Compton cross sections.

$$R \approx R_{pe} / (1 + \sigma_{co}^{+} / \sigma_{pe}^{+})$$

where R_{pe} is the photoabsorption ratio and it has been assumed that σ_{co}^{2+} is small compared to σ_{pe}^{+} in the energy range covered here.

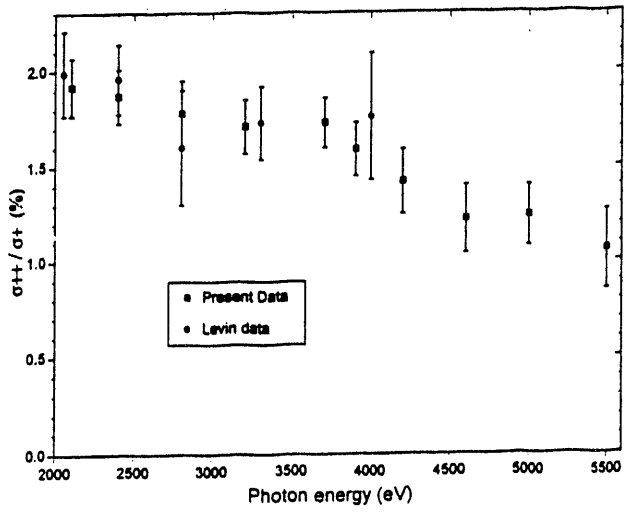

Figure 2. *The measured ratios: note the agreement with Levin; the platform region 2.8- 4.0 keV; and the fall off above 4.0 keV.*

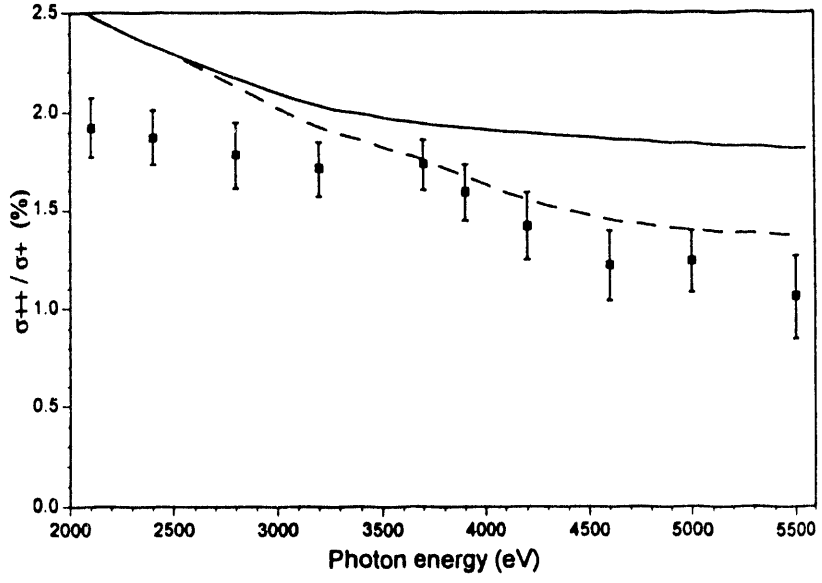

Figure 3. *Some fits to the data (see text)*

Curve fit to the data to find R_{pe}

First use a power series in 1/hν to extract the photoabsorption ratio from the data; fit the first three data points, the ones not expected to be affected by Compton scattering; fit to polynomial in powers of 1/hν and use the calculated asymptotic limit of 1.66%.

i.e. $$R_{pe} = 1.66 + a/h\nu + b/(h\nu)^2$$

Use only the three terms shown and find a and b.

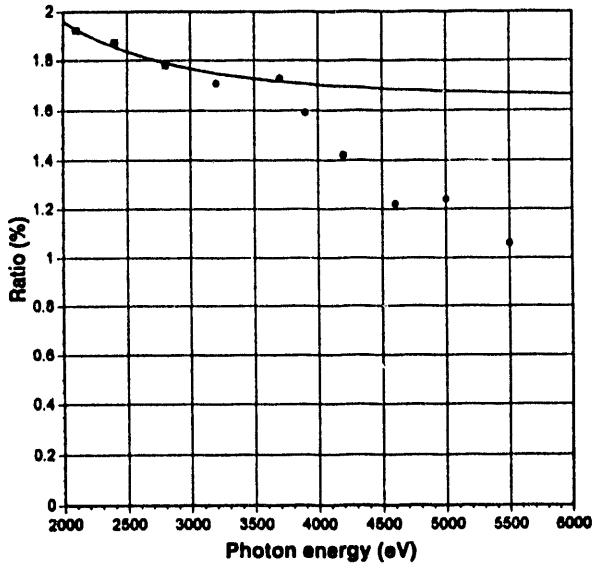

Figure 4. *Fit to the ratio, as described above.*

Ionizing Compton Cross sections

$$\sigma_{co}^{+} = \int d\sigma_{kn} \sim \pi r_e^2 \int d\theta\, (1+\cos^2\theta)\, \sin\theta \,/\, (1+\epsilon(1-\cos\theta))$$

where $d\sigma_{kn}$ is the Klein-Nishina differential cross section, r_e is the classical electron radius, and $\epsilon = h\nu/mc^2$. θ_c is the minimum angle for which energy E_b can be transferred to the bound electron. Based on free electron Compton scattering, $\theta_c = \cos^{-1}(1-mc^2E_b/(h\nu)^2)$. The limits on the integral are from θ_c to π.

$$\sigma_{inc}^{+} = \int d\sigma_{kn}\ S(x,z)$$

where σ_{inc}^{+} is the incoherent scattering cross section that can cause ionization and S(x,z) is the incoherent scattering function taken from Hubbell's paper (J. Phys. Chem. Ref. Data **4**, 471 (1975)). The limits on the integral are the same as above.

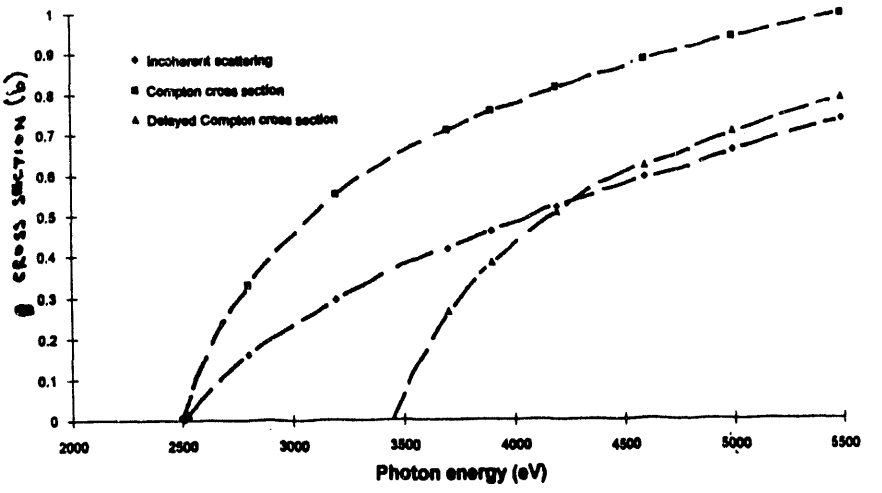

Figure 5. *Compton scattering cross sections*

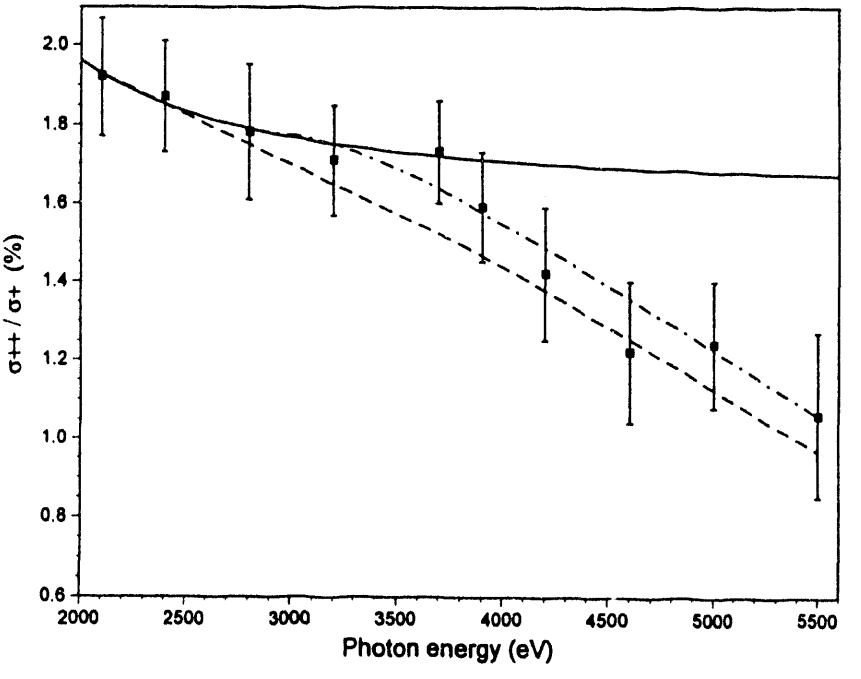

Figure 6. *The ratios from Compton scattering.*

Conclusions

1. Ionizing Compton scattering contributes significantly to the single ionization cross section of helium for hν greater than about 3800 eV.

2. The data are not inconsistent with the predicted asymptotic limit of 1.66%.

3. The data seem to reach a plateau value of 1.7% for energies greater than about 2800 eV and less than about 3800 eV, above which the Compton scattering reduces the ratio.

4. There seems to be a delayed onset of the ionization caused by Compton scattering from what would be expected based on the transfer of the single ionization energy.

Double ionization of helium by photoionization and Compton scattering

Ken-ichi Hino

Department of Physics and Astronomy, University of Tennessee, Knoxville, Tennessee 37996 and Oak Ridge National Laboratory, Oak Ridge, Tennessee 37831

Abstract

The lowest-order many-body perturbation theory is applied to double ionization of helium due to photoionization and Compton scattering. Recent theoretical works are briefly surveyed.

I. Introduction

Helium is a particularly useful paradigm for investigating electron-electron interactions because it is the simplest, abundant atomic system where such correlations are significant. The electron-electron correlation plays a decisive role in the simultaneous ionization of two electrons. A detailed analysis of double ionization by photon impact provides deeper insight into the electron-electron correlation effect on the double ionizing state. At high photon energies, the interaction of photon with electrons occur so quickly that the important processes of the electron-electron correlation may be simplified. Tunable, high intensity radiation from synchrotron sources has recently been applied to experiments measuring the ratio of double to single ionization of helium by photon impact in the asymptotic regions[1].

Early theoretical investigations of helium successfully demonstrated that the high-energy dependence of the double ionization cross section was the same as that of single ionization yielding a constant asymptotic ratio[2-5] between 1.6% and 1.7% . All these calculations used accurate correlated initial-state wave functions, including the shake-off (SO) effect in which rearrangement of electron cloud may occur due to a change of the electron charge screening of a target nucleus during collision. They ignored other effects due to the electron-electron interaction, such as the two-step-1 (TS1) process corresponding to the contribution of one electron, after an interaction with a photon, knocking the other electron out of an atom in a second step of the collision. These are based on the assumption that when a photon energy is much larger than the ionization potential of a target, at least one of the outgoing electrons leaves the target region relatively fast and the electron-electron interactions in the final state are

minimized. In 1990 Samson[6] proposed a simple classical model corresponding to the TS1 process. This model was in reasonable agreement with experimental ratios in the low- to intermediate-energy regions. Subsequently, Ishihara, Hino and McGuire[7] employed the many-body perturbation theory (MBPT) and obtained a ratio of 1.6% at 2.8 keV using the length form of dipole operator. This was in good agreement with the magnitude of earlier predictions. They also found that one of the largest amplitudes came from the two-step-1 (TS1) term. The importance of the TS1 term had also been emphasized in the low-energy region by Carter and Kelly[8]. While the agreement was obtained that the ratio at high energies was about 1.6 \%, there was apparent disagreement as to identifying the dominant mechanism responsible for double ionization.

Dalgarno and Sadeghpour[9] suggested a resolution to this disagreement, namely that this was due to a different choice of dipole operator. They gave mathematical arguments at the limit of high photon energy that while the TS1 term is non-negligible in the length form of dipole operator, it drops off rapidly in the acceleration form. Recently, Hino *et al.*[10] have explicitly demonstrated that an individual MBPT amplitude is strongly dependent on the choice of dipole operator but the coherent sum of these amplitudes is independent of the choice. Accordingly, the separate MBPT amplitudes have no consistent meaning as mechanisms for double ionization unless the form of dipole operator is defined.

While the agreement between theory and experiment has been quite reasonable for photon energies from near threshold to 12 keV, Samson, Greene and Bartlett[11] have recently noted the importance of the Compton scattering process to the interpretation of these measurements. Indeed, most experiments have relied on measuring time of flight of the residual ions, and have not yet been sensitive enough to discriminate ions produced by photoionization from those produced by Compton scattering. Here the ratio of double to single ionization for helium by photon impact reads

$$R = (\sigma_{cs}^{2+} + \sigma_{ph}^{2+}) / (\sigma_{cs}^{+} + \sigma_{ph}^{+}) \qquad (1)$$

where σ_{cs}^{+} and σ_{cs}^{2+} are single and double ionization cross sections by Compton scattering, and σ_{ph}^{+} and σ_{ph}^{2+} are counterparts by photoionization. The inability to distinguish between the two processes becomes problematic at high photon energies, where Compton scattering cross sections become comparable to photoionization cross sections at several keV and are dominant near 10 keV. Although the two distinct processes contribute to the overall ratio R of Eq. (1), experimental measurements for R above 6 keV take similar values to the theoretical asymptotic value 1.68% of photoionization. Recently, Andersson and Burgdörfer[12] have discussed the approach of R to the asymptotic photoionization ratio using a simple estimate based on photoionization data.

In this report, I introduce the lowest-order MBPT calculations of double ionization of helium due to photoionization[10, 7] and Compton scattering[13]. In Compton scattering, the A^2-approximation is employed as the photon-electron interaction. The validity of this approximation is discussed in refs. 13 and 14. According to this framework, the transition amplitude for a respective process

consists of three terms which correspond to the three mechanisms called in the literature as the two-step-1, the shake-off, and the ground-state correlation (GSC). Note that there are generally two amplitudes contributing to GSC as shown in Fig. 1. One of these represents a GSC process mediated by a particle propagating from the electron-electron interaction to the photon-electron interaction, the other means the contribution from a hole propagation. They may be called as GSC-p and GSC-h for simplicity. Here the coherent sum of the two amplitudes is termed as GSC. In photoionization where the dipole approximation is correct, an effect from GSC-h is omitted exactly. The local V^{N-1} potential is used to obtain the Hartree-Fock basis set[10]. In the present calculations, it is understood that the hole-hole interactions are incorporated to all orders to give the correct Hartree-Fock energy for the ground state of helium. Discussions of photoionization and Compton scattering are made separately in Sec.II and III, respectively.

II. Photoionization

Cross sections for double photoionization are evaluated using the lowest-order MBPT in Fig. 1 in the length (L), velocity (V) and acceleration (A) forms of dipole operator. Agreement of all three formulas is necessary condition for the validity of the approximation used here. Figure 2 shows that the present results for the ratios of double to single ionization in the L and V forms are identical at all energies of an incident photon. (The mathematical argument on the identity between the two is discussed in ref. 10.) There are some differences between A form and L (or V) form, which are less than 1% at energies above 2 keV. The results are in excellent agreement with the recent observation in the keV region[1, 15]. (However, it should be noted that these measurements are affected from Compton scattering at energies higher than 6 keV, as discussed in Sec. I and III.) The present ratios are somehow lower than the existing experiments in the low- to intermediate-energy regions due presumably to lack of higher-order correlation effect in the present formalism. Indeed, the inclusion of higher-order electron-electron interaction up to second-order remedies this disagreement to some extent[8, 16].

Figure 3 shows the cross section ratio in the L form. Curves TS1, SO and GSC are the ratios where the double-ionization cross sections are calculated using an individual amplitude in Fig.1. The curve marked "Total" is the cross-section ratio obtained by the coherent sum of these three amplitudes. TS1 and GSC (actually, the contribution from GSC-p) appear to be the largest and the magnitudes are greater roughly by one order than "Total" at high energies. Therefore, it is apparent that the TS1 and GSC amplitudes interfere {*destructively*} in the L-form. The ratios in the A form are shown in Fig. 4. Here, all three amplitudes seem to interfere {*constructively*}, and TS1 falls off at high energies. The energy-dependence of this decline is reasonably close to that given by Dalgarno and Sadeghpour[9]. The tendency in the V form (not shown here) is similar to that in the A form at high energies.

Thus it has been demonstrated that the individual MBPT cross section indeed depends on the form of dipole operator. At high-energy limit, TS1 is dominant in the L form but negligible in the V and A forms. Only SO's in all forms converge consistently to 0.5% at the asymptotic energy. Accordingly, these three amplitudes have no consistent meanings as mechanisms of

double ionization by photoionization unless the form of dipole operator is defined[17].

Before ending this section, I refer to the alternative approach applied to the double ionization by photoionization in helium. Recently, the correlated double continuum wave function has been proposed and employed to the low-energy electron and positron impact ionization of hydrogen[18,19]. This wave function is often termed as the BBK wave function in acronym of authors of ref. 18. In the BBK wave function, the electron-electron correlation is accounted for by the confluent hypergeometric functions, describing the Coulomb distortion between electrons. It satisfies the proper asymptotic Coulomb boundary condition of the three-body break-up channel[20, 21]. This approach has been recently applied to the double ionization by photon impact in keV region[22, 23] and reasonable agreement is obtained with MBPT results and existing measurements. Here the V and A forms of dipole operator have been chosen following the suggestion by Dalgarno and Sadeghpour[9] that the error caused in employing the approximate final-state wave function is diminished in these forms whereas in the L form the error remains unaltered. Subsequently, Kornberg and Miraglia[24] have applied the BBK wave function to all photon energy regions using the L and V forms. They have found that the ratio obtained in the L form fails to account for other theories and experiments and that even in the V form the BBK wave function is unreliable in the low- to intermediate-energy regions. This fact seems to contradict with the recent theoretical prediction[25] using the BBK wave function for the asymmetry parameter of double photoionization in helium at near threshold energy.

III. Compton scattering

First of all, I note that there exist substantial differences between Compton scattering and photoionization:

(1) The most probable ejected energy of electrons, equivalent to the energy transfer of photons to an atom, by Compton scattering is significantly small relative to that of the photoionized electron[11].

(2) In photoionization, the non-relativistic dipole approximation to the photon-electron interaction is known to hold correctly to relatively high photon energy region due to a cancellation effect of relativistic and retardation effects[26]. In contrast, the momentum transfer of photons to an atom is relatively large in Compton scattering and the dipole approximation is not valid. As a result, all terms of the multipole expansion of photon fields should be taken into consideration.

The lowest-order MBPT given in Fig. 1 is applied to double ionization by Compton scattering using the A^2-approximation. The ratio R of double to single ionization in helium is calculated[13] at the energies of 4 to 12 keV where this process is important and where measurements of this ratio have been reported. At 8 keV, for instance, σ_{Cs}^{+} and σ_{Cs}^{2+} are 0.981 b and 14.6 mb, respectively, and then the ratio of double to single Compton scattering is 1.49%. Using these results and photoionization data obtained by MBPT[10], the overall ratio R becomes 1.54%. This value is very similar to the ratio for photoionization equal to 1.66% at this energy. Andersson and Burgdörfer[12] predicted a somewhat smaller ratio using a simple estimate based on the existing

photoionization data.

The double differential cross section with respect to a scattered photon at an incident energy of 8 keV is given in Fig. 5. It is found that a photon is dominantly scattered toward backward angular region, showing the importance of effects of large momentum transfer, namely effects of multipole radiation. Peak structures appearing reflects the Compton profile of a helium atom. By integrating it with respect to scattering angle of a photon, the energy distribution of a final photon is obtained. This distribution corresponds to the distributions of energy transfer to an atom or ejected electron energies. It is found that ejected electrons with a relatively small energy is the most probable compared to photoionization, where large electron energies are dominant.

Finally, I discuss on the dominant process for double ionization by Compton scattering. Evaluating individual cross sections of the four MBPT amplitudes in Fig. 1, it is found that TS1 dominates Compton scattering and SO and GSC are relatively smaller. As in the case of dipole operator used in photoionization calculations, it is known that there is the following identity relation[27]. Letting momentum transfer of photon fields be **k** and an electron coordinate **r**, the photon-electron interaction under the A^2-approximation is of the form

$$V^L = e^{i\mathbf{k}\cdot\mathbf{r}} \tag{2}$$

An alternative operator V^V is here defined using the commutation relation

$$V^V = [V^L, H], \tag{3}$$

where H means the total Hamiltonian of helium. Putting the matrix elements of V^L and V^V bracketed by the exact eigenstates i and f of H as $M^L{}_{fi}$ and $M^V{}_{fi}$, respectively, one obtains the identity relation

$$M^L{}_{fi} = -\omega M^V{}_{fi}\,, \tag{4}$$

where ω is the energy transfer of photon field to helium. Taking the limit of **k** small in Eq. (4) yields the common identity relation of dipole operators in between the L and V forms. In this context, V^L and V^V may be termed here as the L and V forms, respectively.

According to the manipulation similar to that given in ref. 10 for a dipole operator, one can evaluate differences of a respective amplitude of Fig.1 between in the L and V forms defined above. As is the same in the case of photoionization, a difference of a respective amplitude for SO, TS1, GSC-p and GSC-h is not zero, however, the coherent sum of these differences leads exactly to zero. This means that the present approach using the lowest-order MBPT in Compton scattering is independent of the choice of the interaction operator, while the individual amplitude depends on it and has no consistent meaning. The independence is the necessary condition for the validity of the theoretical framework. According to the above argument, one may not discuss the dominant mechanism for double ionization by Compton scattering unless the form of the interaction operator is defined. The interaction operator given in Eq. (2) is also common to the

case of double ionization by charged-particle impact in the sense of a Fourier-transformed Coulomb interaction. Thus the conclusion on Compton scattering holds true to this process.

I appreciate T. Ishihara, J. H. McGuire, P. M. Bergstrom and J. H. Macek for fruitful collaborations.

References

1. J. C. Levin, D. W. Lindle, N. Keller, R. D. Miller, Y. Azuma, N. Berrah Mansour, H. G. Berry, and I. A. Sellin, Phys. Rev. Lett. **67**, 968 (1991); J. C. Levin, I. A. Sellin, B. M. Johnson, D. W. Lindle, R. D. Miller, N. Berrah, Y. Azuma, H. G. Berry and D. -H. Lee, Phys. Rev. **A 47**, R16 (1993).
2. A. Dalgarno and R. W. Ewart, Proc. Phys. Soc. London **80**, 616 (1962).
3. F. W. Byron, Jr. and C. J. Jochain, Phys. Rev. **164**, 1 (1967).
4. T. Åberg, Phys. Rev. **A 2**, 1726 (1970).
5. M. Ya Amusia, E. G. Drukarev, V. G. Gorshkov, and M. P. Kazachkov, J. Phys. **B 8**, 1248 (1975).
6. J. A. R. Samson, Phys. Rev. Lett. **65**, 2861 (1990).
7. T. Ishihara, K. Hino, and J. H. McGuire, Phys. Rev. **A 44**, R6980 (1991).
8. S. L. Carter and H. P. Kelly, Phys. Rev. **A 24**, 170 (1981).
9. A. Dalgarno and H. R. Sadeghpour, Phys. Rev. **A 46**, R3591 (1992).
10. K. Hino, T. Ishihara, F. Shimizu, N. Toshima and J. H. McGuire, Phys. Rev. A 48, 1271 (1993).
11. J. A. R. Samson, C. H. Greene and R. J. Bartlett, Phys. Rev. Lett. **71**, 201 (1993).
12. L. R. Andersson and J. Burgdörfer, Phys. Rev. Lett.**71**, 50 (1993).
13. K. Hino, P. M. Bergstrom, Jr and J. H. Macek, Phys. Rev. Lett. (submitted).
14. P. Eisenberger and P. M. Platzmann, Phys. Rev. **A 2**, 415 (1970).
15. J. A. R. Samson (private communication).
16. C. Pan (private communication).
17. I remark here that the TS1 ratios in the A and V forms are nearly the same as the "Total" in the low- to intermediate-energy region. This observation seems to be consistent with the Samson's TS1 model[6], while the result in the L form does not support this similarity.
18. M. Brauner, J. S. Briggs and H. Klar, J. Phys. **B 22**, 2265 (1989).
19. J. Botero and J. H. Macek, Phys. Rev. Lett. **68**, 576 (1992).
20. P. L. Altick, Phys. Rev. **A 21**, 1381 (1980); **A 25**, 128 (1982); J. Phys. **B 16**, 3543 (1983).
21. R. Peterkop, J. Phys. **B 15**, L751 (1982).
22. Z. Teng and R. Shakeshaft, Phys. Rev. **A 47**, R3487 (1993).
23. K. Hino, Phys. Rev. **A 47**, 4845 (1993).
24. M. A. Kornberg and J. E. Miraglia, Phys. Rev. A (in press).
25. F. Maulbetsch and J. S. Briggs, Phys. Rev. Lett. **68**, 2004 (1992).
26. S. D. Oh, J. McEnnan and R. H. Pratt, Phys. Rev. **A 14**, 1428 (1976).
27. M. Inokuti, Rev. Mod. Phys. **43**, 297 (1971).

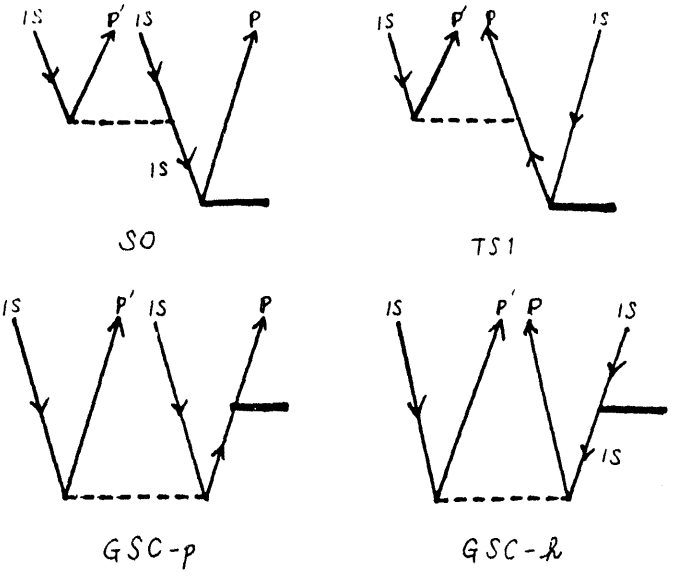

Fig.1 The lowest-order MBPT diagrams for double ionization of helium. The bold solid line represents the photon-electron interaction. This means the dipole interaction in photoionization and $\mathbf{A}^2$ interaction in Compton scattering. The electron-electron interaction is shown by a dotted line. It is understood that the hole-hole interactions are incorporated to all orders to give the correct Hartree-Fock energy for the ground-state of helium. Exchange diagrams are also included in the present calculations.

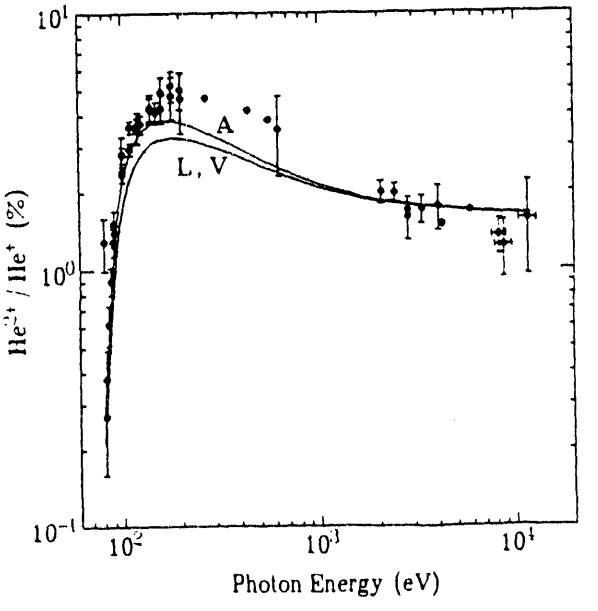

Fig.2 Comparison of the cross-section ratios for double to single photoionization. Curve L, V and A are calculations in the length, velocity and acceleration forms of dipole operator, respectively.

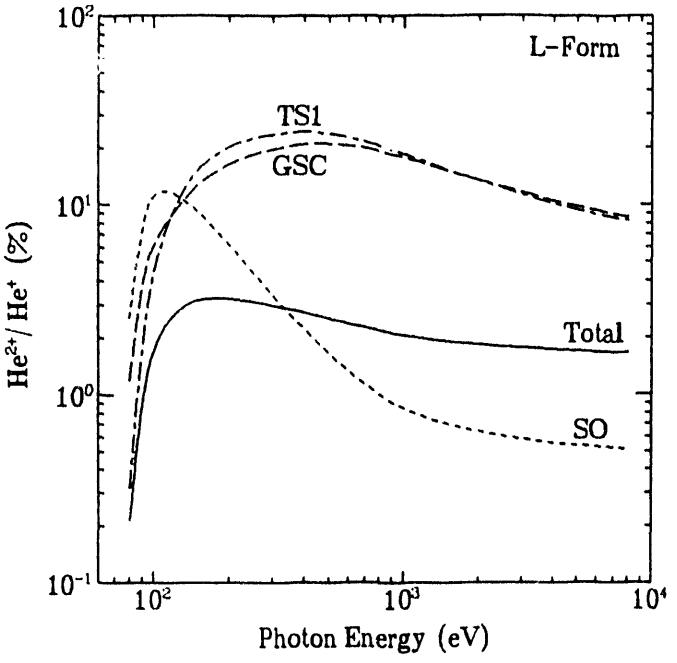

Fig.3 Cross-section ratios of double to single ionization calculated using the length form.

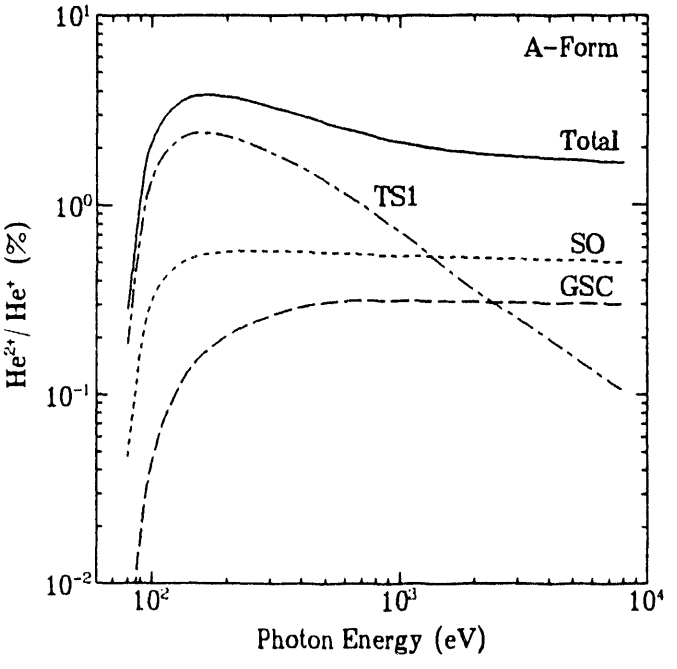

Fig.4 Same as Fig.3 in the acceleration form.

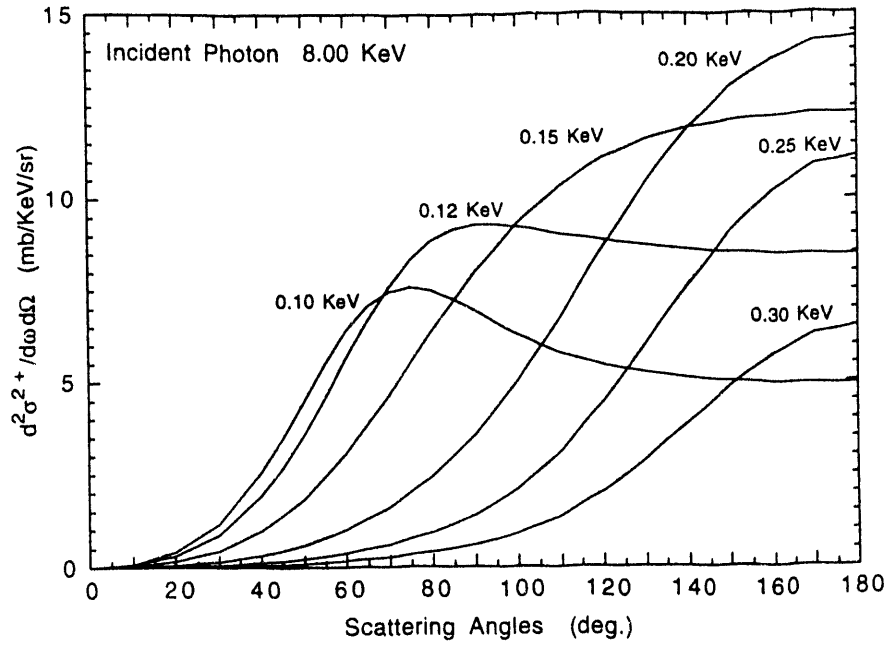

Fig.5 Double differential cross section of double ionization due to Compton scattering with respect to the photon scattering angle at the incident photon energy of 8 keV. Curves are calculated at fixed energy transfer of photon to helium, that is the difference of energies between the incident and scattered photons.

Summary of the workshop on double photoionization of helium with synchrotron x-rays*

Gordon Berry

Physics Division, Argonne National Laboratory, Argonne, IL 60439

A major question arose early in the planning stages for this workshop: whether such a narrow field of research could be covered in a morning or less? A suggestion was made that we include threshold processes, which is, of course, an area of very active research with many more investigators. In fact, we are pleased that we kept the field so restricted and focussed to the higher energy domain. It has been clear throughout the workshop that the border area where photoionization and Compton processes become close in magnitude still has many theoretical and experimental unknowns.

One goal of this workshop has been to identify just where we need to focus future experimental and theoretical research. I think all attendees agree that the lively discussions, especially after the theoretical presentations, have helped in that regard. What comes to mind is discussion of the gauge problem in identifying the electron correlation processes important in the double ionization of helium. Beforehand, it had not been appreciated, at least by myself, that the initial state, final state, and shakeoff processes are not necessarily distinct, but that their relative magnitudes depend on the gauge used in the calculations. As an experimentalist, since we measure the sum of these processes, it is reassuring to find that the theoretical result of the sum is independent of the gauge (length, velocity or acceleration) utilized. (this point was touched on in several of the theory papers, but discussed explicitly by McGuire (paper 2).

So, what are the outstanding problems remaining in the collisions of keV photons with helium atoms?

Azuma's results (paper 1) on photon attenuation in the 2 to 12 keV range show clearly the onset of the Compton scattering cross-section taking over from the photo-absorption cross section. However, distinguishing double photoionization from absorption and from the Compton process is a more difficult task. Samson (paper 6) discussed the possibility of distinguishing the different momentum transfers in the two processes - there is far less momentum transfer in most Compton collisions, where the secondary photon removes a significant fraction, depending on the angle of scattering.

Thus, the experimental task is to identify the outgoing particles in the photon-helium collision, in terms of scattering angle, momentum or energy, or all three.

A major theoretical task remaining is to calculate the asymptotic (or energy dependent) charge

state ratio for Compton collisions. Two important energy regimes are needed for this ratio: the Compton threshold region - this region extends from 2 keV, the classical threshold for single ionization, to above 4.5 keV, the classical threshold for double ionization in the Compton process; and the higher energy region, probably above 10 keV photon energy, where there may be an asymptotic limit to the charge state ratio for the Compton processes.

An integral question to this last discussion is whether the asymptotic charge state ratio for the photoionization process is the same as the ratio for the asymptotic Compton process. The experiments of Levin at 12 keV, (e.g. see paper 4) suggest that the Compton ratio is very similar. Amusia (paper 7) suggests that the ratio should be the same asymptotically for the two processes.

Further work needs to be done both experimentally and theoretically in comparing the charge state ratios obtained from photons and from charged particles. A more inclusive understanding of the theory appears to be in progress.

Once the helium correlation problem in multiple ionization is solved, it should lead the way to further experimental and theoretical work in heavier systems. Lithium and the alkalis appear to be obvious first tests of a more general theory.

David Moncton laughingly suggested that the Advanced Photon Source (the APS) would not be useful for helium experiments. In fact, such experiments may well be among the first experiments to be attempted there in 1995-96: Its enhanced photon fluxes at 4 to 10 keV may make possible some coincidence experiments which are presently very difficult to perform at existing light sources.

We thank the speakers for coming, for their enthusiasm, for their friendly criticisms, and for the manuscripts that make up these Proceedings. The written reports are informal, many of them taken directly from the overheads used in the talks, and should not be considered perfected creations for publication. These Proceedings are only put together in an effort to make the workshop deliberations more generally available, in a timely manner. We hope the reader(s) find them useful in extending our understanding of this interesting field of research.

---

*Work supported by the U.S. Department of Energy, Office of Basic Energy Sciences under contract No. W-31-109-ENG-38.

END

DATE
FILMED
3/15/94